

**FIELD VERIFICATION OF STREAM/AQUIFER INTERACTION,  
COLORADO SCHOOL OF MINES SURVEY FIELD, GOLDEN,  
COLORADO**

by

**Evan R. Anderman and Eileen Poeter**



**Colorado Water**

Resources Research Institute

**Completion Report No. 169**

**Colorado  
State  
University**

**FIELD VERIFICATION OF STREAM/AQUIFER INTERACTIONS  
COLORADO SCHOOL OF MINES SURVEY FIELD  
GOLDEN, COLORADO**

by

**Evan R. Anderman  
Eileen P. Poeter**

Grant No. 14-08-0001-2008  
Project No. 11

June 1993

The activities on which this report is based were financed in part by the Department of the Interior, U.S. Geological Survey, through the Colorado Water Resources Research Institute. The contents of this publication do not necessarily reflect the views and policies of the Department of the Interior, nor does mention of trade names or commercial products constitute their endorsement by the United States Government.

**COLORADO WATER RESOURCES RESEARCH INSTITUTE  
Colorado State University  
Fort Collins, Colorado 80523**

Robert C. Ward, Director

## ABSTRACT

The nature of stream/aquifer interactions is determined in a field study on a stream at the Colorado School of Mines survey field in Golden, Colorado. The field study measured the temporal and spatial variability during the spring and summer of 1992 of hydraulic parameters controlling stream/aquifer interactions at the streambed level of detail. Techniques for obtaining inexpensive measurements of the relevant parameters are developed. The field study included determination of the shallow hydraulic gradient directly beneath the stream; measurement of streambed seepage along the stream reach; in-situ hydraulic conductivity measurement using established piezometers and an air permeameter; and, characterization of the streambed. Samples were collected and grain size distribution was determined. The study area was monitored during a variety of hydrologic conditions in order to determine temporal and spatial controls on the seepage rate.

A number of conclusions are drawn regarding the nature of stream/aquifer interactions at the site. As 1992 received less precipitation than 1991, groundwater did not discharge as long into 1992 as into 1991, indicating that duration of groundwater discharge into summer months is dependent on the amount of precipitation the area has received. The response of the groundwater system to precipitation is on the order of days rather than hours, while the response to changes in stream stage is almost immediate. The shallow groundwater gradients calculated from the water level data indicate the presence of two groundwater discharge zones at the site, corresponding to sharp breaks in stream slope and possible subsurface features. The total reach of stream is generally gaining water from the groundwater system. The range of stream flow velocities observed is fairly uniform and sufficient to transport unconsolidated sediments up to 2 mm in diameter. Mapping of the streambed surface material shows that it is highly variable with poorly sorted large grain sizes predominant. Grain size distribution analysis supports this observation. Measured hydraulic conductivity of the streambed surface material ranges from  $2.2 \times 10^{-6}$  to  $3.2 \times 10^{-4}$  feet per second (ft/s), while hydraulic conductivity of the shallow aquifer material is greater with a range of  $9.5 \times 10^{-6}$  to  $4.3 \times 10^{-4}$  ft/s. The

observed data was combined by predicting the stream seepage using Darcy's Law. All methods adequately predicted observed conditions, but consistently overestimated seepage in the early period and underestimated seepage in the later period, suggesting a time-dependence of one or more of the parameters.

## TABLE OF CONTENTS

	<u>Page</u>
ABSTRACT .....	ii
TABLE OF CONTENTS .....	iv
LIST OF FIGURES.....	vi
LIST OF TABLES .....	viii
LIST OF PLATES .....	viii
Section 1. INTRODUCTION .....	1
1.1 Purpose.....	1
1.1 Study Area Description .....	2
1.2 Previous Work .....	6
Section 2. GENERAL BACKGROUND.....	9
2.1 Background .....	9
2.2 Assumptions and Approach.....	16
Section 3. FIELD DATA COLLECTION AND REDUCTION .....	20
3.1 Piezometers.....	20
3.2 Stream Gaging .....	24
3.3 In-situ Conductivity.....	26
3.3.1 Piezometer Slug Tests .....	26
3.3.2 Bouwer & Rice Slug Test.....	28
3.3.3 Automated Numerical Analysis .....	31
3.3.4 Surface infiltration tests .....	32
3.3.5 Air Permeameter.....	33
3.5 Trenching.....	37
3.6 Surveying.....	38
3.7 Precipitation Data .....	38
3.8 Grain Size Distribution.....	39
3.8.1 Mechanical Analysis.....	39
3.8.2 Hydrometer Analysis .....	40

3.8.3	Sample Classification .....	42
Section 4.	DATA ANALYSIS .....	44
4.1	Precipitation.....	44
4.2	Water Levels.....	46
4.3	Gradients .....	56
4.4	Streamflows .....	61
4.5	Flow Velocity .....	62
4.6	Streambed Materials.....	62
4.7	Slug Tests .....	65
4.7.1	Piezometer Slug Tests .....	65
4.7.2	Surface infiltration tests .....	68
4.8	Grain Size Distribution.....	69
4.9	Air Permeameter .....	70
Section 5.	STREAMFLOW PREDICTION .....	77
Section 6	CONCLUSIONS .....	90
6.1	Stream/aquifer system .....	90
6.2	Observation Techniques .....	92
	REFERENCES CITED .....	93
	SELECTED BIBLIOGRAPHY.....	97
APPENDIX A	FORTRAN Code for Automated Numerical Analysis of Slug Test	
Data	.....	98
APPENDIX B	Daily Precipitation.....	102
APPENDIX C	Water Level Observations .....	106
APPENDIX D	Calculated Shallow Groundwater Gradients .....	111
APPENDIX E	Grain Size Analysis of Surface Sediments .....	118

## LIST OF FIGURES

	<u>Page</u>
1.1 General location map .....	3
1.2 Alluvial and bedrock geology of the study area .....	4
2.1 Conceptual representation of stream/aquifer interactions .....	11
2.2 Physical and conceptual representations of stream/aquifer interactions .....	13
2.3 Conditions causing losing or gaining stream reaches.....	14
2.4 Ripple and pool scale of stream/aquifer interactions .....	17
2.5 Generalized cross-section of study area showing bedrock aquifers.....	19
3.1 Location map showing piezometer and weir.....	21
3.2 V-notched weir dimensions.....	25
3.3 Assumed geometry of Bouwer and Rice slug tests .....	29
3.4 Parameters for Bouwer and Rice slug test.....	31
3.5 General configuration of air permeameter .....	34
3.6 Air permeameter calibration.....	36
4.1 Precipitation summary for field area.....	45
4.2 Water levels in piezometers for period of study .....	47
4.3 Depth of sediment in piezometers .....	51
4.4 Rate of water level decline as a function of sediment thickness .....	53
4.5 Dates of streamflow and piezometers drying up .....	55
4.6 Shallow groundwater gradients between piezometers.....	57
4.7 Streamflow measured at weirs .....	63
4.8 Streamflow velocities measured at piezometer locations.....	63
4.9 Streambed material type.....	64
4.10 Results from the in-situ and lab slug tests .....	67
4.11 Results from grain size distribution analyses.....	71
4.12 Hydraulic conductivity of streambed and shallow aquifer material .....	75
5.1 Geometry used in streamflow prediction .....	80
5.2 Gradients used in streamflow prediction.....	81

5.3	Relative areas assigned to each piezometer as a function of date .....	82
5.4	Streamflow predictions .....	84
5.5	Streamflow prediction using hydraulic conductivity from surface infiltration tests and grain size distribution analysis .....	86
5.6	Estimated time dependence of hydraulic conductivity .....	89



## LIST OF TABLES

	<u>Page</u>
Table 1.1 Bedrock geology.....	5
Table 1.2 Alluvial geology.....	5
Table 3.1 Piezometer nests.....	23
Table 3.2 Parameter values for slug test analysis.....	30
Table 3.3 Sieve sizes used in mechanical analysis.....	40
Table 3.4 Unified soil classification.....	43
Table 4.1 Precipitation summary for field site.....	45
Table 4.2 Water level decline and thickness of sediment in piezometers.....	52
Table 4.3 Hydraulic conductivities from slug tests.....	66
Table 4.4 Slug tests of station 1+80 3 foot piezometer.....	68
Table 4.5 Grain size distribution of surface sediments.....	70
Table 4.6 Hydraulic conductivities from air permeameter.....	74
Table 5.1 Hydraulic conductivities used in streamflow prediction.....	79
Table 5.2 Effective hydraulic conductivities used in streamflow prediction.....	81
Table 5.3 Observed and predicted streamflows.....	84
Table 5.4 Predicted hydraulic conductivities using surface infiltration and grain size distribution analysis.....	86

## LIST OF PLATES

Plate 1 .....	pocket
---------------	--------

## Section 1. INTRODUCTION

### 1.1 Purpose

Many computer models of groundwater flow represent the interaction between streams and the aquifers underlying them on a grid size scale. Therefore, the user must assume that the conductance and other properties of the streambed do not vary significantly within a given grid cell. MODFLOW (McDonald & Harbaugh, 1987), a widely used code for simulating stream/aquifer interactions, allows the user to change the stream conductance at times the user selects. Although this and other codes simulate variations in conductance, field data are not available for use in estimating streambed conductance and so its value is almost always an educated guess. The purpose of this study is to measure hydraulic parameters controlling stream/aquifer interactions, some as a function of location and some as time on a stream reach in the field. Techniques for obtaining inexpensive accurate measurements of the controlling parameters are developed. The validity of the measurements is tested by comparing the calculated stream seepage over a given reach of stream using these measured values to the observed seepage. There are two hydraulic parameters which control seepage between the stream and underlying aquifer: 1) the head gradient between the stream and the aquifer and 2) the hydraulic conductivity of the porous medium comprising the streambed. There may be processes by which the hydraulic conductivity of the streambed varies, spatially or temporally. This will have a direct effect on the ability of the stream to gain or lose water. This study assesses the possible variations of these parameters at the streambed level.

A variety of measurements were taken to determine the nature of stream/aquifer interactions at the Colorado School of Mines Survey Field on Golden, Colorado. The study area was monitored during a variety of hydrologic conditions in order to determine controls on the seepage rate. The field study included: measurement of head at various

depths below the streambed to determine the hydraulic gradient; measurements of streamflow at the upper and lower bounds and intermediate points along the stream reach; in-situ hydraulic conductivity measurements using the established piezometers; and, characterization of the streambed. Samples were collected and analyzed in the lab to determine the grain size distribution of the samples. All measurements were taken at various locations along the streambed and analyzed statistically to characterize the spatial and temporal variation of the relevant parameters.

### **1.1 Study Area Description**

The Colorado School of Mines Survey Field, located approximately one mile southwest of the main campus in Golden, Colorado, provides an environment well suited for the purposes of this study (see Figure 1.1). The proximity to and ownership by Colorado School of Mines are heavily weighted factors in the decision to study the site, because of the ready access and approval for field activities. However, from a hydrologist's point of view, the limited size of the tributary basin and the fact that during the majority of the year the stream makes the transition from a flowing to a non-flowing condition along this reach makes this site even more attractive. The creek flowing through the site is an ephemeral tributary to Kenney's Creek and is large enough to flow for several months out of the year but small enough that flows can be measured without great expense. The alluvium is of limited thickness so that piezometer installation is also inexpensive. An annual average of 23 inches of precipitation falls on the study area, much greater than the reported average of 18 inches (Hansen et al., 1978, p. 39). The 420 acre basin contains only limited development, especially in the direct proximity of the study area, and there are no wells or other disturbances of the natural hydrology.

The site is located between the first line of foothills of the Rocky Mountain Front Range and a sandstone hog back associated with uplift on a reverse fault, so the bedrock and alluvial geology are complex (Figure 1.2). The narrow quaternary alluvial valley is eroded in and deposited on Paleozoic and Mesozoic sediments. No less than seven formations of sedimentary origin, ranging in age from Pennsylvanian to Upper Cretaceous,

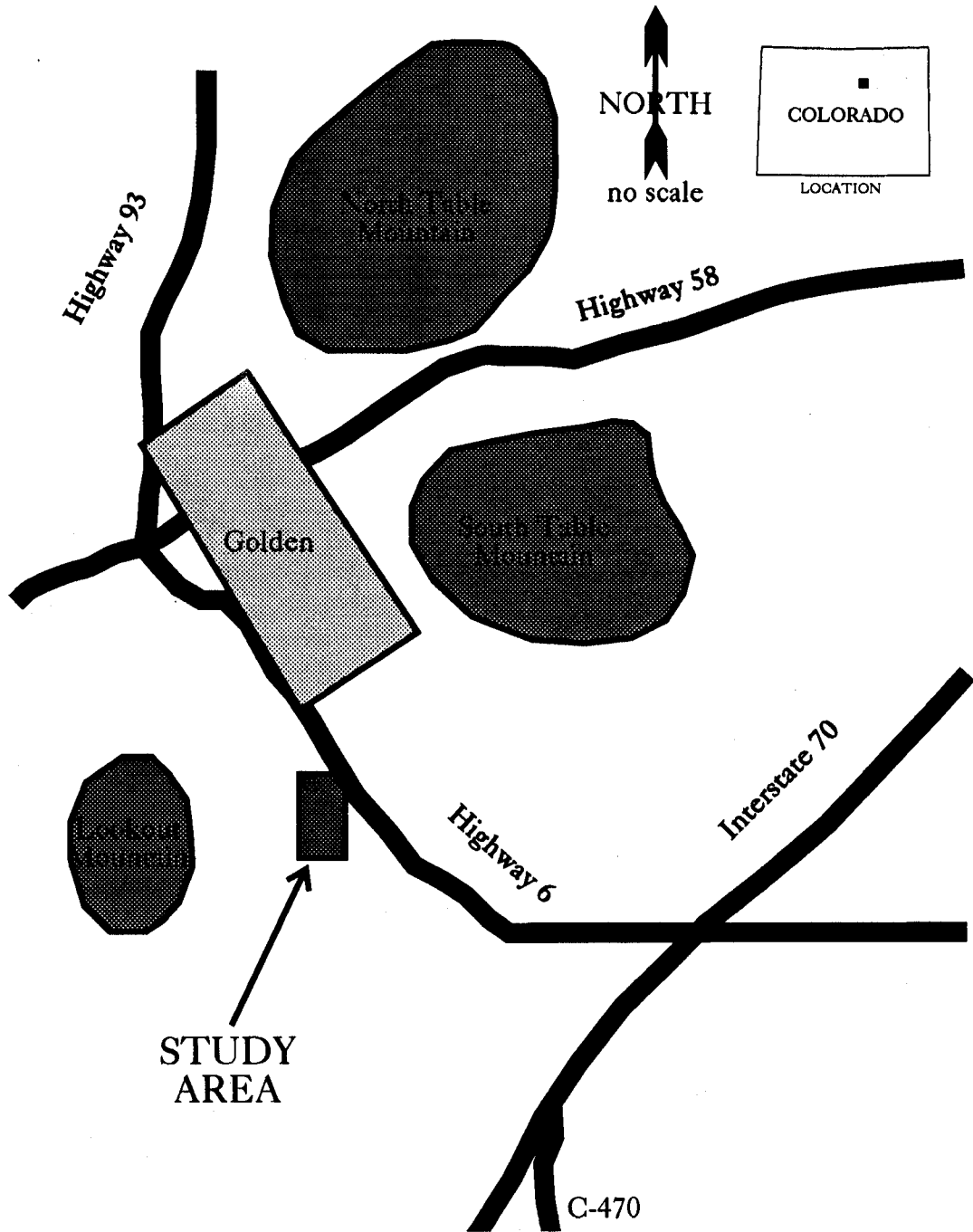


Figure 1.1 General location map of the study area.

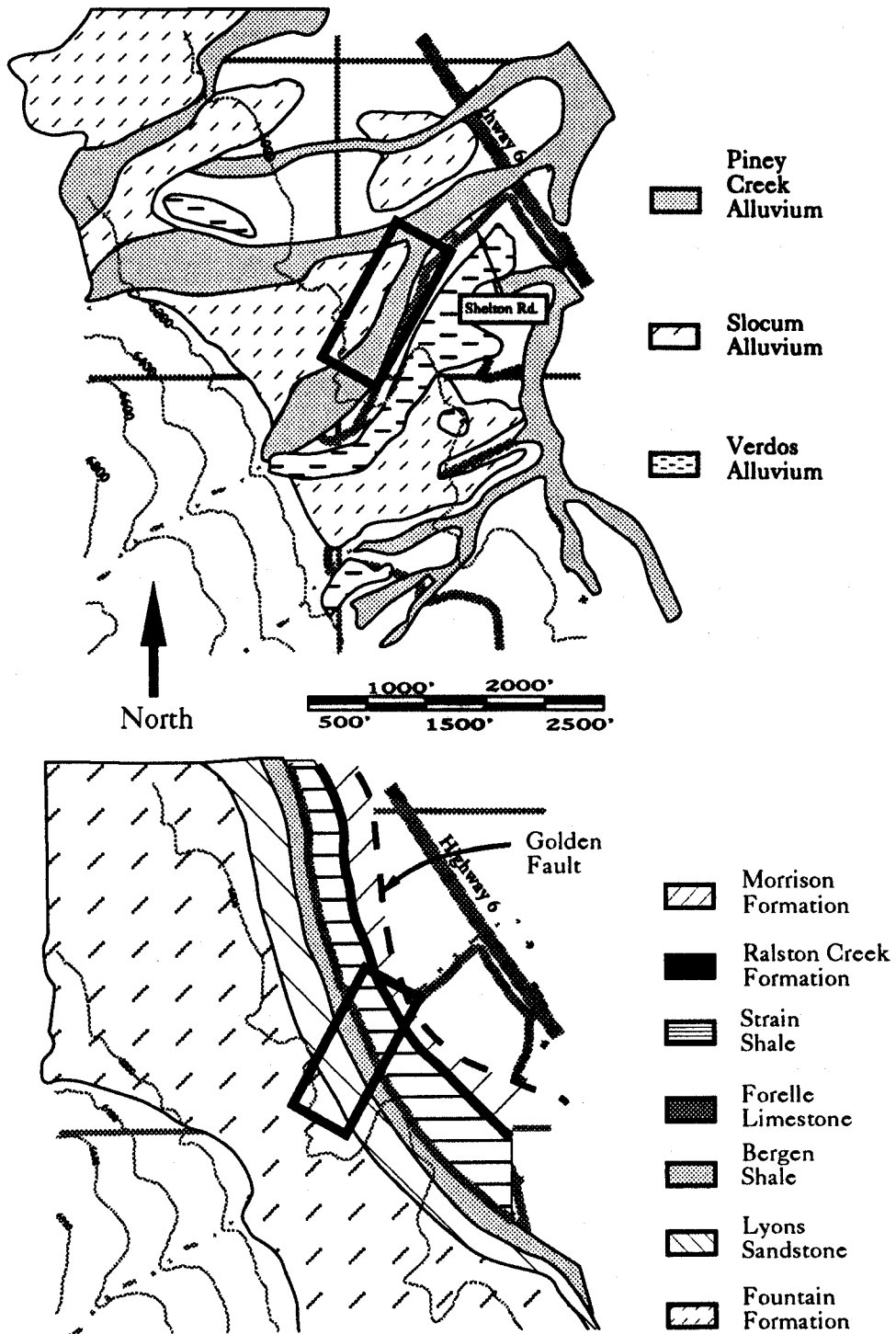


Figure 1.2 Alluvial and bedrock geology of the study area (after Scott, 1972a).

**Table 1.1 Bedrock Geology<sup>1</sup>**

Unit	Age	Description	Thickness	Relative <sup>2</sup> Hydraulic conductivity
Morrison Formation	Upper Jurassic	Siltstone with thin sandstone beds in upper part and limestone in middle part, sandstone in lower part.	300 feet	Low
Ralston Creek Formation	Upper Jurassic	Sandstone and siltstone underlain by silty sandstone containing limestone.	90	Low
Strain Shale	Triassic/ Permian	Fine-grained silty sandstone and siltstone.	300	Low
Forelle Limestone	Permian	Sandy marine limestone containing algal stromatolites.	17	Low
Bergen Shale	Permian	Siltstone containing laminated sandy limestone.	133	Low
Lyons Sandstone	Permian	Conglomerate with up to 2 inch detritus grading downward to fine-grained sandstone.	190	Medium
Fountain Formation	Permian/ Pennsylvanian	Thick bedded coarse-grained sandstone and conglomerate containing silty sandstone.	1650	Medium

**Table 1.2 Alluvial Geology<sup>1</sup>**

Unit	Age	Description	Thickness	Relative <sup>2</sup> Hydraulic conductivity
Piney Creek Alluvium	Upper Holocene	Clayey silt and sand containing layers of pebbles, grading upslope into colluvium.	5-20 feet	Medium
Slocum Alluvium	Illinois Glaciation	Pebbly silt and clay interlayered with gravel containing more and larger boulders near mountains.	15	High
Verdos Alluvium	Kansan Glaciation	Pebbly silt and clay interlayered with gravel containing more and larger boulders near mountains.	15	High

<sup>1</sup> Scott, 1972a.

<sup>2</sup> Scott, 1972b.

crop out on the property owned by Colorado School of Mines. Because of the proximity to the uplift block, formations are nearly vertical in orientation. Beneath the study area itself from southwest to northeast are the Fountain Formation, Lyons Sandstone, Bergen Shale, Forelle Limestone, Strain Shale, Ralston Creek Formation, and the Morrison Formation (Scott, 1972a). The description, thickness, and relative permeability of these units are presented in Table 1.1. The alluvial geology is simple by comparison; there are three different alluviums present in the study area, as described in Table 1.2. The Slocum alluvium occupies the hill to the west of the area and Verdos alluvium, the ridge to the east. The streambed consists of Upper Holocene Piney Creek alluvium of clayey silt and sand with layers of pebbles. The thickness of the Piney Creek alluvium in the Morrison Quadrangle ranges from 5 to 20 feet, but because of the proximity of the study area to the foothills, it is believed that the thickness of alluvium is between 5 and 10 feet. Upstream of the study area, the stream flows directly across bedrock for short reaches. The alluvium consists of 6- to 12-inch cobbles and larger boulders with a sand and pebble matrix. The small thickness and large grain size of the alluvium can be explained by proximity to the rugged foothills and the resultant steep stream slope.

## 1.2 Previous Work

Although stream/aquifer interaction concepts were presented in the 1960's (Freeze, 1969), plentiful water supply precluded the need to study them in general. Thus the occurrence of studies in the literature are periodic and brief. The emphasis of research to date has been on numerical modeling of certain aspects of stream/aquifer interactions, with a fraction of studies concentrating on collection of field data. The numerical modeling studies are predominantly event based, that is they model the response of some form of stream/aquifer system to a given precipitation event. The series of articles generated by Freeze (1969, 1972a, 1972b, 1974) forms a comprehensive overview of streamflow generation due to precipitation in a basin. The first article (Freeze, 1969) discusses water table fluctuations due to recharge through the unsaturated zone from rainfall. The next article (Freeze, 1972a) presents the physical mechanisms of baseflow generation from which a model coupling three-dimensional saturated and unsaturated subsurface flow with

one-dimensional gradually varied unsteady channel flow is derived. The third article (Freeze, 1972b) presents a basin-scale model which illustrates that overland flow in response to a precipitation event is a rare occurrence. The numerical modeling suggests that vertical infiltration of rainfall causes the water table to rise and overland flow only occurs for short distances as the water table intersects the land surface and increases the wetted perimeter of the channel. The occurrence of subsurface storm flow is also rare and exists when the saturated hydraulic conductivity is greater than a threshold value of  $3 \times 10^{-5}$  ft/s and where convex hill slopes feed deeply incised channels. The final article (Freeze, 1974) recapitulates previous work and presents concepts, theory, and modeling of the generation of streamflow from a storm.

Concurrently, a number of other authors published articles regarding the modeling of stream/aquifer interactions. Hornberger et al. (1970) used the Boussinesq equation with a groundwater recession technique to model discharge to a stream and groundwater flow in response to changes in stream stage. Using a coupled groundwater/surface water model, Pinder and Sauer (1974) analyzed the interaction of a flood wave hydrograph with the increase in groundwater storage. This work showed that the leakage rate increases with increasing flood stage resulting in attenuated flood waves. Morel-Seytoux (1975) used a similar approach to simultaneously predict the two-dimensional drawdown in an aquifer in response to a one-dimensional propagation of a flood wave.

There are two references concerning ephemeral streams. Flug et al. (1980) modeled the recharge from an ephemeral stream subject to flow events due to periodic precipitation. Dillon and Liggett (1983) used the boundary integral equation method to represent the interaction between an ephemeral stream which is periodically not hydraulically connected with the water table and the unconfined aquifer.

There are only a few occurrences in the literature of field studies of stream/aquifer interactions. The most comprehensive one is that of Kennedy et al. (1986) conducted in a northern California basin. The increase in dissolved chemical load observed at peak discharge illustrates several aspects about stream/aquifer interactions. First, extensive interaction with the soil occurred as evidenced by the large increase in dissolved species in the river water which had a different isotopic signature than the rain water. The penetration of the soils by the rainwater was quick because the increase occurred shortly after the initiation of the storm event. The nature of the dissolved species indicates that



there was not great enough infiltration to cause the displacement of groundwater, rather the rain water reacted with shallow subsurface soils before discharging into the river. A possible explanation for this shallow subsurface stormflow is that the infiltrating water encounters soil layering sub parallel to the hill slope and is discharged shortly downslope. The Hill (1990) study of groundwater discharge to a gully in a small alluvial headwater valley in Nevada showed that bedrock contribution to streamflow is significant. Castro and Hornberger (1991) used a tracer test to determine groundwater/surface water interactions in an alluvial mountain stream. This study showed that there is significant interaction between water in a stream and both the shallow gravel bed and in deeper alluvial infill material. An examination of water quality and stream-aquifer interaction during drought periods of the Truckee River in California and Nevada (McKenna, 1990) concluded that there was a significant amount of groundwater entering the Truckee River during the drought of 1988. Analysis of the hydrogen isotope ratios indicated that a component of the water gained was released from bank storage but this process could not account for the total amount of water gained.

A number of observations can be drawn from the articles outlined above. First, numerical models have been a predominant and useful method of research into stream/aquifer interactions. A numerical model is a good first step in conceptual understanding of a system as it allows one to test hypotheses without the expense of a field study. The next logical step is to determine whether the phenomenon observed in the model is actually occurring in the field. The data obtained from field studies should then be analyzed in light of the conceptual model to help refine the conceptual understanding of the system.

## **Section 2. GENERAL BACKGROUND**

It is important to have a thorough conceptual understanding of the system in order to understand the data being gathered. The purpose of this part of the report is to present the concepts of stream/aquifer interactions within the overall context of basinwide hydrologic processes. This approach considers a variety of scales, dependent on the processes which are of interest and the amount of information available. While presenting the theory of stream/aquifer interactions, the area being investigated in this study is described and the necessary assumptions are stated.

### **2.1 Background**

There are a number of scales from which the study of stream/aquifer interactions can be approached, depending on the level of detail desired and the available resources. These levels vary from the basin level at the greatest, to the sub-basin or watershed level, streambed level and finer. On the basin level stream/aquifer interactions can be a significant and important part of the entire watershed character, while at the streambed level different processes predominate and broader scale influences are less important. Likewise, there are different mathematical approaches to representing these processes depending on the scale of interest. An important contemporary issue is that of scaling up an analysis so that the overall character of the porous media is retained while the specific details are neglected.

On the basin level, stream/aquifer interactions form one part of the many hydrologic processes contributing to the overall water budget of the basin. These hydrologic processes in a basin include: precipitation, infiltration, groundwater recharge, overland flow, channel flow, evapotranspiration, groundwater discharge, exfiltration, and streamflow. Groundwater flow in this sense can take place in either the very shallow soil/alluvial aquifer, or in deeper bedrock aquifers. At this basin scale of analysis,

contributions from individual hydrologic and geologic units are less important to understanding the basin character than the overall processes.

Focusing on the watershed level, of which there are many within a basin, these same processes predominate; but, at this level contributions from individual elements can be discerned. Figure 2.1 shows both the physical and conceptual representation of stream/aquifer interactions within a watershed (Freeze, 1974). There are three mechanisms by which water can flow into a channel: overland stormflow, subsurface stormflow, and groundwater flow. Overland flow occurs when the rainfall intensity exceeds the infiltration capacity of a given soil and the surplus water flows off the soil into the stream. Subsurface stormflow is that water which infiltrates the shallow subsurface and flows laterally through the upper soil horizons to a stream before recharging the groundwater aquifer. Groundwater flow into a stream, only one of the components of streamflow, is the baseflow which sustains the streamflow between storm events. On the long term, subsurface contributions to streamflow are as significant as surface contributions. The mechanism which predominates varies spatially and temporally and depends on such geographic factors as climate, geology, topography, soil characteristics, vegetation, and land use, to name a few. Flow duration, runoff volume, stream cross section, wetted area, hydraulic gradient, soil properties, moisture content, aquifer type and depth, and vegetative cover are storm events and watershed specific characteristics controlling the recharge from an ephemeral stream within a watershed. While at this level all these processes should be accounted for, the amount of information needed is hard to obtain, much less the interactions between the processes. Streamflows can change rapidly, altering the nature of the streambed and thereby the efficiency with which it transmits water. Groundwater levels fluctuate seasonally, perhaps hydraulically disconnecting a streambed and the underlying aquifer and changing the flow characteristics. These are the problems encountered at the watershed level.

The streambed level is the next level of detail from which stream/aquifer interactions can be explored. At this level of detail there are two factors which control streamflow loss or gain: 1) the hydraulic head gradient between the stream and the underlying aquifer and 2) the hydraulic conductivity of the porous media separating the

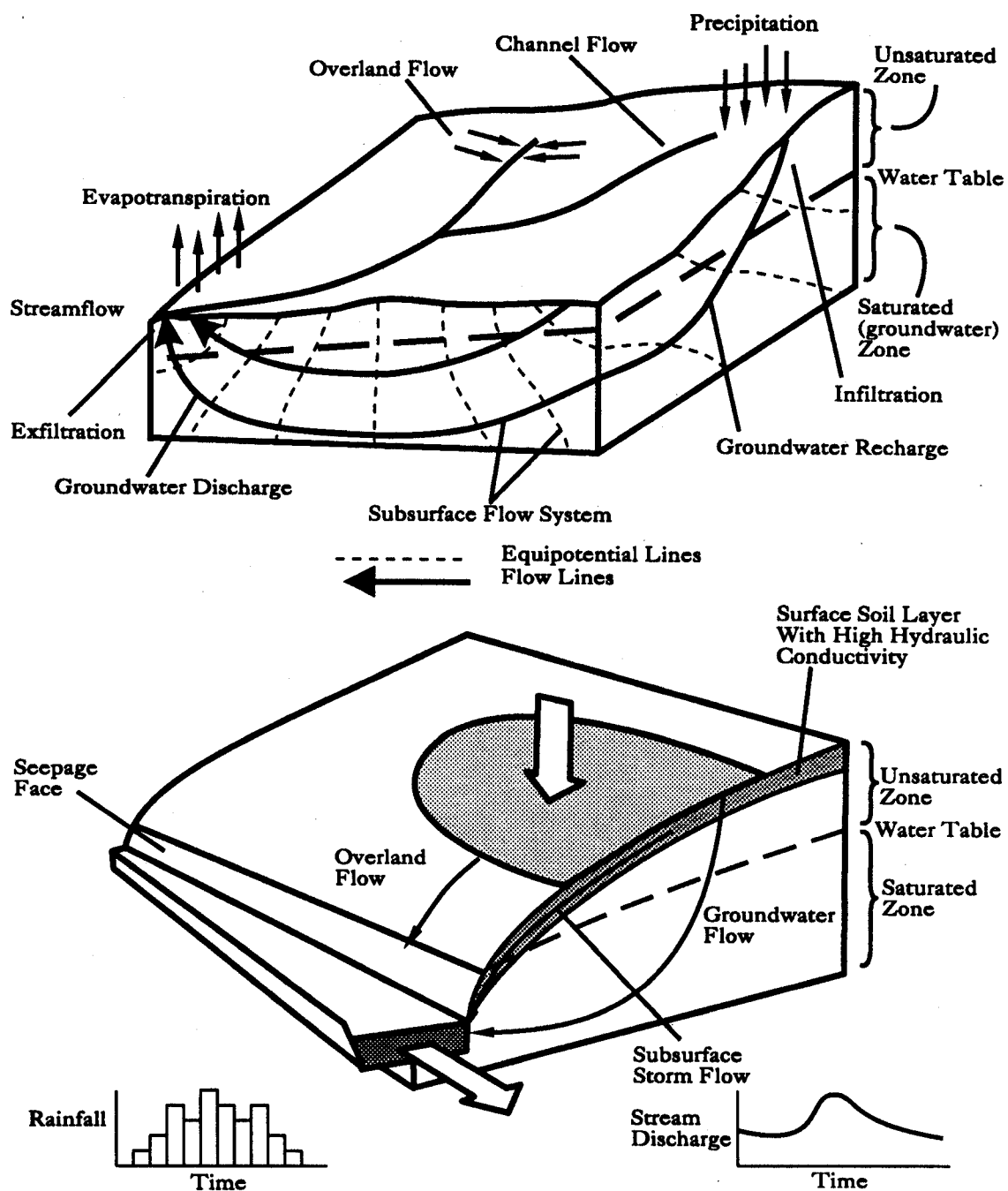


Figure 2.1 Conceptual representation of stream/aquifer interactions (after Freeze, 1974).

two. One conceptual representation of the relationship of these two factors is that of McDonald and Harbaugh (1988) showing the low hydraulic conductivity streambed and the relationship of the head in the aquifer relative to the stream, as seen in Figure 2.2. The controlling characteristics of these factors are discussed in further detail below.

The hydraulic head gradient is measured using nested piezometers consisting of piezometers measuring the head at various depths in the aquifer; if the head in the aquifer is higher than the stage in the stream, the stream will gain water from the aquifer and vice versa (Figure 2.3). Groundwater movement in shallow alluvial aquifers is controlled largely by surface topography (Larkin and Sharp, 1992). The depth to water is controlled by topography and the magnitude of groundwater recharge; as topography is controlled by the nature of the surface materials, it follows that the depth to water is also dependent on the nature of the materials and thus topography. In all terrains, the water table generally follows topography, but with a lower slope (Coates, 1990), as groundwater moves down slope from areas of recharge. Because of this, groundwater movement is dependent on topography. The response of the water table to small scale features depends on the hydraulic conductivity of the material, with zones of lower hydraulic conductivity exhibiting greater water table slopes. Subsurface topography features constrict or enlarge flow area and consequently affect the head gradient. Constriction of an alluvial aquifer valley by some subsurface feature may cause the water table to rise above the ground surface, causing a losing stream to become gaining for short reaches. Deeper erosion into less competent bedrock units results in enlarged flow area and a lower water table, resulting in a losing stream.

The hydraulic conductivity of the porous media can be complicated by the degree of heterogeneity of the porous media. Some form of a relationship between grain size and hydraulic conductivity has long been recognized (Hazen, 1910). In some geological settings, the aquifer material is coarse-grained and homogeneous and consequently the low hydraulic conductivity streambed material controls the rate of loss or gain. In other situations, the differences between the two materials are not as distinct and the controlling hydraulic conductivity is difficult to identify. There may be transient hydrogeologic events complicating the system by changing the magnitude of the hydraulic conductivity of the streambed. Examples of such events are high velocity streamflows which scour the low

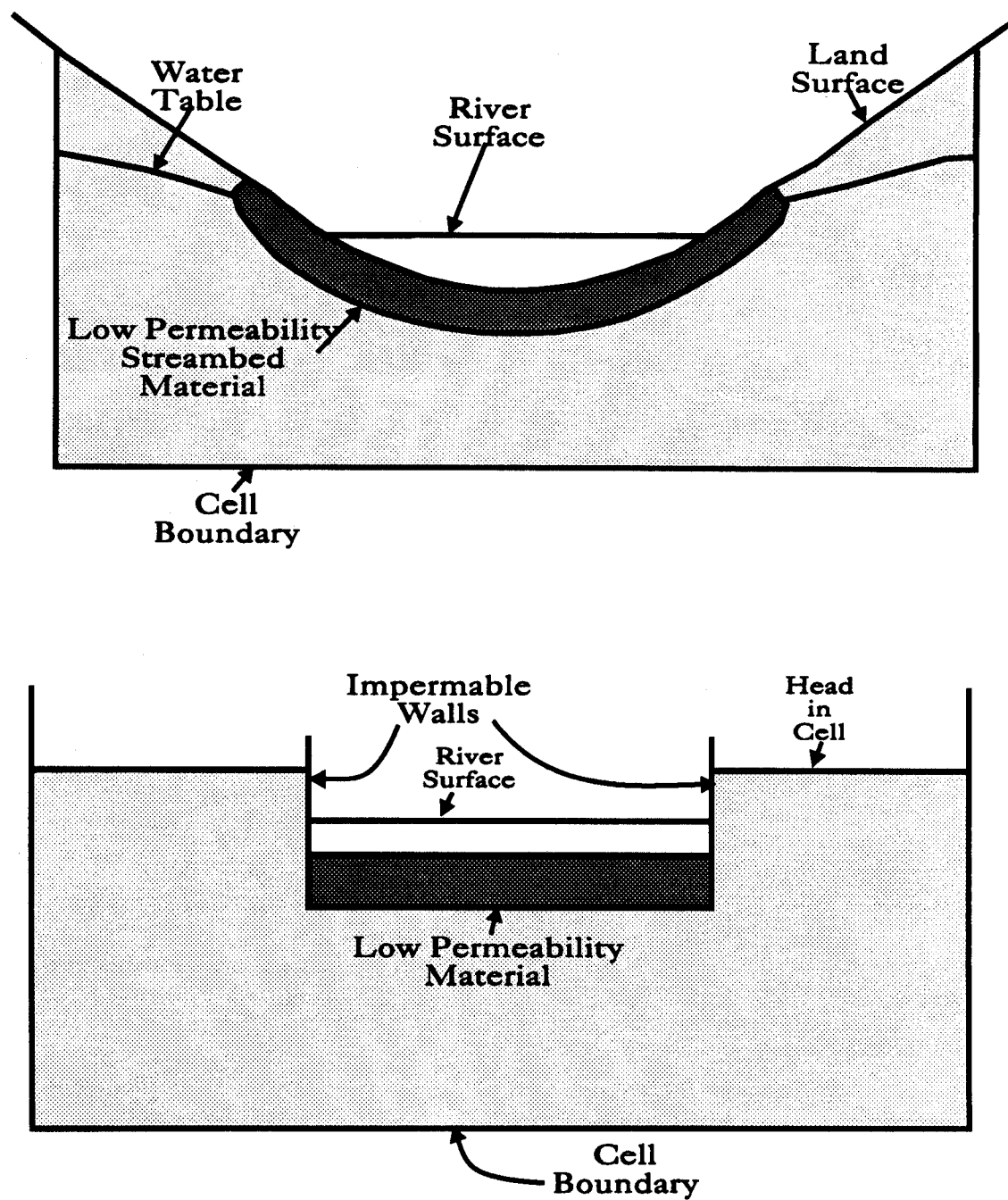


Figure 2.2 Physical and conceptual representation of stream/aquifer interactions (after McDonald and Harbaugh, 1988).

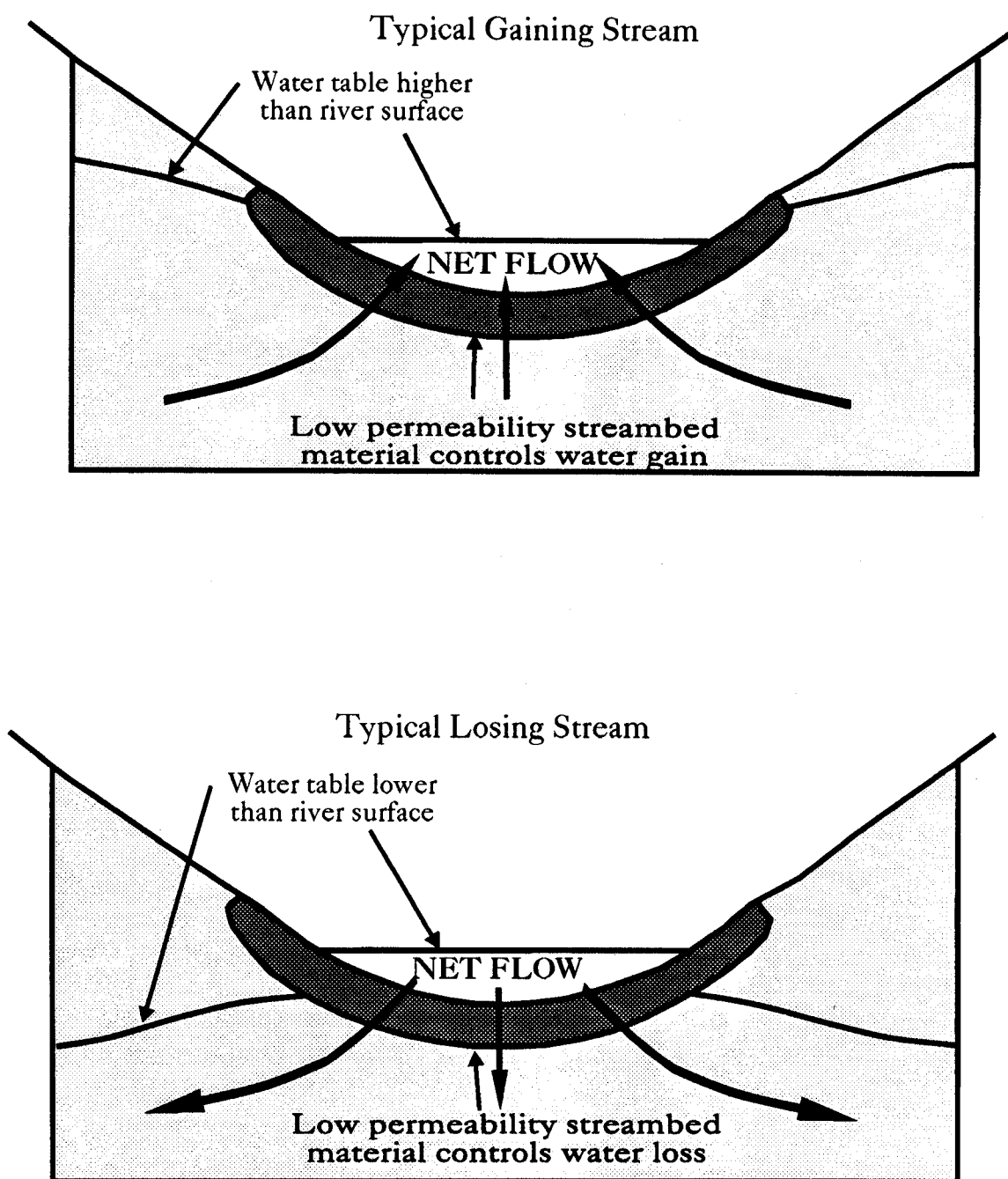


Figure 2.3 Conditions causing losing or gaining stream reaches (after McDonald and Harbaugh, 1988).

hydraulic conductivity material from the streambed and deposit it in an area with low stream velocity. This has the effect of increasing streambed hydraulic conductivity in one area while decreasing it in another. Alternatively, the upward head gradient below a gaining stream can become great enough to effectively float the grains off the bed, thereby changing the packing and grain size distribution of particles. It has long been recognized that seepage through the streambed will alter the flow configuration near the bed, but the specific role it plays remains unclear. Harrison and Clayton (1970) observed (in a field study of a small stream) that in areas where the stream was gaining water, it was transporting pebbles and cobbles while in areas where the stream was losing water it was transporting nothing larger than sand. The apparent increase in competence of the stream bed is most likely due to fine-grained material plastered on the streambed. They were not able to support or deny these findings in their laboratory study. In a flume study, Watters et al. (1971) came to the opposite conclusion. Because the velocity boundary layer is forced away from the streambed in a gaining stream, the drag forces are decreased for a particle in and above the bed while the lift forces are increased for particles in the bed and decreased for particles above the bed. This means that gaining streams inhibit sediment transport at the streambed. If any conclusion to be drawn from these studies, it is that gaining streams may have little effect on sediment transport and losing streams may inhibit sediment transport (Keller et al., 1990). These concepts are as yet controversial and additional research needs to be conducted to substantiate these results.

The effect heterogeneities have on the hydraulic conductivity of the aquifer material itself is also important to stream seepage. Less research has been conducted on this because of the complexities involved in characterizing a three-dimensional system. The degree of heterogeneity is introduced during the deposition of sedimentary materials forming the alluvium. The preferred path of groundwater movement will be through the interconnected zones of high hydraulic conductivity material with little to no flow in the lower hydraulic conductivity units. The size, shape, and connectivity of these materials depends on the depositional environment. Incorporating heterogeneities into numerical models can be computationally intensive. Bachu and Cuthiell (1990) formulated a two-dimensional numerical model of a heterogeneous core of shale clasts in a sand matrix to determine the effect that heterogeneity has on effective hydraulic conductivity. This research concluded that the reduction in effective hydraulic conductivity has a first-order



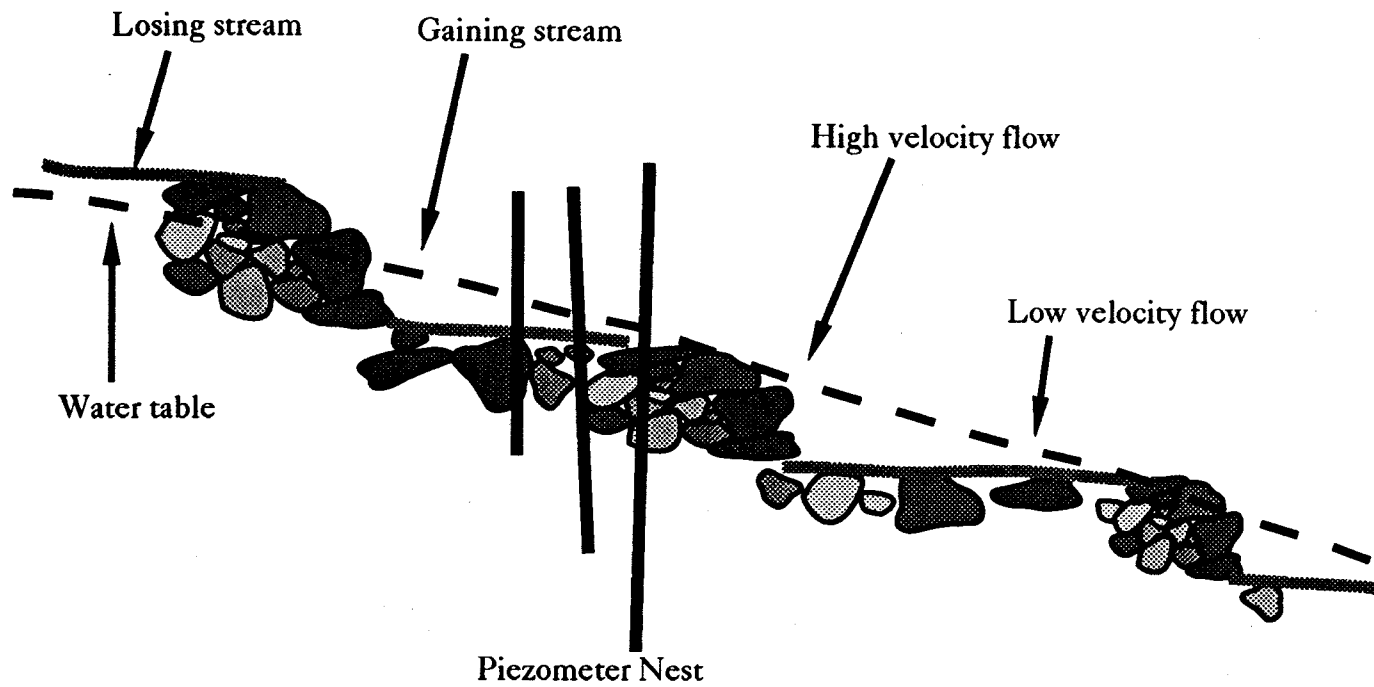
dependence on heterogeneity fraction and conductivity contrast and a second-order dependence on the shape, size, orientation, and distribution of the heterogeneity in the matrix. The effective hydraulic conductivity is not reduced for contrasts in hydraulic conductivity greater than two orders of magnitude. This implies that in groundwater flow systems which have a hydraulic conductivity contrast greater than two orders of magnitude the majority of flow is occurring in the higher hydraulic conductivity materials. Further work (Bachu et al., 1990) with three-dimensional block models of homogeneous sand matrix with varying amounts of impervious quartzite pebbles came to the same conclusions. In this work, there was less of a reduction in the effective hydraulic conductivity because of dimensional and shape differences.

## 2.2 Assumptions and Approach

In an ideal study, all parameters associated with the system are measured. In this study a number of simplifying assumptions are necessary, reducing the conceptual system to one which is manageable and can be examined by measuring head and hydraulic conductivity. The hypothesis of this study is that streamflow gain or loss varies over short distances due to variations in topographic and hydrogeologic characteristics of a stream. As mentioned previously, there are two main parameters which control stream/aquifer interactions at this level: 1) the hydraulic head gradient between the stream and underlying groundwater system and 2) the hydraulic conductivity of the porous media connecting the two. At this level of detail, the particular parameters of the groundwater system, such as recharge from underlying bedrock and geometry of the alluvium are not important.

At the Colorado School of Mines survey field, the stream gradient is not uniform on the streambed level but is broken into a series of ripples and pools (Figure 2.4). This has the effect of reducing the stream gradient in the pools while maintaining the overall gradient. The flow in the ripples is high velocity and turbulent in comparison with tranquil flow in the pools. This should have an effect on the groundwater seepage into or out of the stream. The head gradient may be upward in areas of steep topographic drops as the water table cannot respond to the abrupt change in slope. Additionally, the stream

Figure 2.4 Ripple and pool scale of stream/aquifer interactions.



Overall stream gradient is maintained while gradient in pools is reduced

velocity may be high enough to scour the fine-grained material in steep areas, lessening the resistance of the streambed and allowing more water to be gained by the stream. The opposite would be true in areas where the stream gradient is shallow where the water table follows the topography such that the stream loses water, while fine-grained material is deposited increasing the resistance to loss.

A generalized cross-section of the study area, constructed from the topographic map and information taken from the geologic map (Scott, 1972a), is shown in Figure 2.5. Thickness of the alluvium is approximate, and variations of the subsurface topography are based on relative competence of the bedrock units. In the absence of direct information on the bedrock aquifers, their contributions to flow in the alluvium are not addressed in this study. Since the study area is a likely recharge area for some of the bedrock aquifers, they probably do not seep water to the alluvium but they may carry water away from the alluvium. Alternatively, if the bedrock aquifers are in communication with the nearby crystalline rock, the potentially high heads in the crystalline rocks due to the steep rise in topography could result in substantial discharge from the bedrock aquifers.

The approach to estimating seepage in this study is to measure spatial and temporal variations in the hydraulic head gradient, and spatial variations in the hydraulic conductivity of the porous media. This assumes that, at this scale, stream/aquifer interactions are only dependent on those two factors, with all other influences being incorporated into these parameters.

## Study Area Cross Section

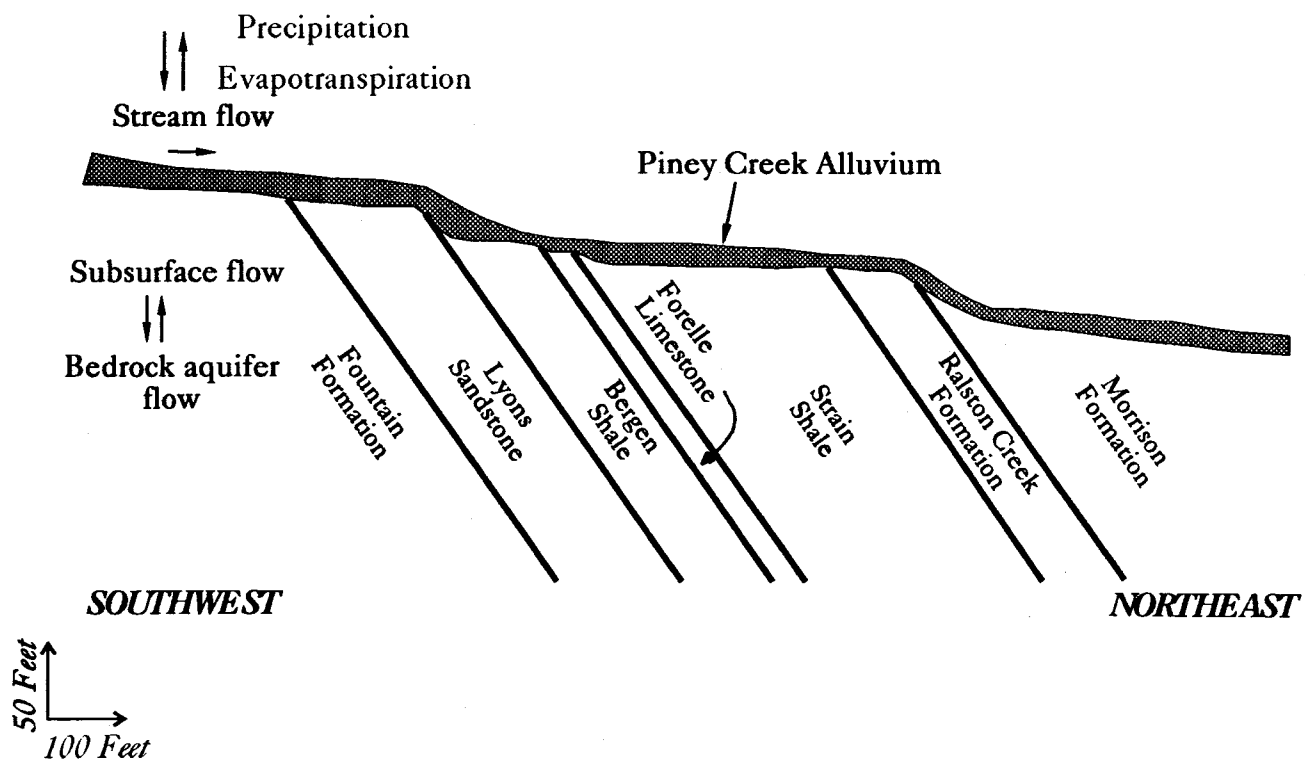


Figure 2.5 Generalized cross-section of study area showing bedrock aquifers (after Scott, 1972a).

### **Section 3. FIELD DATA COLLECTION AND REDUCTION**

The stream reach documented in this study was selected with the criteria that, in order to document a variety of hydrologic conditions, there should be a flowing and non-flowing segment of stream reach. This allowed the collection of data for both losing and gaining stream reaches. The stream reach selected runs for a length of approximately 1200 feet along the main branch of the stream, in the study area just west of State Highway 6 (Figure 3.1). A tributary joins the stream reach just downstream of the study area. Stream/aquifer interactions were documented during different types of precipitation events to characterize interactions during a variety of environments. The field study included: measurement of the head at various depths below the streambed to determine the hydraulic gradient; measurements of streamflow at the upper and lower bounds and intermediate points along the stream reach; in-situ hydraulic conductivity measurements using the established piezometers and an air permeameter; and characterization of the streambed. Sediment samples were collected from the streambed and sieved to determine their grain size distribution.

#### **3.1 Piezometers**

Piezometers were installed to monitor the shallow groundwater gradient beneath the streambed. A number of factors influenced the design and installation of the piezometers and the low budget of the project required an innovative approach. Because of the coarse-grained nature of the sediments in the stream valley, a variety of installation techniques were attempted prior to the final piezometer design and installation. Use of a drill rig was not only too expensive for the project budget, but would also have had problems with the large cobbles and boulders in the subsurface, disturbing the porous media. Hand installation required a piezometer small enough to avoid large cobbles but large enough to withstand sledge hammer blows. The final design consists of standard

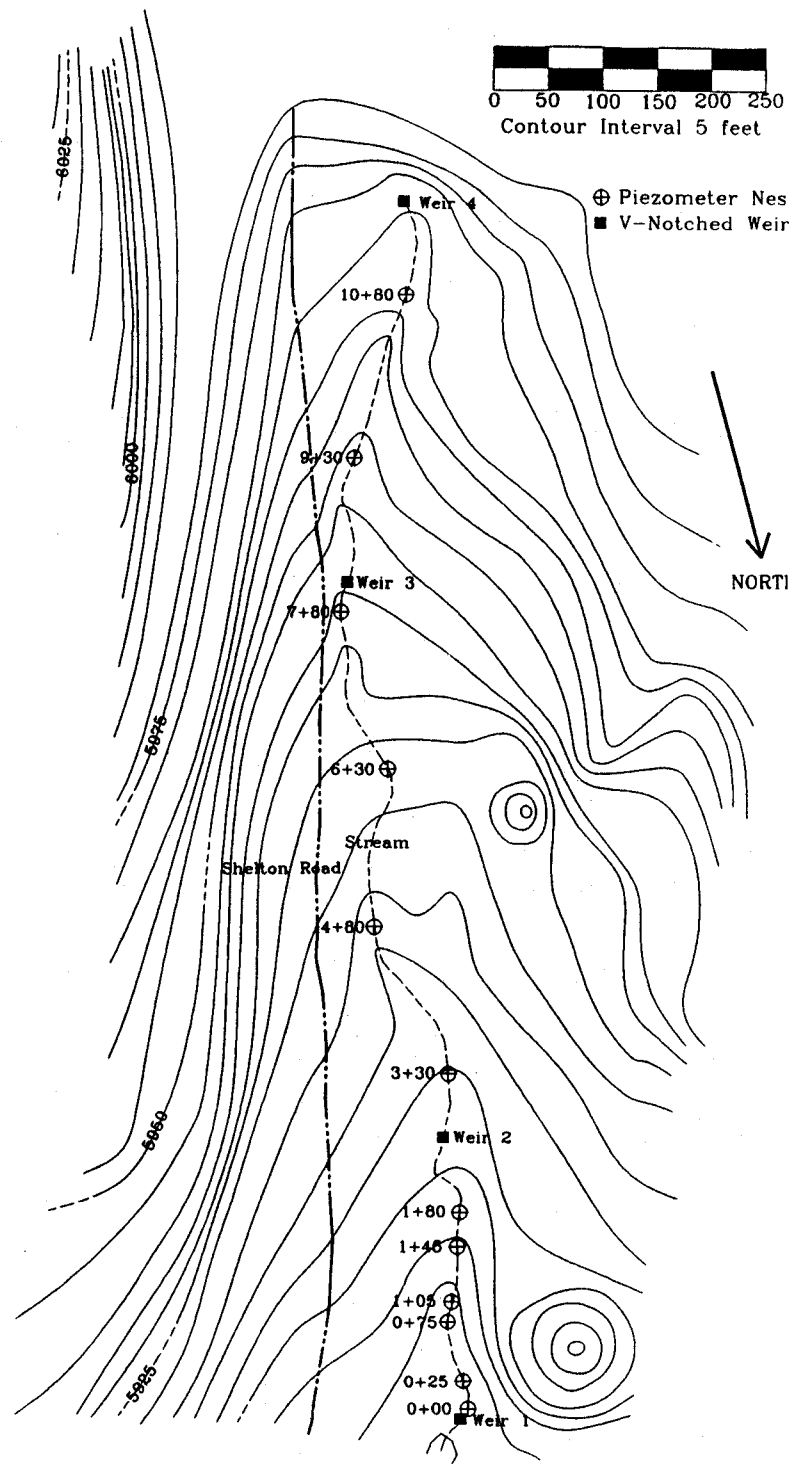


Figure 3.1 Location map showing piezometers and weirs.

half-inch electrical conduit cut to various lengths with the lower end pinched closed and approximately 12 1/8 inch holes drilled in the sides near the tip. The end was pinched closed to facilitate insertion of the tube into the porous media while inhibiting material from entering the tube. The 1/8 inch holes were drilled for two inches, along the tube, in a random radial pattern, starting one inch from the pinched end. The size and orientation of the holes were selected to allow adequate communication with the porous media while preventing fine-grained material from entering the tube during installation. Head loss in the holes was determined to be negligible as the tube would empty in a fraction of a second when filled with water. Fifteen sets of three piezometers were manufactured, each consisting of approximate lengths of 3, 4, and 5 feet, allowing 2 feet of tube to remain above ground when installed to depths of 1, 2, and 3 feet, respectively.

Two techniques were used to install the piezometer tubes. The first consisted of pounding the tubes straight into the ground with a sledge hammer, trying to keep the tubes as vertical as possible at the desired location. A mandrill of slightly larger pipe and cap was used to protect the upper end of the tube. Two major problems arose with this technique: 1) the presence of large cobbles in the subsurface caused the tube to deviate from the vertical or make installation to the desired depth impossible in some cases, and 2) the upper end of the electrical conduit, even with the protective mandrill, was compressed and deformed due to the softness of the metal. Piezometer nests 1 through 5 were installed using this technique and largely show a great deviation from vertical and insufficient penetration depth (Table 3.1). At this point, a technique of pre-driving the hole was developed to overcome these problems. This technique consisted of driving a 3 foot long 3/4 inch hardened steel drilling rod into the streambed, removing it and quickly placing the piezometer tube into the resulting cavity. Pea gravel and powdered bentonite were used to pack the oversized hole and isolate the screen from communication with the surface stream. This technique was advantageous because the piezometer tubes were generally close to vertical and installed at the proper depths. The technique of using powdered bentonite could only be used where the streambed was dry because it was necessary to ensure that the bentonite was in place before it expanded to seal the hole. Piezometer nests 6 through 12 were installed with this method.

**Table 3.1 Piezometer nests**

Piezometer No.	Station		1 Foot	2 Foot	3 Foot
1	0+00	Angle	7.0 degrees	5.1	2.0
		Depth	0.99 feet	1.99	3.00
		Collar Elevation	5890.65 feet	5890.89	5890.83
2	0+25		2.0	1.6	7.9
			1.00	2.00	2.77
			5891.34	5891.52	5891..18
2a	0+25		0.0	0.0	
			1.00	2.00	
			5889.71	5889.87	
3	0+75		7.1	19.3	11.2
			0.99	1.60	1.77
			5892.95	5893.36	5894.32
4	1+05		20.7		
			0.94		
			5894.34		
5	1+45		9.8	11.1	15.9
			0.99	1.96	2.88
			5895.95	5896.17	5896.36
6	1+80		12.3	15.8	7.2
			0.98	1.92	2.73
			5897.83	5897.88	5898.36
7	3+30		11.1	5.2	10.8
			0.98	1.89	2.16
			5907.25	5907.42	5908.19
8	4+80		13.4	6.6	7.0
			0.97	1.99	2.98
			5914.41	5914.82	5914.68
9	6+30		5.2	7.8	11.2
			1.00	1.98	2.40
			5925.13	5925.37	5925.79
10	7+80		11.6	9.5	7.2
			0.98	1.97	2.08
			5934.34	5934.52	5934.39
11	9+30		12.2	17.8	13.7
			0.98	1.67	2.23
			5944.05	5944.46	5944.93
12	10+80		8.3	7.4	8.7
			0.99	1.98	2.47
			5954.31	5954.53	5954.41



The spacing of the piezometers was selected based on the gaining or losing regime of the stream and on the success of installation. Piezometer nests 1 through 7 are spaced tightly to gain insight into the generally gaining reach of stream which they encompass. They are irregularly spaced due to difficulties associated with the first installation technique and the resulting need to attempt to install piezometer nests in less adverse conditions. Once the predriving technique was established at piezometer nest 7, a regular spacing of approximately 150 feet was established for the remainder of the study area. The locations were chosen as close to the 150 foot spacing as possible, using a fiberglass tape so as not to introduce bias from stream features, such as ripples or pools. The piezometer nests are referred to by their station location, which is the distance of the piezometer nest upstream from the most downstream piezometer nest. The angle, depth of emplacement, and absolute elevation of the collar of each piezometer is shown in Table 3.1.

Once the installation of the piezometer nests was complete, the water levels in the tubes were monitored on a regular basis. Observations at each tube consisted of two measurements: 1) the distance from the top of the tube to the water level in the stream, and 2) the distance to the water level in the tube. Two measurements were taken since accurate elevations of the piezometer tubes were not available until late in the study. This allowed the water level in each of the piezometers to be referenced to a datum that was consistent and controlling at each piezometer nest site. The water levels in the various piezometers at each nest could then be compared to determine the shallow gradient and regime of the stream. The water levels were monitored during various flow regimes to determine the hydraulic gradient along the stream reach.

### **3.2 Stream Gaging**

Accurate measurement of the flow in the stream at several locations along the length of the study area is also important data for the project. Again, the small budget necessitated an innovative approach to the acquisition of this data. Four v-notched weirs were installed at various locations to monitor the variations in flow along the stream reach

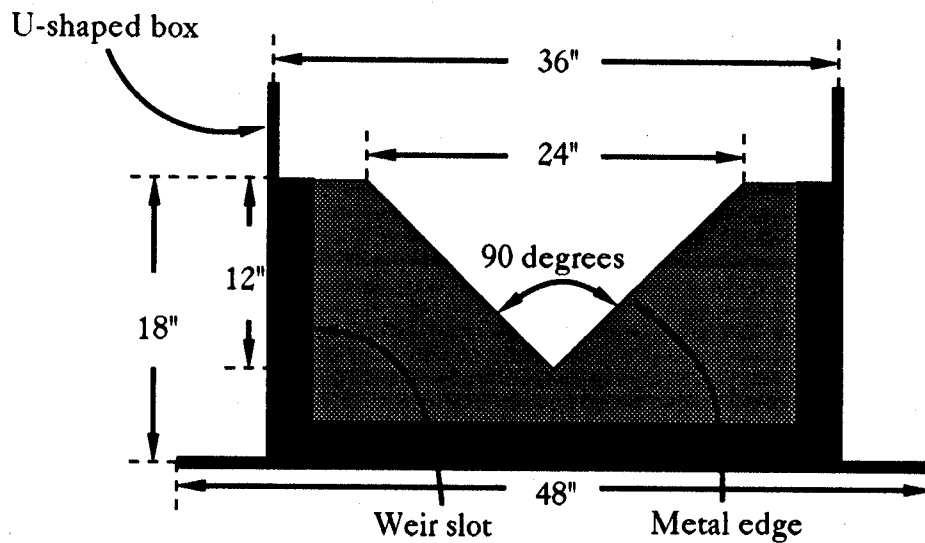


Figure 3.2 V-notched weir dimensions

as well as in time. The flow rate in cubic feet per second (cfs) is calculated from the depth of water in feet ( $h$ ) flowing over the weir as (Buchanan and Somers, 1969):

$$Q = 2.46h^{3/2} \quad (3.1)$$

Installation of the weirs during the spring runoff complicated the installation procedure, consequently a two part design was used. The first part is a u-shaped box consisting of a 2-foot by 4-foot floor with two 2-foot by 2-foot walls forming the u. The walls were placed 6 inches in from the edge of the floor to provide a base for securing the entire structure in place with earth. A slot was placed in the u-shaped opening towards the front of the structure to take advantage of the weight of the water on the base behind the notch as a long moment arm preventing leakage which might occur under the weir. The v-notched weir was cut from 1/8 inch steel and mounted on a piece of plywood to fit into the slot in the box. Garage door weather stripping was mounted on the track in the box to prevent any leakage through the track. To prevent leakage around the entire structure, a rubberized canvas skirt was placed on the front of the box and buried in the pool upstream of the emplaced weir. Installation of the weirs while the stream was flowing presented problems in that it was difficult to dig a large, flat, level area on which to initially set the

weir, while simultaneously ensuring a proper seal along the bottom of the box floor. Once a suitable pad was obtained, the box was placed in the stream and the sides were backfilled while the stream flowed over the floor of the box. The weir was then slid into the channel once the box and skirt were securely positioned.

The depth of water flowing through each weir was monitored on the same schedule as the piezometers so that the stream discharge could be compared with the stream seepage. The difference in flow along each stream reach is calculated from these discharge measurements and compared with stream bed seepage determined from the head gradient and hydraulic conductivity measurements using Darcy's Law.

### **3.3 In-situ Conductivity**

The in-situ conductivity of the porous aquifer material was measured using both slug tests in the piezometers and an air permeameter in trenches. The following sections describe the two procedures.

#### **3.3.1 Piezometer Slug Tests**

The in-situ, near horizontal, hydraulic conductivity of the streambed material was measured at various locations using slug tests on the installed piezometers. Slug testing was chosen because of its ease of application and low cost. The method consists of introducing or removing a volume of water from the piezometer and monitoring the recovery of head over time. The basis of slug testing was first discussed by Hvorslev in 1951 when he observed that upon installation of a well the "hydrostatic pressure within the hole or device is seldom equal to the original pore water pressure." Subsequent flow of water must occur to equalize this pressure gradient, the rate of which is controlled by the hydraulic conductivity of the porous media as well as the geometry of the monitoring hole. The rate of flow from the piezometer decreases with time as the head gradient approaches zero (initial equilibrium conditions). The equation for determination of hydraulic conductivity from the slug test is based on the same assumptions as for a falling head

permeameter, namely that Darcy's Law is valid and that both the water and the porous media are incompressible. The flow into a piezometer with a recovering water level is described as (Hvorslev, 1951):

$$Q = FK(z - y) = FKH, \quad (3.2)$$

where F describes the shape of the piezometer point (L),

K is the hydraulic conductivity (L/T),

z is the initial head difference at t=0 (L),

y is the head difference at time t (L), and

H is the height of the water table above or below equilibrium.

The volume of flow over a period of time is described as (Hvorslev, 1951):

$$Qdt = Ady \quad (3.3)$$

where A is the cross-sectional area of the pipe (L<sup>2</sup>).

Substituting (3.2) into (3.3) results in the governing differential equation (Hvorslev, 1951):

$$\frac{dy}{z - y} = \frac{FK}{A} dt \quad (3.4)$$

Given the geometry of the installed piezometers, the equation for determination of horizontal hydraulic conductivity in velocity units is (Hvorslev, 1951):

$$K_H = \frac{d^2 \ln\left(\frac{2ml}{D}\right)}{8L(t_2 - t_1)} \ln\left(\frac{H_1}{H_2}\right), \quad (3.5)$$

where  $K_H$  = hydraulic conductivity derived from Hvorslev method,

D = diameter of the piezometer,

m = anisotropy ratio of horizontal to vertical hydraulic conductivity,

$$= \sqrt{K_h/K_v} = 1,$$

L = length of the intake,

$H_1$  = piezometric head for t=t<sub>1</sub>, and

$H_2$  = piezometric head for t=t<sub>2</sub>.

Taking  $H_1=H_0$  when t<sub>1</sub>=0 and  $H_2=H_t$  when t<sub>2</sub>=t yields:

$$K_H = \frac{d^2 \ln\left(\frac{2L}{D}\right)}{8L} \frac{1}{t} \ln\left(\frac{H_0}{H_t}\right) \quad (3.6)$$

The flow equation that this is based on was determined empirically through experiments conducted by Harza(1935) and radial flow nets by Taylor(1948).

### 2.3.2 Bouwer & Rice Slug Test

An alternative method for analyzing slug test drawdown data was developed by Bouwer and Rice (Bouwer and Rice, 1976, Bouwer, 1989). This method combines work done by Cooper (1967), Skibitzke (1958), Lohman (1972), and Bouwer and Jackson (1974). The slug test analysis developed here is appropriate for partially penetrating or partially perforated wells in confined or unconfined aquifers. The particular solutions developed by Bouwer are valid for the range of geometries common to piezometers. The basis of the technique is the Thiem equation (see Figure 3.3) in the form (Bouwer, 1989):

$$Q = 2\pi KL \frac{y}{\ln(R_e/r_w)}, \quad (3.7)$$

where Q is the rate of flow into the well,

K is the hydraulic conductivity,

L is the perforated, screened, or uncased length of the well bore,

y is the height of the piezometric surface, above or below equilibrium,

$R_e$  is the effective radius of the well, and

$r_w$  is the borehole radius.

The assumptions upon which this equation is based are that 1) drawdown around the well is negligible, 2) flow above the water table can be ignored, 3) well losses are negligible, and 4) the aquifer is homogeneous and isotropic. The rate of water level change in a well in which water has been added or removed is described as (Bouwer, 1989):

$$\frac{dy}{dt} = -\frac{Q}{\pi r_c^2} \quad (3.8)$$

Equating (3.7) and (3.8), rearranging, integrating, and solving between limits  $y_0$  and  $y_t$  yields (Bouwer, 1989):

$$K_B = \frac{r_c^2 \ln(R_e/r_w)}{2L} \frac{1}{t} \ln\left(\frac{y_0}{y_t}\right) \quad (3.9)$$

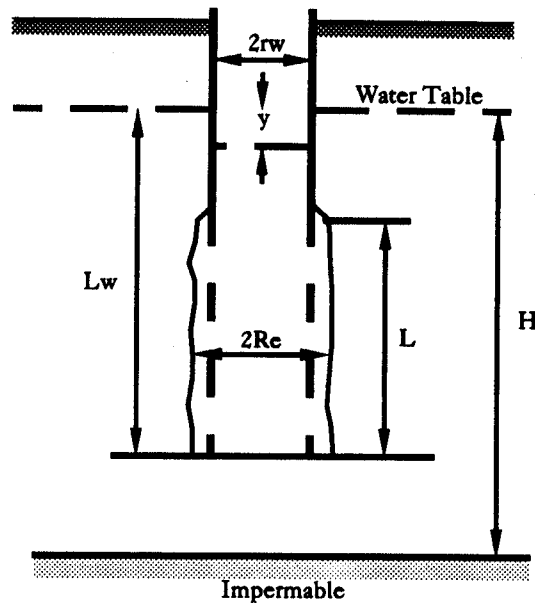


Figure 3.3 Assumed geometry of Bouwer and Rice slug test (after Bouwer and Rice, 1976).

The effective radius  $R_e$  is defined as the equivalent radial distance over which the head difference  $y$  in the flow system is dissipated and depends on the geometry of the well installation. An electrical resistance analog network was used to determine an empirical relationship between  $R_e$  and the terms representing the geometry of the well  $H$ ,  $r_w$ ,  $D$ , and  $L$ . The equation derived for a partially penetrating well is (Bouwer, 1989):

$$\ln\left(\frac{R_e}{r_w}\right) = \left[ \frac{1.1}{\ln(H/r_w)} + \frac{A + B \ln[(D-H)/r_w]}{L/r_w} \right] - 1 \quad (3.10)$$

The dimensionless coefficients  $A$  and  $B$  are determined graphically using the value of  $L/r_w$  (Figure 3.4). For the well geometry such that  $D \gg H$ , the term  $\ln[(D-H)/r_w]$  has an effective upper limit of 6 above which there is no change in  $\ln(R_e/r_w)$ . Bouwer suggests that the value 6 be used for these cases. There are two sets of values for  $A$  and  $B$  for the two different well installation techniques used in this study. These two techniques are the

driven piezometer and driven point (discussed in Section 3.1). The corresponding values of A and B are presented in Table 3.2.

**Table 3.2 Parameter values for slug test analysis**

Parameter	Driven Piezometer	Driven Point
$r_c$	0.275 inches	0.275 inches
$r_w$	0.35 inches	0.5 inches
L	2 inches	2 inches
$L/r_w$	5.7	4
D	10 feet	10 feet
A	1.65	1.6
B	0.25	0.25

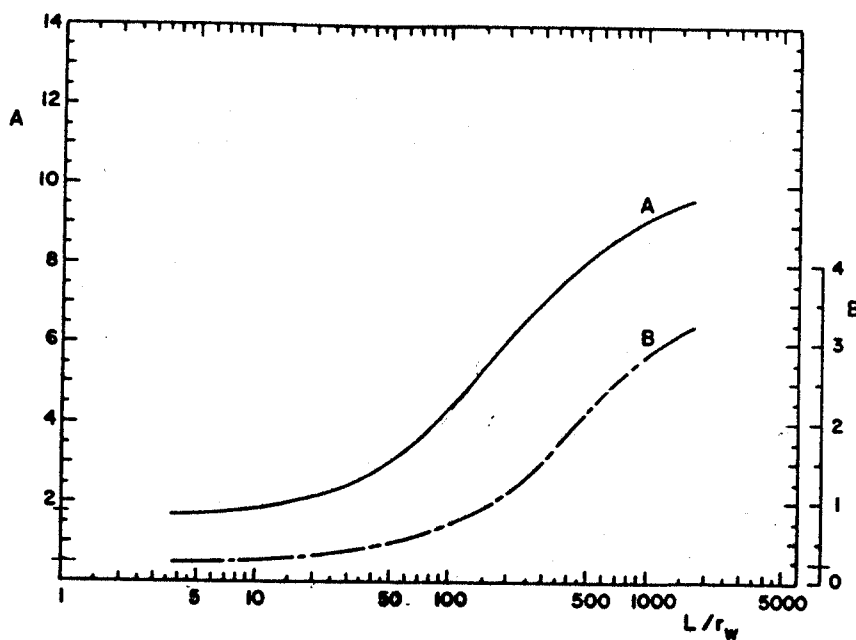


Figure 3.4 Parameters for Bouwer and Rice slug test (Bouwer and Rice, 1976).

### 3.3.3 Automated Numerical Analysis

Because the final form of the equations for the two different methods of analysis rely on fitting a straight line to the drawdown data, the analysis of the data can be performed numerically through parameter estimation (Kemblowski & Klein, 1988). Both equations (3.5) and (3.8) can be expressed in the same form (Kemblowski & Klein, 1988):

$$K = \frac{D_{\alpha}}{t} \ln \frac{y_0}{y_t} \quad (3.11)$$

where  $D_{\alpha}$  for the Hvorslev (H) and Bouwer and Rice (B) methods, respectively, are:

$$D_H = \frac{d^2 \ln \frac{2L}{D}}{8L} \quad (3.12a)$$

$$D_B = \frac{r_c^2 \ln \frac{R_e}{r_w}}{2L} \quad (3.12b)$$

The terms in these two equations are similar and so the two different methods give similar results. Rearranging equation (3.11) drawdown can be expressed as a function of time and hydraulic conductivity (Kemblowski & Klein, 1988):

$$y_t(K) = y_0 e^{-Kt/D} \quad (3.13)$$

The parameter estimation process iteratively minimizes the squared differences between the predicted and observed drawdowns to update the estimate of the hydraulic conductivity. A Taylor series expansion is used to estimate this total square error curve with respect to hydraulic conductivity. The minimum occurs when the slope, or first derivative, is equal to zero. A FORTRAN code was written by the author to perform the parameter estimation and is contained in Appendix A.

### 3.3.4 Surface infiltration tests

In a procedure similar to the piezometer slug tests, the hydraulic conductivity of the streambed surface material was determined using slug test analyses. The difference from the piezometer slug test is that a four-inch diameter California sampling tube was used to conduct the test. The tube was inserted into the streambed far enough to prevent sidewall leakage while not disturbing the streambed material. The bottom edge of the



sampler has tapered edges to minimize disturbance. The tests were conducted at various locations along the stream near the lower edge of the study area where the stream was flowing and the material was saturated. The tubes were filled with water and the decline in water level was monitored. The slug test analysis method was applied, using the geometry of the sampling tube, to interpret the drawdown data and calculate the hydraulic conductivity of the streambed material.

### 3.3.5 Air Permeameter

An air permeameter was used as an alternative method to obtain hydraulic conductivity of the permeable media. The air permeameter was attractive due to its ability to quickly and cheaply obtain a large number of non-destructive hydraulic conductivity measurements. While some form of air permeameters have long been used in the petroleum industry, portable devices have only recently been introduced to the hydrogeology industry. Initial work by Goggin et al. (1988) addressed the issues of the extent of material effected by an air permeameter as well as gas slippage for low permeabilities and high velocity flow effects for high hydraulic conductivity. A correction method is laid out by the authors. More recent work by Davis et al. (unpublished Masters research, New Mexico Tech.) presents development of a portable air permeameter using a medical glass syringe and an electronic timing device which was used as a basis for the design of the apparatus used in this study. The device forces a steady flow of air under constant pressure into the permeable medium through an injection tip. The response of the flow depends on (Goggin et al., 1988):

- 1) hydraulic conductivity of the sample,
- 2) viscosity of the injected gas,
- 3) gas slippage effect for low hydraulic conductivity samples,
- 4) high velocity effects for high hydraulic conductivity samples,
- 5) sealing quality of the tip to the sample, and
- 6) gas flow geometry.

The rate of flow is measured and, given the pressure and injection tip and sample geometry, the hydraulic conductivity of the sample is calculated using a modified form of

Darcy's Law. The calculated hydraulic conductivity must be corrected for gas slippage or high velocity flow effects and geometry (Goggin et al., 1988).

The mini air permeameter used for this study consists of a 3 cm glass syringe, connected to a standard rubber flask stopper by flexible tubing, and an electronic timing device (Figure 3.5). To ensure a sufficient seal with the permeable media, spongy material of a donut shape with a grommet forming the hole was fastened to the bottom of the stopper. To prevent any foreign matter from entering the system when the syringe is lifted, a standard filter assembly was inserted between the injection tip and syringe. The

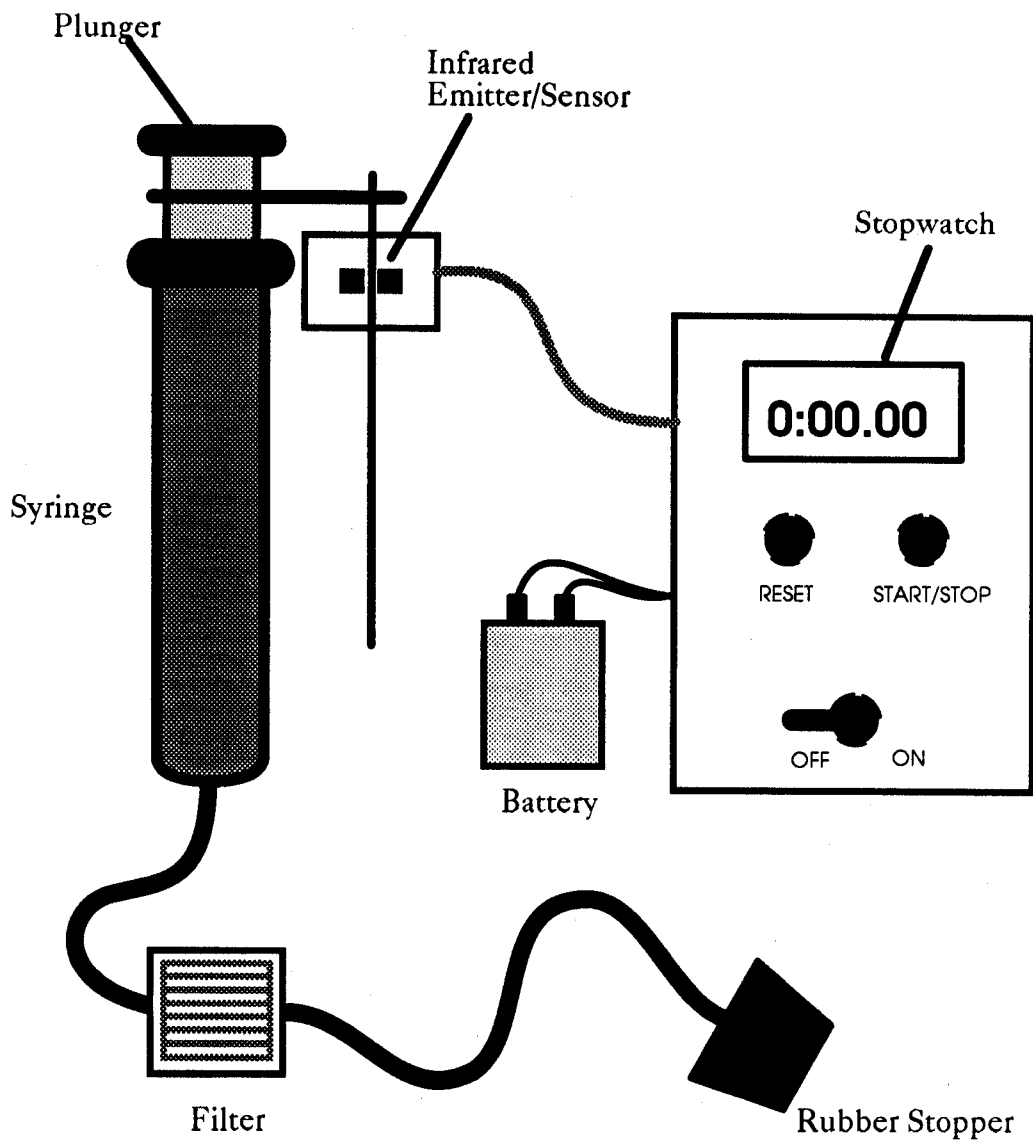


Figure 3.5 General configuration of air permeameter.

electronic timing device consists of an infrared emitter and sensor assembly which trips a standard stopwatch. An aluminum bar connected to the syringe plunger has two notches placed exactly 10 cm apart and passes through an infrared assembly when the plunger is dropped. The air permeameter is operated by raising the plunger high enough above the bottom notch to ensure steady state flow is achieved before the first notch starts the timer. As the stopper falls the second notch stops the timer and the elapsed time is read. Adequate care must be taken to ensure the injection tip is in proper contact with the permeably media and that no air leakage is occurring.

Because the modified form of Darcy's Law may need correction for gas slippage or high velocity effects, the mini air permeameter was calibrated using samples of known hydraulic conductivity and a regression equation was obtained. This calibration curve is plotted as the time of plunger fall versus hydraulic conductivity. The mini air permeameter was calibrated using core samples of known hydraulic conductivity as determined independently by Core Labs, Inc., Dallas, Texas. Multiple points along three different cores, having a range of hydraulic conductivity of  $10^{-4}$  to  $10^{-8}$  ft/s, were used to obtain the calibration. These cores were selected on the basis of their range of permeabilities and because the location of each measurement could be identified from the remaining core plug hole. The actual material measured by Core Labs was not available. Therefore, where feasible, measurement was repeated at the same location to obtain an accurate value. With the higher hydraulic conductivities ten measurements were taken, while with the lower permeabilities three to five measurements were taken. The average time of all the measurements at each location was used in the calibration calculation. Unfortunately, the highest hydraulic conductivity sample available was only  $1.7 \times 10^{-4}$  ft/s, the hydraulic conductivity of a silty to clean sand. Some of the material at the site are of higher hydraulic conductivity than this and so are outside the range of calibration. Calibration was performed using a total of eighteen measurements and results are presented in Figure 3.4. As the relationship between time of plunger fall and hydraulic conductivity is apparently linear, a linear regression was used to obtain the relationship between  $\log(t$  in seconds) and  $\log(K$  in ft/s). The resultant equation is:

$$\log(K) = -3.43 - 1.116 \log(t) \quad (3.14)$$

with an  $r^2=0.87$ . The regression line is also shown in Figure 3.6 along with the joint 95% confidence interval calculated using the Working-Hotelling technique (Neter et al., 1990).

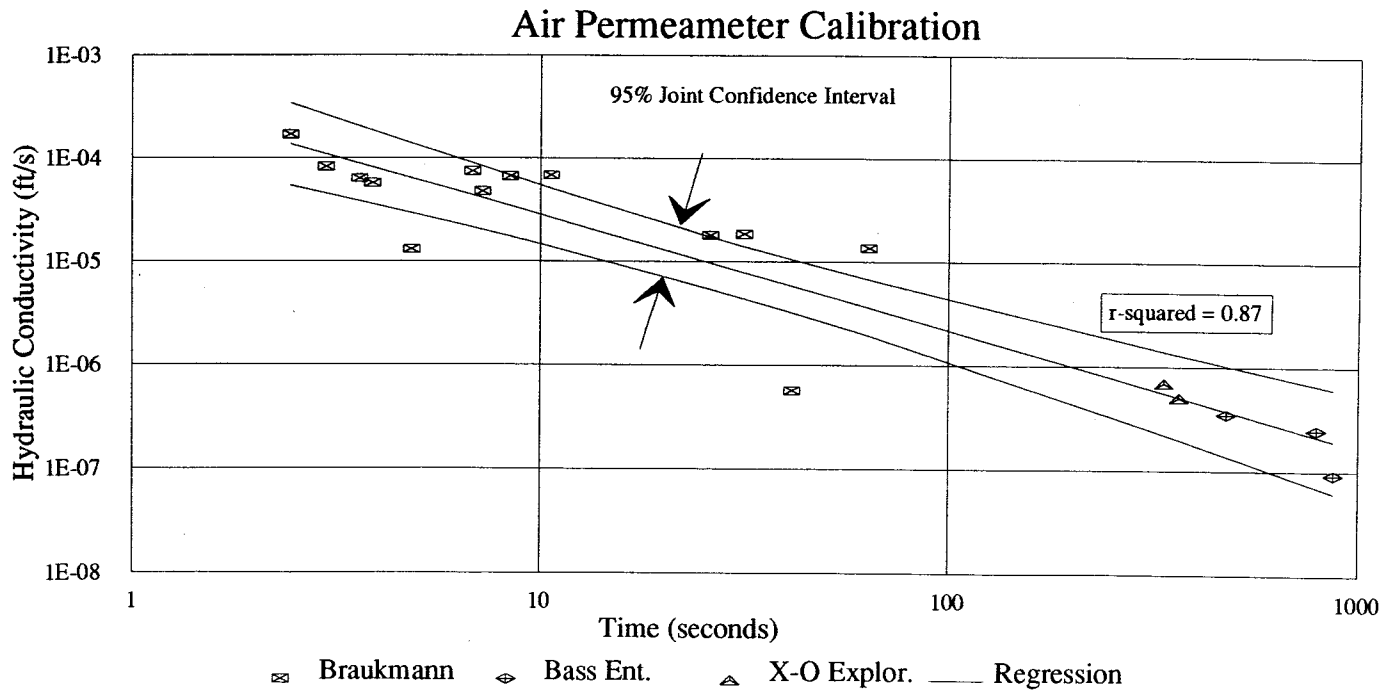
Figure 3.6 Air permeameter calibration.

Core	Interval	k(mD)	k(ft/s)	time	SDEV	n	log(time)	log(k)	Ws (Yh)
Braukmann	6862 - 6863	5350	1.7E-04	2.457	0.234	10	0.39	-3.77	0.400
Braukmann	6860 - 6861	2600	8.2E-05	3	0.147	10	0.48	-4.08	0.381
Braukmann	6864 - 6865	2000	6.3E-05	3.625	0.181	10	0.56	-4.20	0.363
Braukmann	6865 - 6866	1800	5.7E-05	3.898	0.368	10	0.59	-4.24	0.357
Braukmann	6856 - 6857	411	1.3E-05	4.857	0.387	10	0.69	-4.89	0.338
Braukmann	6876 - 6877	2350	7.4E-05	6.8	0.027	10	0.83	-4.13	0.312
Braukmann	6869 - 6870	1500	4.8E-05	7.19	0.021	10	0.86	-4.32	0.308
Braukmann	6870 - 6871	2100	6.7E-05	8.42	0.028	10	0.93	-4.18	0.297
Braukmann	6867 - 6868	2150	6.8E-05	10.65	0.046	10	1.03	-4.17	0.282
Braukmann	6871 - 6872	570	1.8E-05	26.27	0.191	10	1.42	-4.74	0.253
Braukmann	6872 - 6873	585	1.9E-05	31.73	0.213	10	1.50	-4.73	0.253
Braukmann	6875 - 6876	18	5.7E-07	41.52	0.611	10	1.62	-6.24	0.257
Braukmann	6868 - 6869	429	1.4E-05	63.59	0.628	10	1.80	-4.87	0.272
X-O Explor.	4527 - 4528	22		338.6	23.870	5	2.53	-6.16	0.399
X-O Explor.	4537 - 4538	16		368	9.540	3	2.57	-6.30	0.408
Bass Ent.	8330 - 8331	11	3.5E-07	481	19.290	3	2.68	-6.46	0.434
Bass Ent.	8329 - 8330	7.8	2.5E-07	792	20.100	3	2.90	-6.61	0.487
Bass Ent.	8316 - 8317	2.9	9.2E-08	869.8	75.800	5	2.94	-7.04	0.497

Regression Output:		Low Limit	predicted	Upper lim
Constant	-3.43	5.4E-05	1.4E-04	3.4E-04
Std Err of Y Est	0.398	4.5E-05	1.1E-04	2.6E-04
R Squared	0.871	3.8E-05	8.8E-05	2.0E-04
No. of Observations	18	3.6E-05	8.1E-05	1.8E-04
Degrees of Freedom	16	2.9E-05	6.4E-05	1.4E-04
		2.1E-05	4.4E-05	8.9E-05
X Coefficient(s)	-1.116	2.0E-05	4.1E-05	8.3E-05
Std Err of Coef.	0.1072	1.7E-05	3.4E-05	6.8E-05
		1.4E-05	2.6E-05	5.1E-05
		5.4E-06	9.7E-06	1.7E-05
		4.4E-06	7.8E-06	1.4E-05
		3.2E-06	5.8E-06	1.0E-05
		1.9E-06	3.6E-06	6.7E-06
		2.2E-07	5.6E-07	1.4E-06
		2.0E-07	5.1E-07	1.3E-06
		1.4E-07	3.8E-07	1.0E-06
		7.0E-08	2.2E-07	6.6E-07
		6.2E-08	1.9E-07	6.1E-07

Xbar =	1.461352
Xi-Xbar =	13.7717
MSE =	0.158173
W =	2.699



### 3.4 Streambed Mapping

A qualitative visual assessment of variation of sediment characteristics longitudinally along the stream reach was mapped to determine if there is a correlation between such characteristics and hydraulic conductivity of the streambed. There is a general correlation between the two. Sediment clasts range in size from silt to cobbles several feet in diameter. In a given stream reach a smaller subset of sizes is represented, depending on the morphologic characteristic of the stream reach. With this in mind, five ranges of grain size were used to map the streambed:

- organics predominate (sediment not visible)
- silt to sand
- larger than golfball size
- larger than baseball size
- larger than basketball size

The general grain size in a stream reach was observed and transitions were mapped with a resolution of five feet. The distances were measured relative to the existing piezometers using a 100-foot fiberglass tape.

### 3.5 Trenching

In order to gain qualitative insight into the spatial variability and distribution of sediments in the streambed, a trench was dug into the streambed. This trench was dug to a depth of approximately three feet with an areal extent of roughly three feet by five feet. The trench was placed such that one wall of the cut was directly beneath the centerline of the stream itself. The trench is located at station 3+40 and was chosen in a reach of stream with a very slight stream gradient. This location was chosen so that there would be a large thickness of fine-grained material on the surface of the streambed grading down to coarser material. Generally, the surface layer consists of alternating coarse-grained and fine-grained sand beds of a half to two inches in thickness each. These sands are penetrated by roots to a depth of six to nine inches. The surface layer in the trench extends to a depth of approximately 18 inches. Below the surface layer, the grain size

increases dramatically and the degree of sorting decreases. The matrix consists of approximately 1 mm sand particles and finer, while the coarse-grained material includes grains up to 12 inches in diameter. The hydraulic conductivity of the materials was measured using the air permeameter.

### **3.6 Surveying**

Surveying was conducted in order to get a more detailed base map than the USGS 7.5 minute quadrangle topographic map, as well as to obtain the locations and absolute elevations of the piezometers. The topographic mapping was conducted using a plane table located at three separate locations within the study area. As the study area is contained in the Colorado School of Mines survey field, control points were available from which the absolute elevation relative to a benchmark was known. Using this process, elevations were obtained at 133 different locations from which a topographic map was constructed. The absolute elevations of the piezometers were obtained using a level, taking readings in a loop starting at a control point, measuring each piezometer, ending at the control point. Using this technique the error of closure was 0.06 feet over approximately 2,000 feet of traverse. The elevations obtained are accurate to 0.01 feet. The elevations for the piezometers are shown in Table 3.1.

### **3.7 Precipitation Data**

The nearest precipitation gage to the study area is operated at the home of Dr. Greg Holden, Assistant Department Head of Geology and Geological Engineering at the Colorado School of Mines. The gage is located approximately 2 miles northwest of the study area at an elevation of 6,000 feet. The gage consists of a 5-inch Plexiglas outer cylinder containing an inner graduated cylinder capable of measuring to the nearest 0.01 inches. The precipitation is fed to the graduated cylinder via an inverted cone with a razor

edge on top and an approximately 1/2 inch diameter hole in the bottom. The size of the bottom hole prevents excessive evaporation from decreasing the reading. The gage is located away from any obstructions or disturbances. Snow is measured in an open area, away from disturbances and where the snow does not drift. The measurement is taken by inverting the cylinder and placing it down in the snow, which is then cleared away from the sides before the cylinder is again inverted. Both the depth of snow and equivalent depth of moisture were recorded. Measurements were obtained on a daily basis except for some periods in the summer where the cumulative precipitation over several days was recorded due to Dr. Holdens absence.

### **3.8 Grain Size Distribution**

In order to classify the grain size distribution of the streambed sediments, samples were collected and sieved. The less than 200-screen fraction was analyzed using a hydrometer. Information from these classifications can be used to correlate grain size distribution and other parameters as well as to relate the findings of this study to other streams. The samples were collected at the sites where the surface hydraulic conductivity slug tests were conducted. The samples were collected using a large spoon and placed in ziploc plastic bags.

#### **3.8.1 Mechanical Analysis**

The samples were dried in shallow baking pans at 105<sup>o</sup> C for at least 48 hours. For samples where roots were prevalent, tweezers were used to remove as much organic matter as possible. The samples were pulverized with a mortar and pestle and then placed in a sieve stack. Two sieve stacks were needed due to the great visible range in grain size distribution from inches in diameter to silt size. The sieve sizes used in the two stacks are shown in Table 3.3. Each sieve stack was placed in a mechanical vibrator and agitated for 5 minutes. In order to reduce errors, the weight of material remaining on each screen was



obtained by taking the difference of the stack with and without the sample as each screen was removed. The percent retained on each sieve was calculated and from this the percent passing each sieve. The uniformity coefficient and coefficient of gradation were then calculated as (Bowles, 1986):

$$C_u = \frac{D_{60}}{D_{10}} \quad (3.15)$$

$$C_c = \frac{D_{30}^2}{D_{60} \times D_{10}} \quad (3.16)$$

where  $D_{10}$ ,  $D_{30}$ , and  $D_{60}$  are the diameters corresponding to 10%, 30%, and 60% finer in the particle distribution curve, respectively.

**Table 3.3 Sieve sizes used in mechanical analysis**

	Stack 1		Stack 2
2 inches	50.8 mm	#16	1.190 mm
1	26.67	#30	0.600
3/4	18.85	#50	0.300
1/2	13.33	#60	0.246
#4	4.75	#100	0.147
#8	2.362	#200	0.074

### 3.8.2 Hydrometer Analysis

For samples with more than 10 percent passing the #200 sieve, a hydrometer analysis was conducted to distinguish the silt/clay character of the sample. Exactly 50 grams of sample were mixed with 125 ml of 4% sodium metaphosphate (defloculent agent) and enough water to make 500 ml in a malt mixer cup. The mixture was then stirred, for approximately 5 minutes, using a malt mixer. The mixing was complicated by the frothing action of the mixture which had the tendency to cause the mixture to

overflow. When overtopping was imminent, the mixing was stopped to allow the froth to settle. Once mixing was complete, the mixture was transferred to a sedimentation cylinder, rinsing the mixer cup to remove the entire sample. When the froth had settled, the cylinders were topped off to exactly 1000 ml total. The cylinder was agitated by hand for 1 minute and readings were obtained at 2 and 4 minutes elapsed time. This process was repeated until the 4 minute readings agreed, then hydrometer and temperature readings were obtained at 8, 15, 30, and 60 minutes, and approximately 2, 4, 8, 16, 32, 64, and 96 hours. The readings were corrected using data from a control cylinder containing only water and flocculent agent. The hydrometer measures the specific gravity of the mixture at the center of the bulb. Any grains larger than those still suspended between the water surface and the center of the bulb have already passed this zone. The procedure for analyzing the data is given by Bowles (1986). This length ( $L$ ) increases during the hydrometer test and for the hydrometer used is related to the raw reading ( $R$ ) as:

$$L = 16.5 - 0.1641R \quad (3.17)$$

The hydrometer reading is corrected for temperature and to zero as:

$$R_c = R_{actual} - \text{zero correction} + C_T \quad (3.18)$$

Assuming grains to have a density of  $2.65 \text{ gm/cm}^3$  and also to be spherical, the percent finer is computed as:

$$\text{Percent Finer} = \frac{R_c}{W_s} 100 \quad (3.19)$$

The diameter for which the reading at time  $t$  is taken is calculated as:

$$D = K \sqrt{\frac{L}{t}} \quad (3.20)$$

where  $K$  is a function of temperature, grain density, and dynamic viscosity.

### 3.8.3 Sample Classification

In order to compare the grain size distribution of these samples to similar samples, they were classified using the Unified Soil Classification system. This system was developed in the 1940's, subsequently adopted by the U.S. Corps of Engineers and is used

widely in the United States. The basic designations of this classification system are (Bowles, 1986):

- coarse-grained, if more than 30% is retained above the #200 sieve
- coarse-grained material is divided into:
  - gravel if more than 50% of the coarse-grained fraction is retained on the #4 sieve
  - sand if more the 50% of the coarse-grained fraction passes the #4 sieve
- fine-grained material is distinguished as silt (M), clay (C), or organic (O)

The full classification is presented in Table 3.4.

Major divisions		Group symbol	Typical names	Classification criteria for coarse-grained soils		
Coarse-grained soils (more than half of material is larger than No. 200)	Gravels (more than half of coarse fraction is larger than No. 4 sieve size)	GW	Well-graded gravels, gravel-sand mixtures, little or no fines	$C_U = D_{60}/D_{10} > 4$ $C_C = 1 < D_{30}^2/D_{10} \times D_{60} < 3$		
		GP	Poorly graded gravels, gravel-sand mixtures, little or no fines	Not meeting all gradation requirements for GW		
		GM	s.i.a.	Silty gravels, gravel-sand-silt mixtures	Atterberg limits below A line or $I_p < 4$	Above A line with $4 < I_p < 7$ are borderline cases requiring use of dual symbols
		GC		Clayey gravels, gravel-sand-clay mixtures	Atterberg limits above A line with $I_p > 7$	
	Sands (more than half of coarse fraction is smaller than No. 4 sieve size)	Clean sands (little or no fines)	SW	Well-graded sands, gravelly sands, little or no fines	$C_U = D_{60}/D_{10} > 6$ $C_C = 1 < D_{30}^2/D_{10} \times D_{60} < 3$	
			SP	Poorly graded sands, gravelly sands, little or no fines	Not meeting all gradation requirements for SW	
		SM	s.i.a.	Silty sands, sand-silt mixtures	Atterberg limits below A line or $I_p < 4$	Limits plotting in hatched zone with $4 \leq I_p \leq 7$ are borderline cases requiring use of dual symbols
		SC		Clayey sands, sand-clay mixtures	Atterberg limits above A line with $I_p > 7$	
Fine-grained soils (more than half of material is smaller than No. 200)	Sils and clays (liquid limit $< 50$ )	ML	Inorganic silts and very fine sands, rock flour, silty or clayey fine sands, or clayey silts with slight plasticity	<ol style="list-style-type: none"> <li>Determine percentages of sand and gravel from grain-size curve.</li> <li>Depending on percentages of fines (fraction smaller than 200 sieve size), coarse-grained soils are classified as follows: Less than 5%—GW, GP, SW, SP More than 12%—GM, GC, SM, SC 5 to 12%—Borderline cases requiring dual symbols</li> </ol>		
		CL	Inorganic clays of low to medium plasticity, gravelly clays, sandy clays, silty clays, lean clays			
		OL	Organic silts and organic silty clays of low plasticity			
	Sils and clays (liquid limit $> 50$ )	MH	Inorganic silts, micaceous or diatomaceous fine sandy or silty soils, elastic silts			
		CH	Inorganic clays of high plasticity, fat clays			
		OH	Organic clays of medium to high plasticity, organic silts			
	Highly organic soils	Pt	Peat and other highly organic soils			

Table 3.4 Unified Soil Classification (Bowles, 1986).

## Section 4. DATA ANALYSIS

The purpose of this section is twofold; first, the data which was collected using the methods outlined in sections above are presented and general trends are discussed; second, the data are combined to estimate stream/aquifer interactions. These results are discussed to provide insight into the stream/aquifer interactions of this field site.

### 4.1 Precipitation

The period of record for the precipitation gage is March 1983 to present. The total monthly precipitation for this period is presented in Table 4.1, along with the average monthly and total annual computed values. The total monthly values are presented in Figure 4.1, along with the average monthly computed values; the values for the period of study are highlighted. The daily values for the period March 1983 to August 1992 are tabulated in Appendix B. Precipitation is well distributed throughout the year, with the summer months (May through October) receiving 56% of the average total annual precipitation and the remaining months receiving 44%. Analysis of this data suggests that while some months during the period of study were abnormally wet (March and August), 1992 was a drier year than average. For the first eight months of 1992 the study area received 15.64 inches of precipitation which is 7% lower than the average of 16.81 inches. For the same period in 1991, the study area received 18.84 inches, which may be why the stream was observed to be flowing as late as August, 1991, when it was not flowing in the same month in 1992. This suggests that the groundwater system is recharged from precipitation during the winter and spring, and discharges water to the stream throughout the winter, spring, and summer months. As more data become available, a correlation between the amount of precipitation and the last date of streamflow may become apparent. The expected precipitation events occurred but without the intensity of previous years.

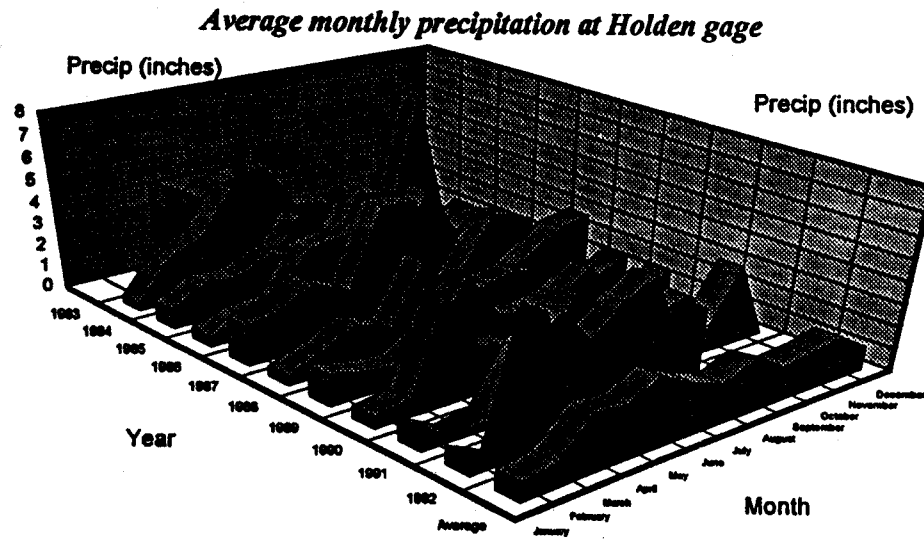


Figure 4.1 Precipitation summary for field area.

**Table 4.1 Precipitation summary for field site**

Total monthly precipitation in inches

Year	Jan	Feb	Mar	Apr	May	Jun	Jul	Aug	Sep	Oct	Nov	Dec	Ann
1983			4.32	3.52	4.12	4.30	2.19	1.85	0.45	0.15	5.07	1.45	27.42
1984	0.30	2.10	2.70	4.66	0.66	2.69	0.67	3.23	1.59	7.01	0.18	1.10	26.89
1985	0.89	1.70	1.65	2.32	1.66	1.83	2.28	0.77	3.55	1.16	1.75	0.60	20.16
1986	0.47	1.00	1.13	3.28	3.47	2.45	0.93	1.66	0.60	2.69	2.26	0.80	20.74
1987	1.80	2.08	2.86	2.11	5.55	5.38	0.43	2.55	0.76	1.54	2.41	2.65	30.12
1988	0.44	1.08	1.89	1.22	3.86	1.43	1.99	2.26	1.61	0.20	0.77	1.45	18.20
1989	1.45	1.09	0.95	1.85	3.91	1.86	1.50	1.81	2.73	0.84	0.57	1.37	19.93
1990	0.56	0.76	4.81	2.15	1.88	0.28	3.26	1.69	2.09	0.98	1.40	0.28	20.14
1991	1.06	0.17	0.37	2.87	4.06	2.40	3.60	4.31	0.94	1.07	3.55	0.10	24.50
1992	0.87	0.07	5.76	0.58	2.31	1.01	1.30	3.74					15.64
Avg.	0.87	1.12	2.64	2.46	3.15	2.36	1.82	2.39	1.59	1.74	2.00	1.09	23.12

The typically high period of precipitation in March occurred as three different storms over a week, with about 1.5 inches precipitation each. This was sufficient to initiate the spring runoff event. The typical long-duration low-intensity spring precipitation event did not occur until the end of May and was only appreciable enough to bring the total monthly precipitation up to 73% of average. Another long-duration low-intensity precipitation event occurred near the end of August, pushing August's total precipitation to 56% above average. However, the stream had been dry well over a month by this time, no streamflow was observed, and only one piezometer rewetted.

## 4.2 Water Levels

During the period of this study, water levels in the piezometers and stream were monitored intermittently. At each piezometer, both the depth to water in the piezometer and to the stream surface were recorded from the piezometer collar. These distances were then subtracted from the absolute elevations of the piezometer collar to obtain the absolute elevations of the piezometric surface at each level of the piezometer nests. The stream water surface elevation was taken as the average of the values obtained from each of the piezometers at a given piezometer nest. There were 60 measurements of these water levels recorded over a six-month period in 1992, starting at the end of February and ending at the beginning of September. The data are plotted as a function of time in Figure 4.2 and are included in tabular form in Appendix C.

A number of problems with the piezometers became apparent as the study progressed causing the data from some of the piezometers to be questionable. First, the piezometer nest located at station 7+80 went dry early in the study, even though the stream was flowing and the other piezometers held water. The 1-foot piezometer rewetted a number of times after that, but the data will not be used because they are questionable. This could be a natural phenomenon that is being observed, but this hypothesis could not be confirmed. The second, more critical, problem was encountered when the slug tests were performed in June. The slug test procedure was to fill the piezometer with water and monitor the decline as the water drained from the tube. Unfortunately, a number of the piezometers either did not drain or drained extremely

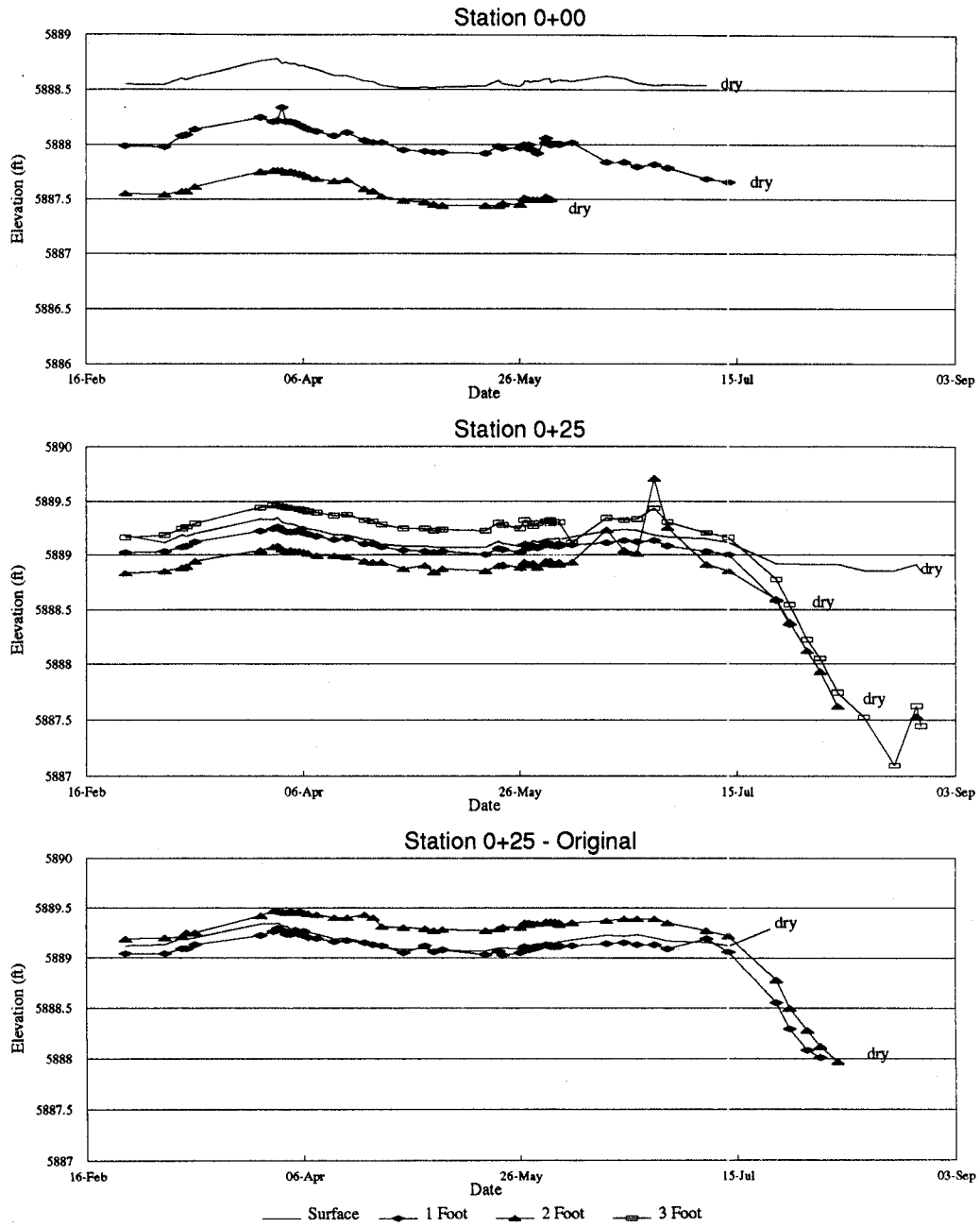


Figure 4.2 Water levels in piezometers for period of study.



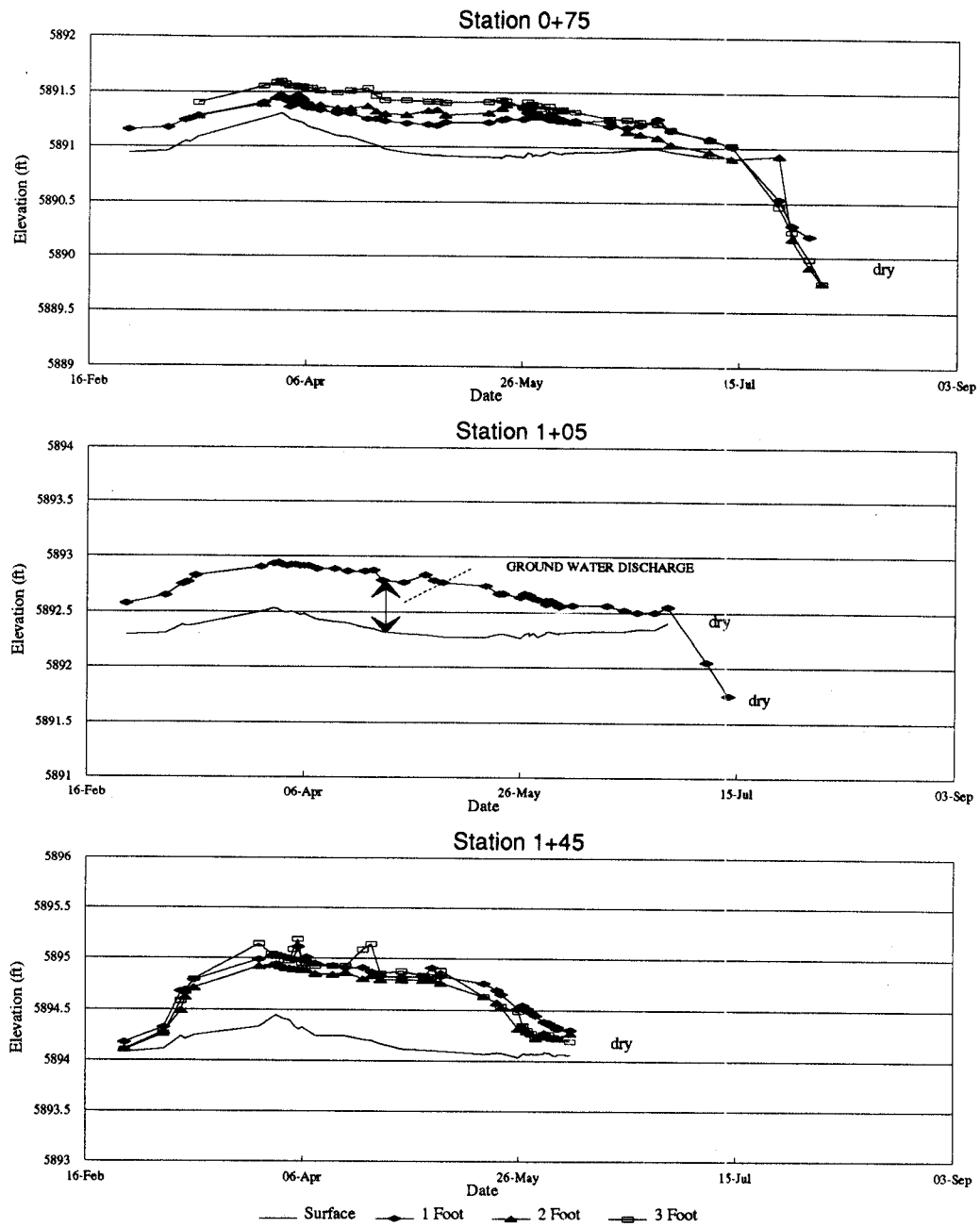


Figure 4.2 (cont.) Water levels in piezometers for period of study.

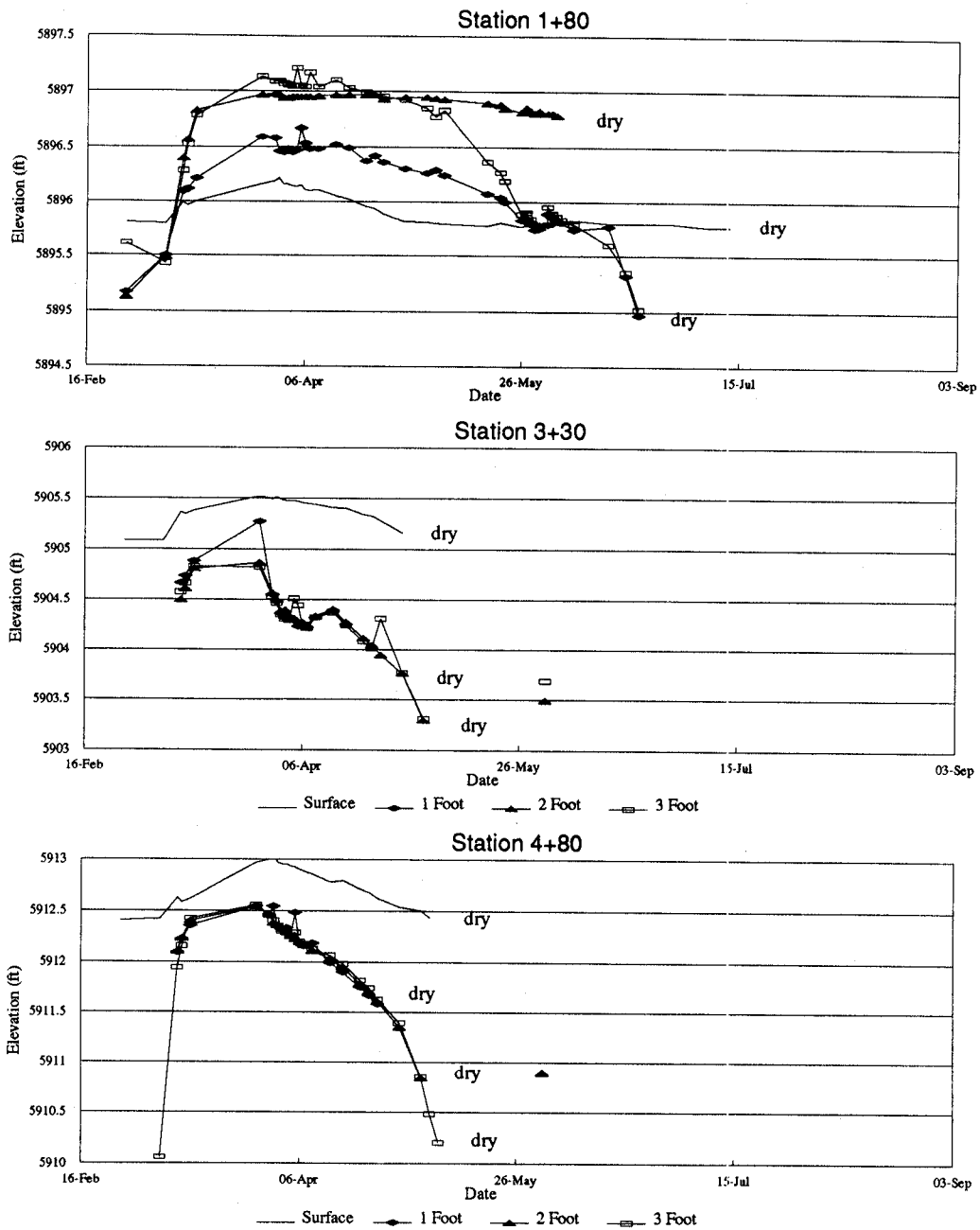


Figure 4.2 (cont.) Water levels in piezometers for period of study.

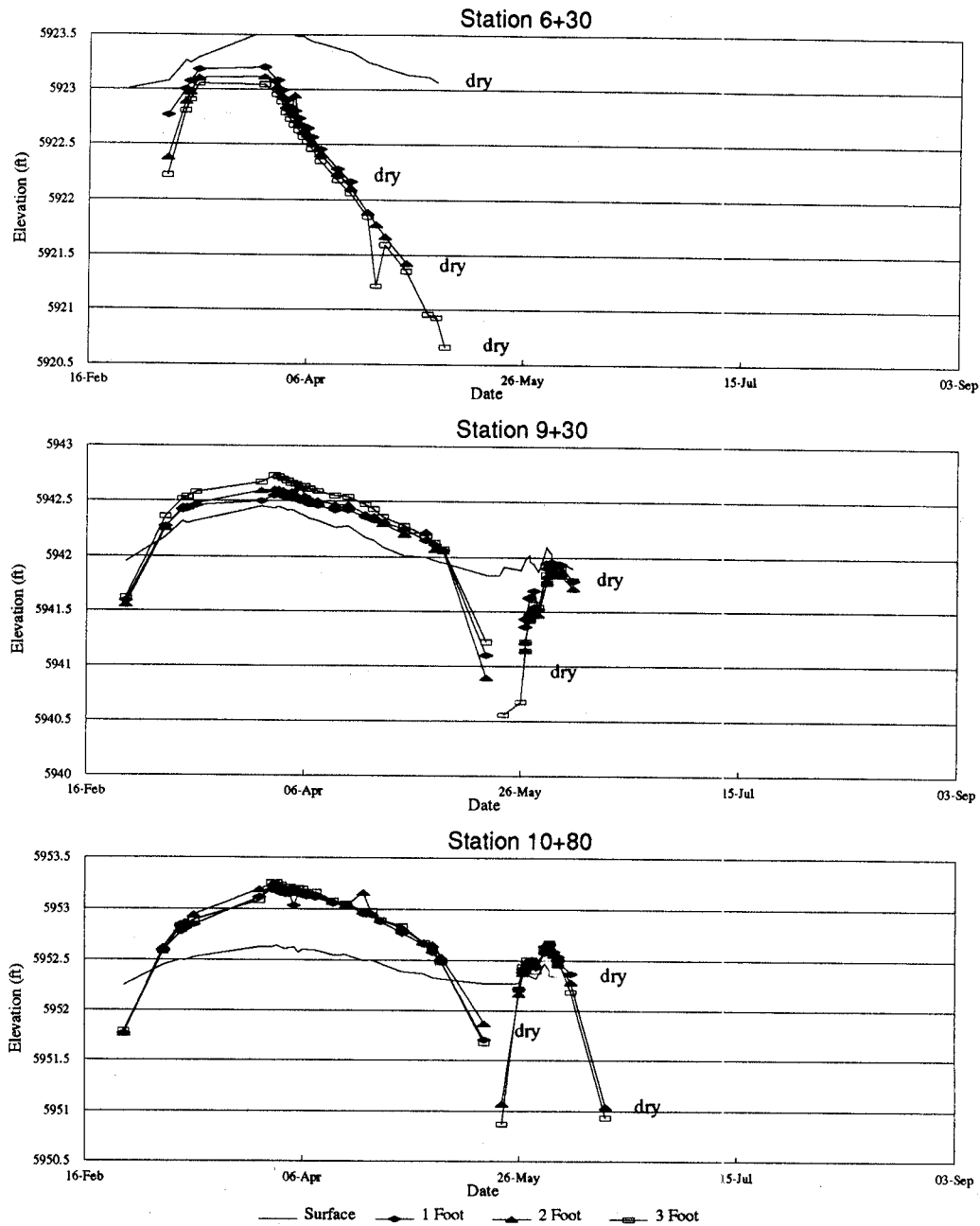


Figure 4.2 (cont.) Water levels in piezometers for period of study.

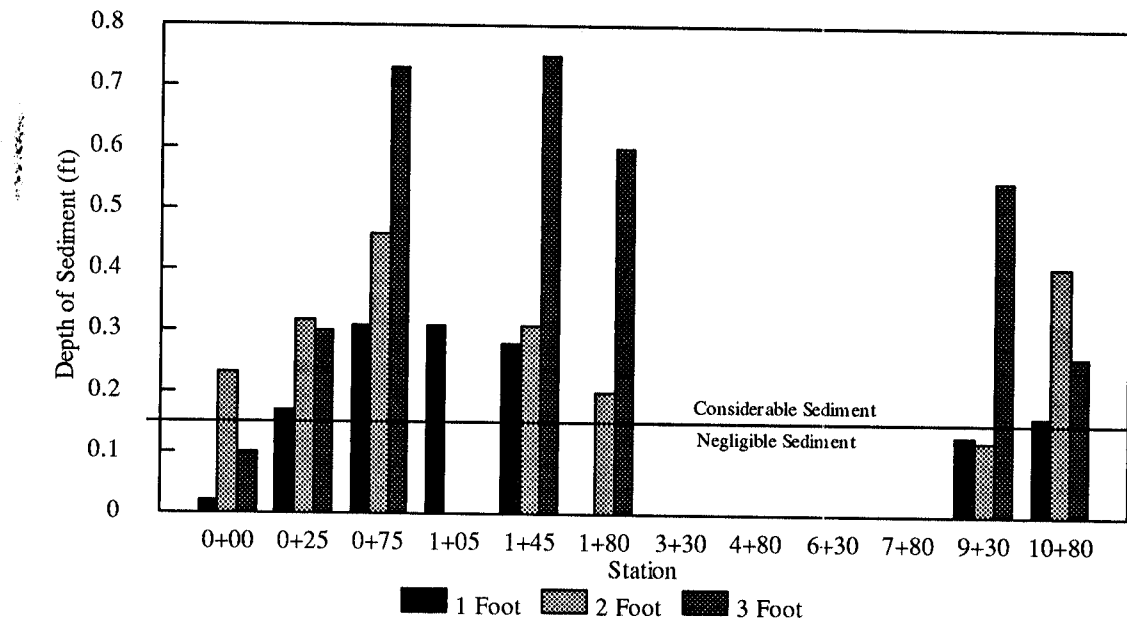


Figure 4.3 Depth of sediment in piezometers.

slowly. The reason for this was that some of the piezometers were plugged with fine-grained material. Later, the amount of sediment in each piezometer tube was determined by measuring the maximum depth inside each tube and subtracting it from the depth to the centerline of the screen holes. This information is presented in Figure 4.3. The ramifications of sediment in the piezometers are threefold: first, hydraulic conductivity values obtained from slug tests conducted in the piezometers are not reliable; second, water levels obtained in some of the piezometers could be inaccurate due to the plugging; and third, water levels obtained are questionable due to the possible slow response time of the piezometer.

While the amount of sediment in each piezometer is known, the nature of the sediment is not known. This makes determination of a critical amount of sediment difficult. The more important factor is the lag time in water-level response in the piezometer caused by the sediment in the bottom. Table 4.2 shows the thickness of sediment in each piezometer, along with the average amount of time required for the

**Table 4.2 Water level drop time and thickness of sediment in piezometers**

Station	1 Foot	2 Foot	3 Foot
0+00	0.02 feet 5.5 minutes	0.23 471	0.10 N/C
0+25	0.17 335	0.32 1693	0.30 728
0+75	0.31 904	0.46 414	0.73 139
1+05	0.31 1560		
1+45	0.28 8581	0.31 8518	0.75 12717
1+80	0 8.1	0.20 N/C	0.60 30
3+30	0 N/T	0 N/T	0 N/T
4+80	0 N/T	0 N/T	0 N/T
6+30	0 N/T	0 N/T	0 N/T
7+80	0 N/T	0 N/T	0 N/T
9+30	0.13 2.2	0.12 17	0.55 3789
10+80	0.16 N/T	0.41 2625	0.26 15

N/T = no slug test performed in piezometer.

increased head level during the slug test to drop one foot. The range of times are from 5.5 minutes in the station 0+00 1-foot piezometer to 8.8 days in the station 1+45 3-foot piezometer, with a mean response of 1.6 days and a median of 600 minutes (0.4 days). These data are plotted in Figure 4.4, where no relationship is apparent. Using this analysis it can be seen that the response time in a number of piezometers is prohibitive. With an arbitrary cutoff of 1,440 minutes (1 day) the following seven piezometers should be suspected as having exceedingly long response times for the purposes of this study:

- station 0+25 2-foot piezometer,
- station 1+05 1-foot piezometer,
- station 1+45 1-foot piezometer,

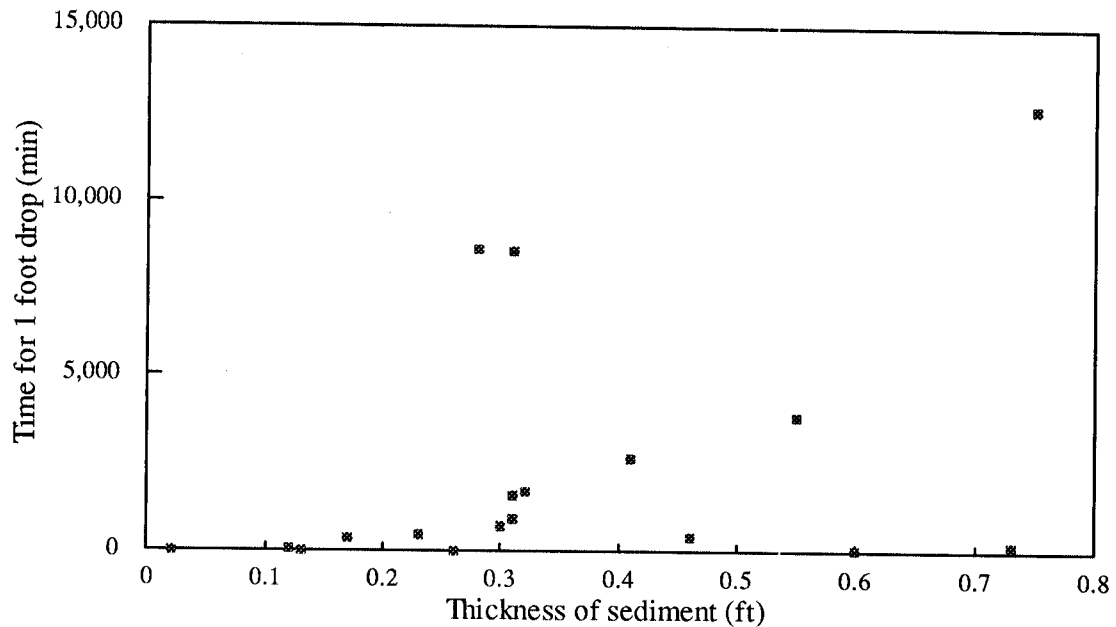


Figure 4.4 Rate of water level decline as a function of sediment thickness.

station 1+45 2-foot piezometer,  
 station 1+45 3-foot piezometer,  
 station 9+30 3-foot piezometer, and  
 station 10+80 2-foot piezometer.

It is suggested that the piezometer design be modified by future users to prevent fine sediment material from entering the piezometer. A possible alternative would be to insert a piece of fine steel wool into the piezometer tube next to the holes. The steel wool would have to be finer than the sediment material but coarse enough that it does not inhibit water from entering or exiting the piezometer tube.

The response time of the system to precipitation was determined to be on the order of days as illustrated by two stress periods. The first period followed the initiation of the spring runoff event at the end of March. During an eight-day period water levels were

monitored on a daily basis to determine the rate and magnitude of water level rise. During that eight-day period water levels in the stream and piezometers rose an average of 0.15 feet. The second stress period was a low intensity, but long duration precipitation event at the end of May and beginning of June. During this eight-day period the water levels were measured twice on some days, yielding a total of 13 measurements during the period. The water levels rose an average of 0.1 feet, less than they rose during the previous intensive measuring period, with little response seen in some piezometers. The infrequency of the remaining measurements are justified because of the slow response time observed during these two periods. Water level response to changes in stream stage appears to be immediate as illustrated by the water levels closely following the stream stage (Figure 4.2).

The magnitude of the change in water levels is generally the same for all piezometers. The duration that the piezometers contain water varies from location to location. There are two groundwater discharge zones which can be identified from this data: the first is located at the upstream end of the study area between piezometer nests at stations 9+30 and 10+80; the next discharge zone is located at the downstream end of the study area, between the station 0+25 and 1+80 locations. Figure 4.5 shows when the stream is flowing and when the piezometers go dry, the light shading showing the periods of stream flow and the circles and dark lines showing when individual piezometers and entire piezometer nests go dry, respectively. The piezometers at the upper discharge zone do not go dry for six weeks after the end of the spring runoff event. While the water levels decline somewhat rapidly, they rebound with the two precipitation events at the end of May and beginning of June. They go dry about three weeks after the second event, indicating that the water table in that area is responsive to precipitation events and drops quickly when recharge is not sustained. The lower recharge zone exhibited a much greater longevity. This zone discharged water for five weeks after the last major precipitation event, with the piezometers going completely dry over six weeks later.

The intervening piezometers between the discharge zones always indicate a losing stream and are only wet for a fraction of the monitoring period. This suggests that the water table in that area is well below the surface for most of the year. Water is present in the piezometers at stations 3+30, 4+80, and 6+30 for a short period in March and April

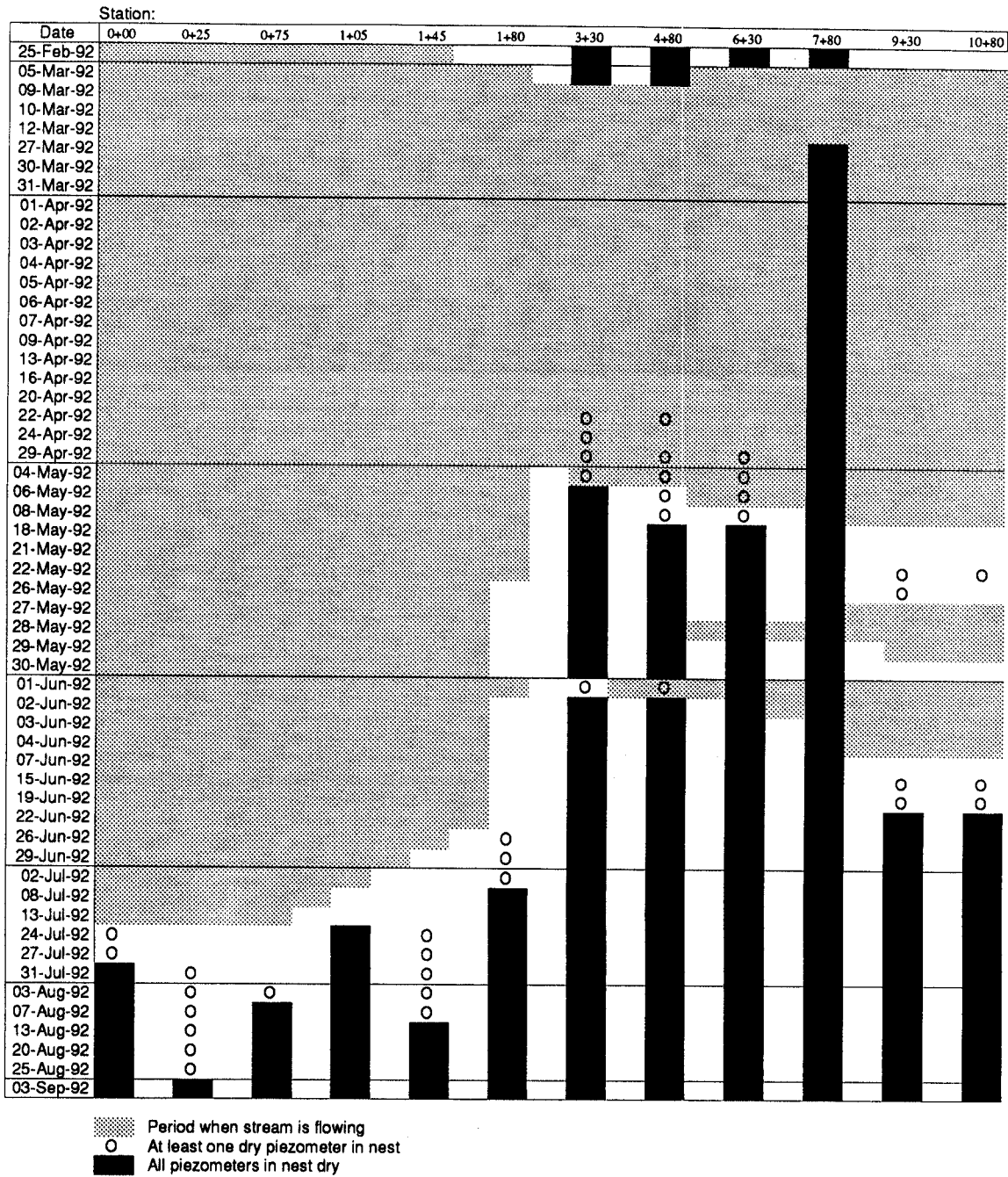


Figure 4.5 Dates of streamflow and piezometers drying up.



due to the spring runoff event. This could be due to two mechanisms, either from the water table, normally deeper than the piezometer tubes, rising with the increased recharge from the spring runoff event; or alternatively could be due to a wetting front descending from the stream bottom to the water table. Because the latter mechanism would cause pressures less than atmospheric in the subsurface, the piezometers would be dry and so this mechanism can be discounted. These piezometers went dry shortly after the stream went dry.

### 4.3 Gradients

Shallow groundwater head gradients were calculated using the water-level data gathered and the depth of the screen of each piezometer. Gradients were calculated as the head difference between any two consecutive piezometers divided by the thickness of porous medium between the screened intervals. Gradients are shown as a function of time in Figure 4.6. The graphs are all plotted at the same scale so that they can be compared easily. This information is also presented on Plate 1 which shows the longitudinal cross-section of the stream with the piezometer locations relative to topography. Calculated gradients are tabulated in Appendix D. The gradients generally have a magnitude between zero and one, with some piezometers having gradients greater than one. Using the hydraulic conductivities of the subsurface material and average grain size diameters obtained from the grain size distribution analysis indicates that the Reynolds numbers are much less than 1 and the flow is laminar. Piezometers with large gradients do not correspond to those that indicated large lag times. It appears that, while the presence of sediment in piezometers affects the water-level response time, it does not affect the magnitude of response. Thus, the gradients may not be reflective of the aquifer conditions on the day on which they were measured but of some previous time. This is a limitation of the data which have been obtained.

The gradients indicate the presence of two groundwater discharge zones. From Plate 1 it can be seen that these discharge zones generally coincide with areas where there

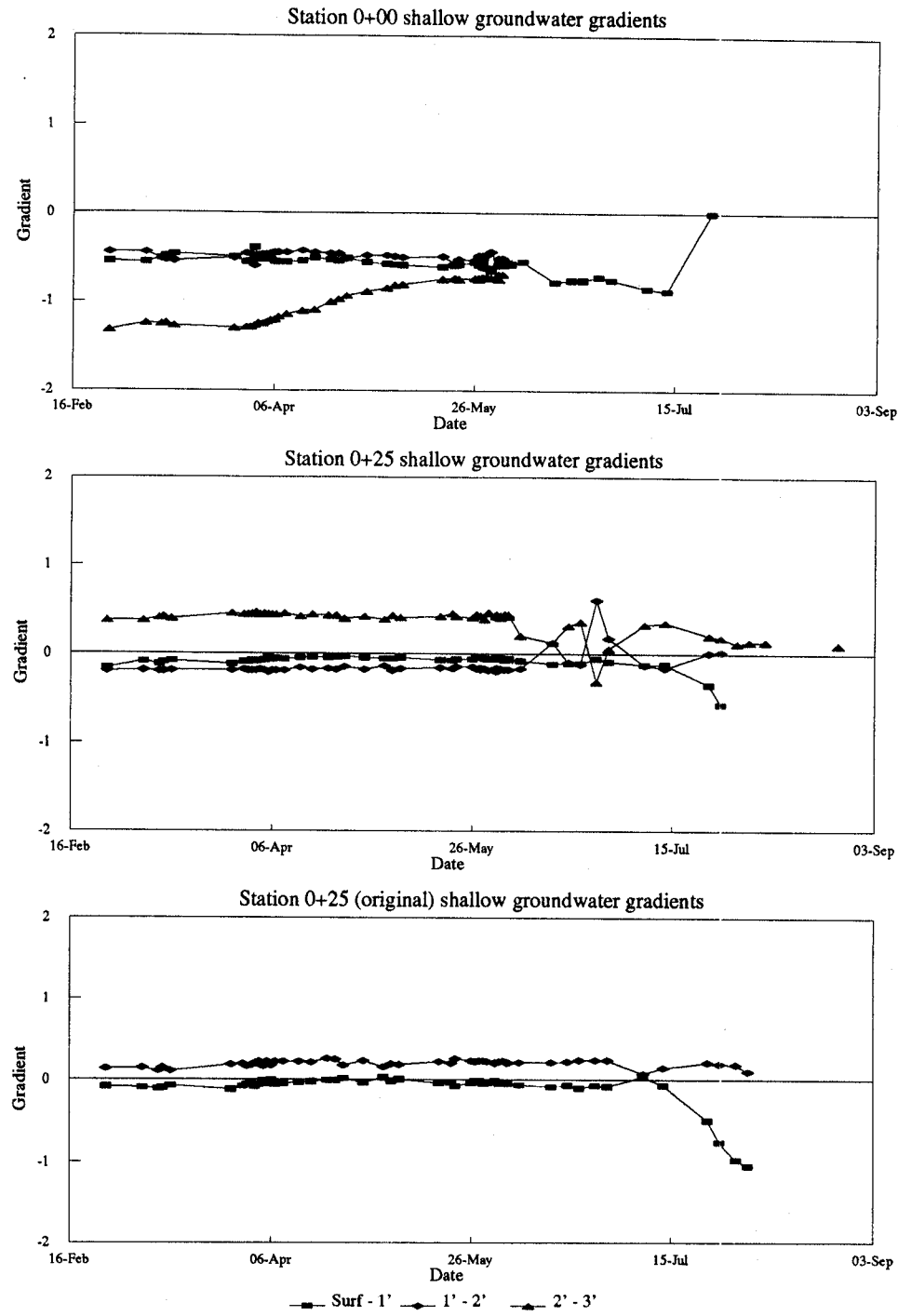


Figure 4.6 Shallow groundwater gradients between piezometers.

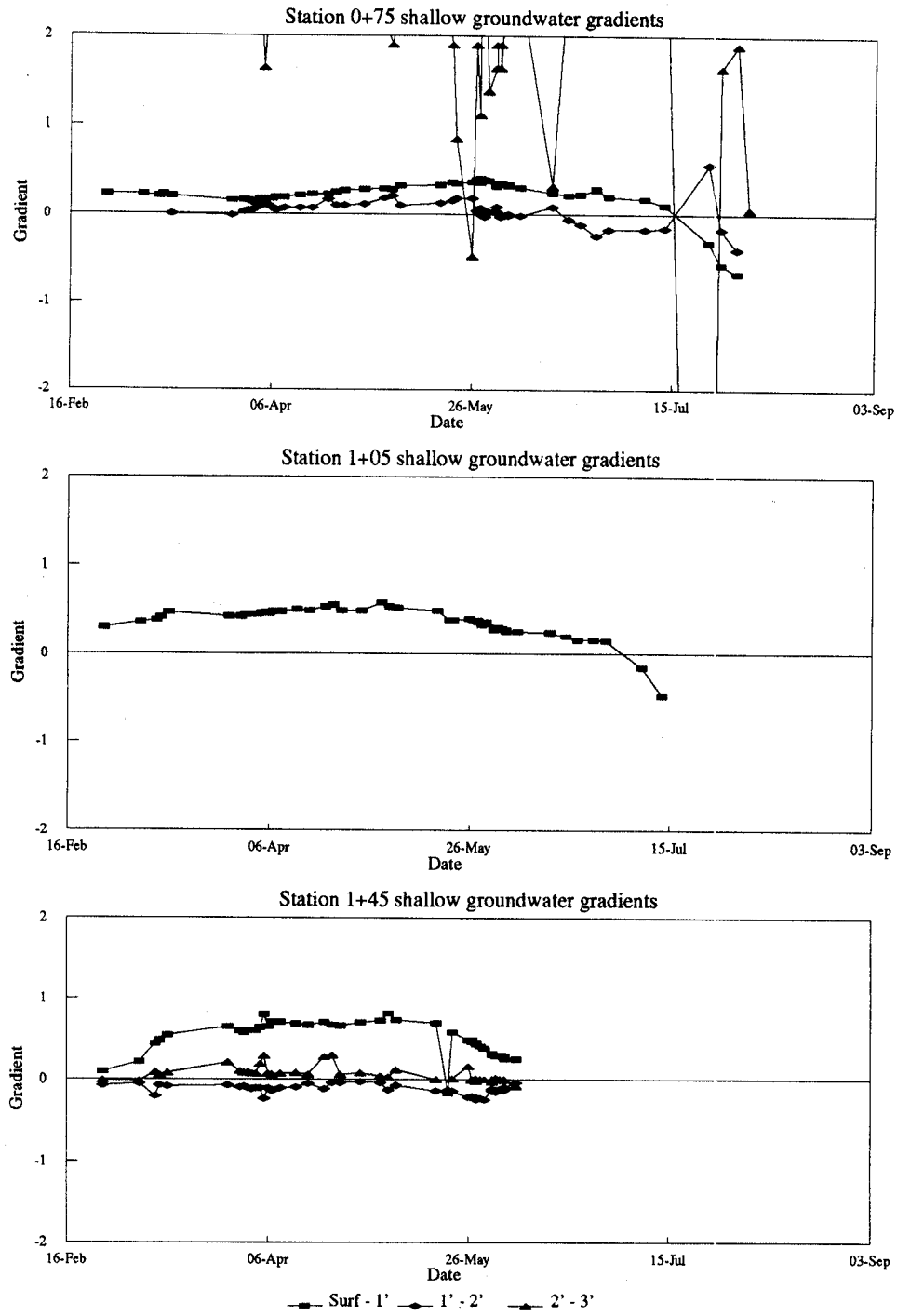


Figure 4.6 (cont.) Shallow groundwater gradients between piezometers.

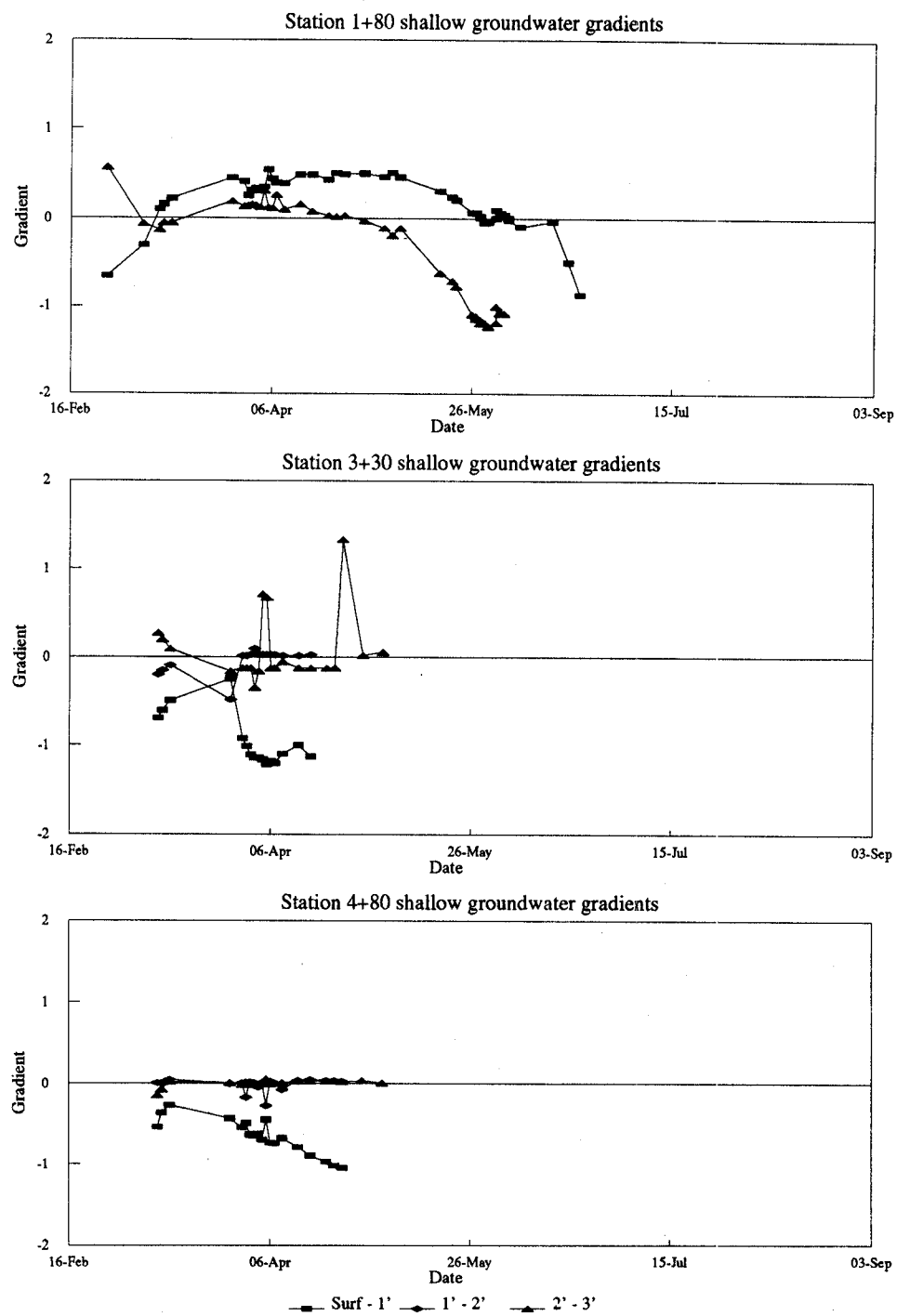


Figure 4.6 (cont.) Shallow groundwater gradients between piezometers.

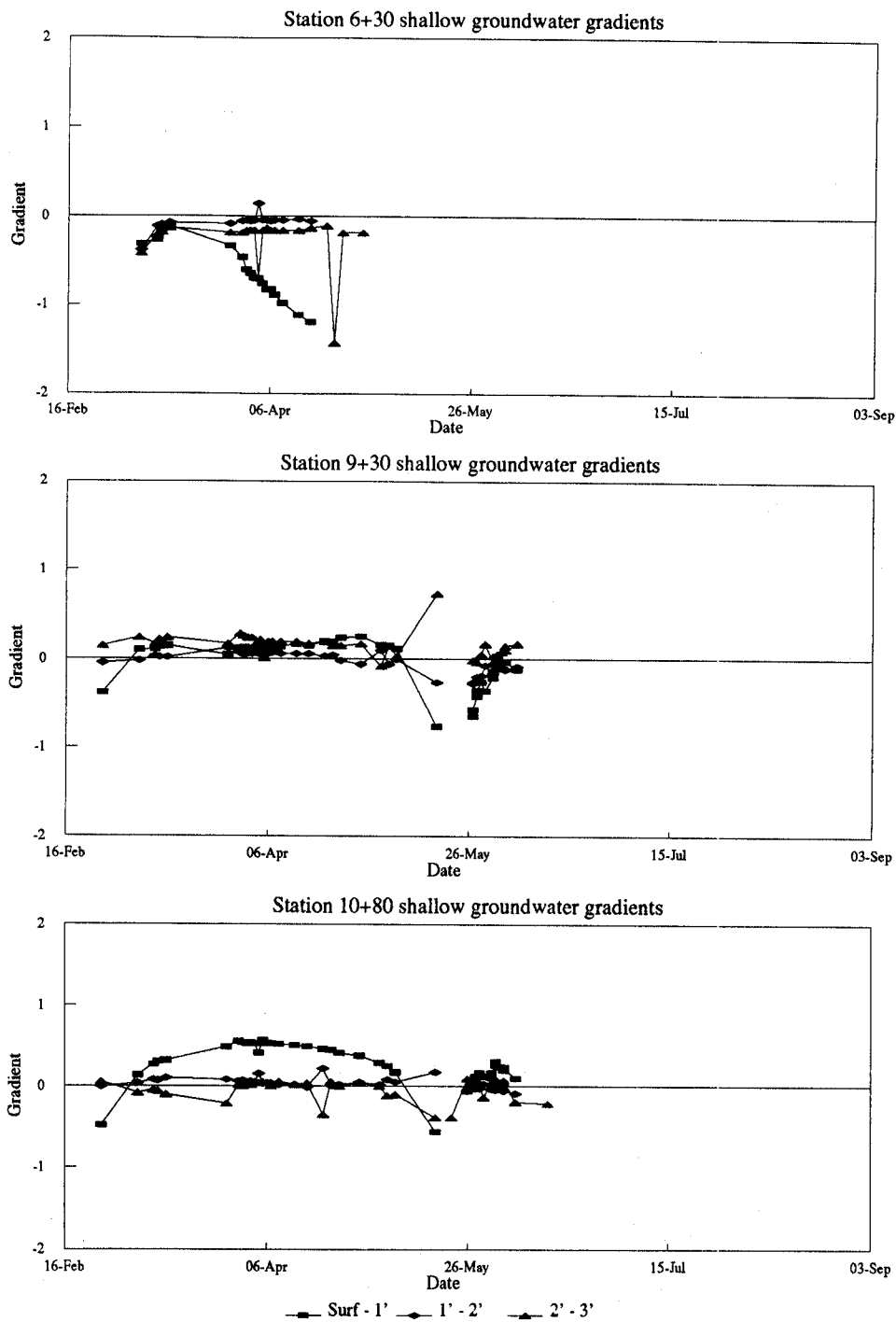


Figure 4.6 (cont.) Shallow groundwater gradients between piezometers.

is a sharp increase in the slope of the stream gradient. The break in slope at the upper discharge zone is greater than that of the lower discharge zone, suggesting that some other mechanism may be responsible for the longevity of the lower discharge zone. This could be caused by a low hydraulic conductivity heterogeneity in the subsurface. All three levels of gradients in the lower discharge zone are upward. The subsurface topography determined from shallow seismic refraction surveys (Bissett, unpublished) indicates that the thickness of alluvium is increasing in that area, so this is not a possible mechanism. A velocity reversal detected in the analysis of several of the lines in this survey indicate the presence of a hidden layer in the subsurface of unknown geometry. The velocity reversal can be attributed to a fine grained lens of material, or to a wetting front descending into the subsurface. While this has no effect on the calculation of the total thickness of alluvium down to bedrock, it does indicate the presence of some layer or process in the subsurface which would alter the groundwater flow system. This layer could isolate the shallow alluvial groundwater system associated with the stream from a deeper one below the clay layer. Without further subsurface information, the process causing this reversal cannot be identified.

#### **4.4 Streamflows**

As mentioned previously, because of the difficulties in obtaining accurate stream gaging data, this information was not available until the end of April for the weirs on the boundaries of the study area and later for the intermediate ones. By this time, the spring runoff event had declined to the extent that the flow was intermittent along the length of the stream within the study area. No flow was ever measured at weir 2 after it was installed. The most valuable data come from weir 1 at the downstream end of the study area. Because the piezometers in the lower 150 feet of the stream-reach studied went dry well after the stream went dry, the gradient data from the piezometers overlap with the streamflow information. The streamflow was measured on 25 different days, and is shown in Figure 4.7. At weir 1 the flow steadily declines except for a slight peak on June 1 during the long precipitation event. The data from weir 4 show a steady decline to a no-flow condition and followed by a resurgence of flow on several occasions. Flow at weir 3

behaves similar to flows at weir 4. Integrating the streamflow data from weir 1 after the end of the spring runoff period on April 29 to the end of flow on July 13 results in a total approximate discharge from groundwater of 5.7 acre-feet or 1.85 million gallons. This is equivalent to a depth of 0.16 inches over the entire 420 acre basin.

#### **4.5 Flow Velocity**

The velocity of water flowing in the stream was approximated at each piezometer nest on April 9 during the spring runoff event. The velocity was estimated by three times measuring the amount of time a tracer (twig) took to travel 10 feet. The average velocity at each location is presented in Figure 4.8. The velocity appears to be within a range of 1.5 to 2.5 feet per second (fps). Several trends can be noticed from this figure, progressing from upstream to downstream. The velocity at piezometer nests 10+80 and 9+30 are similar with a sharp increase downstream. The velocity gradually decreases until peaking again locally at piezometer 3+30. The velocity then increases until piezometer 0+75 and then shows a local minimum at piezometer 0+25. The range of velocities indicates that the stream is capable of transporting unconsolidated sediments up to 2 millimeters in diameter (Leet et al., 1982), the typical upper limit for sand grain size. If the sediments are consolidated, a velocity three times those observed would be needed before particles of any size could be eroded from the streambed. This indicates that the entire reach of stream in the study area is capable of transporting sand-size particles.

#### **4.6 Streambed Materials**

The streambed material types are shown in Figure 4.9 for the entire study area. The predominant characteristic is that the prevalent material type is highly variable with

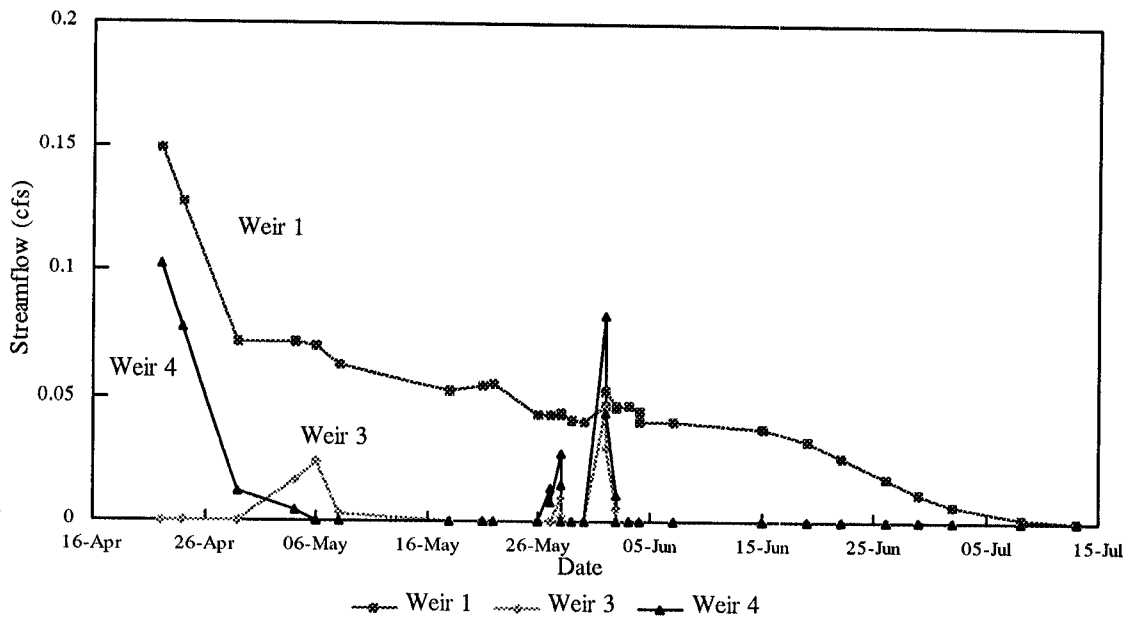


Figure 4.7 Streamflow measured at weirs.

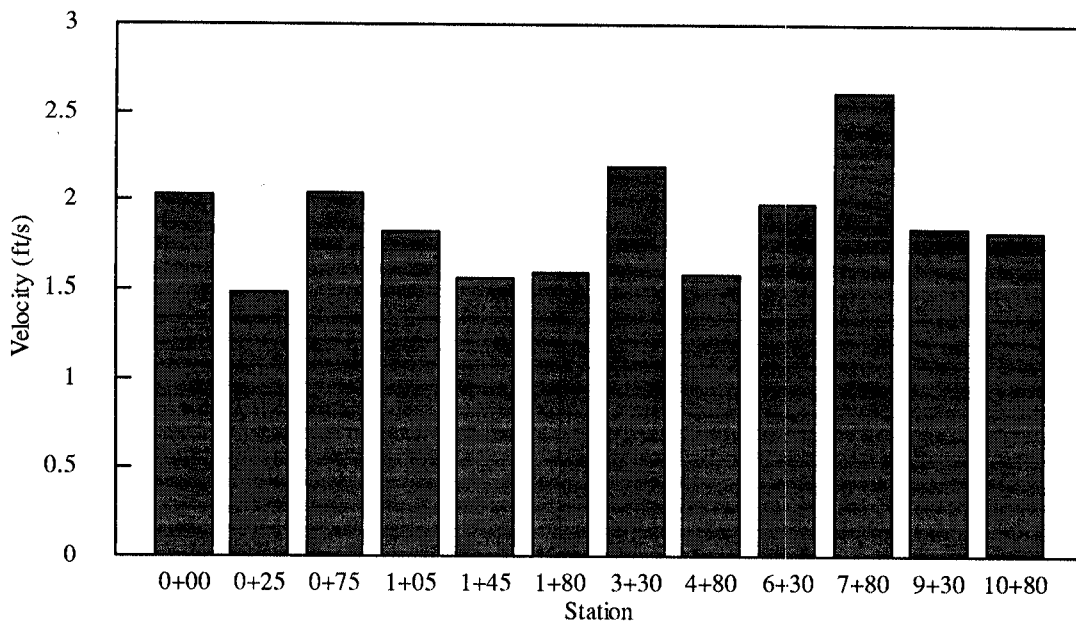


Figure 4.8 Streamflow velocities measured at piezometer locations.



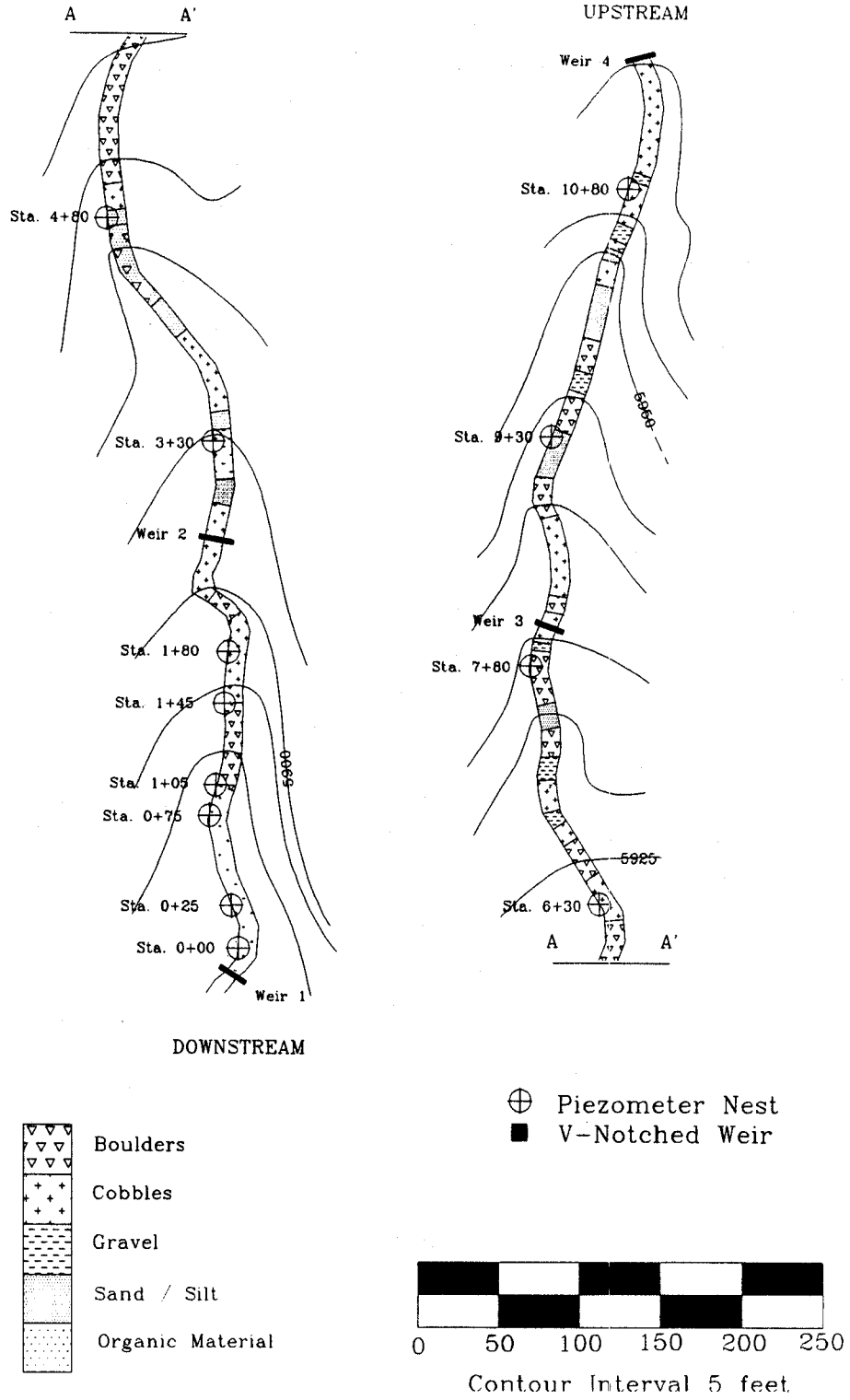


Figure 4.9 Streambed material type.

location along the stream. This has to do with the ripple and pool nature of the stream, as created by the steep stream gradient of 350 ft/mile. This effect can be seen on the map where the areas of cobbles are followed immediately by the areas where sand is deposited due to the decrease in velocity. Throughout the study reach, larger grain sizes predominate, with 81% of the length of the reach having a grain size larger than sand, 77% larger than gravel, and 36% larger than cobbles. This is not unusual because the Piney Creek alluvium is described as having predominant cobbles closer to the mountains. The study area is less than half a mile from the foothills of the Front Range and consequently the occurrence of large cobbles in the streambed is expected. It is important to note that the sediment is well sorted with the smallest grain size in the sand range, thus the Piney Creek alluvium is mapped as having a medium relative hydraulic conductivity (Scott, 1972b).

#### **4.7 Slug Tests**

##### **4.7.1 Piezometer Slug Tests**

The results from the Bouwer and Rice slug test analyses for the piezometers tested are presented in Table 4.3. Without discussing the results, it is sufficient to say that due to the presence of fine-grained material in the piezometers, as discussed in Section 4.1, the results of the slug tests are questionable for many of the piezometers. When the piezometer nest at station 1+80 was removed to conduct the air permeameter analysis, slug tests were conducted in the laboratory to compare with the field measurements. The tubes were placed in a five-gallon bucket full of water to provide some resistance to flow out of the piezometer; then filled with water and the decline in head was observed over time. The 1-foot piezometer tube would not hold any water due to the lack of any sediment within it, so the slug test conducted on it in the field should be accurate. The 2-foot piezometer tube drained over a period of approximately 36 hours, reinforcing the fact that it would not drain when in situ. The 3-foot piezometer drained over a period of 90

Table 4.3 Hydraulic conductivities from slug tests.

		Hydraulic Conductivities in ft/s													
		DOWNSTREAM										UPSTREAM			
		0+00	0+25	0+55	0+75	0+85	1+05	1+45	1+80	3+30	4+80	6+30	7+80	9+30	10+80
Surface	Test #1	2.2E-06	5.7E-06	1.0E-05	1.3E-05	2.8E-06	8.6E-05	9.8E-05	*	*	*	*	*	*	*
	Sigma	1.2E-04	1.1E-04	1.9E-04	1.5E-04	8.8E-05	7.3E-05	3.8E-04							
	R-Squared	0.989	0.999	0.985	0.997	0.998	0.999	0.992							
Surface	Test #2						7.7E-05	1.6E-04							
	Sigma						1.5E-04	1.0E-03							
	R-Squared						0.999	0.983							
Average		2.2E-06	5.7E-06	1.0E-05	1.3E-05	2.8E-06	8.2E-05	1.3E-04							
1 Foot	Test #1	2.3E-06	4.9E-08	N/I	3.9E-08		1.7E-08		2.3E-06	*	*	*	*	5.3E-06	*
	Sigma	1.6E-03	6.9E-04		2.1E-03		4.4E-04		6.5E-04					4.8E-04	
	R-Squared	0.977	0.995		0.939		0.997		0.993					0.998	
1 Foot	Test #2	1.8E-06	1.1E-07		4.1E-08		1.8E-08	3.5E-09		*	*	*	*		
	Sigma	2.3E-04	1.1E-03		2.8E-03		9.4E-04	3.6E-04							
	R-Squared	0.999	0.990		0.922		0.980	0.981							
Average		2.0E-06	7.9E-08		4.0E-08		1.7E-08	3.5E-09	2.3E-06					5.3E-06	
2 Foot	Test #1	4.3E-08	1.0E-08	N/I	5.0E-08	N/I	N/I		N/A	*	*	*	*	3.7E-07	4.7E-09
	Sigma	7.8E-04	2.8E-04		9.5E-04									2.0E-03	
	R-Squared	0.996	0.998		0.992									0.976	
2 Foot	Test #2	1.3E-06	6.6E-07		3.5E-06			2.5E-07							
	Sigma	1.5E-01	6.2E-02		4.0E-02			1.0E-02							
	R-Squared	0.971	0.981		0.997			0.997							
Average		6.5E-07	3.4E-07		1.7E-06			2.5E-07						3.7E-07	4.7E-09
3 Foot	Test #1	N/A	2.7E-08	N/I	1.0E-07	N/I	N/I		4.8E-07	*	*	*	*	2.4E-09	4.7E-07
	Sigma		1.9E-03		1.7E-03				6.7E-04					3.6E-04	
	R-Squared		0.963		0.978				0.994					0.998	
3 Foot	Test #2		3.9E-08		8.4E-08			3.7E-09							
	Sigma		2.4E-03		1.8E-03			2.0E-04							
	R-Squared		0.958		0.991			0.990							
Average			3.3E-08		9.5E-08			3.7E-09	4.8E-07					2.4E-09	4.7E-07

Note: N/A = not hydraulically connected; N/I = no piezometer installed; \* = no test performed.

minutes, similar to the test in the field. Analysis of this test gives a hydraulic conductivity of  $1.9 \times 10^{-7}$  ft/s, as compared to  $4.8 \times 10^{-7}$  ft/s observed in the field. Figure 4.10 presents the drawdown data and hydraulic conductivity results of the two tests. The differences in the two results are attributable to the lab test being conducted in a five gallon bucket. The drawdown with respect to time for the two tests is almost identical, as shown in Table 4.4.

While the 2-foot piezometer contained less sediment it was relatively impermeable compared to the material in the 3-foot piezometer. The amount of material in the 2-foot and 3-foot piezometers was 0.20 and 0.60 feet, respectively. Visual inspection of the material shows that the material in both piezometers is fine-grained, sand size (1 mm) and smaller. Also a number of clumps were present in both piezometers indicating that the lower end of the grain size is most likely silt or clay. In either case, the tendency of the material to clump indicates that it could significantly impede the flow of water into or out

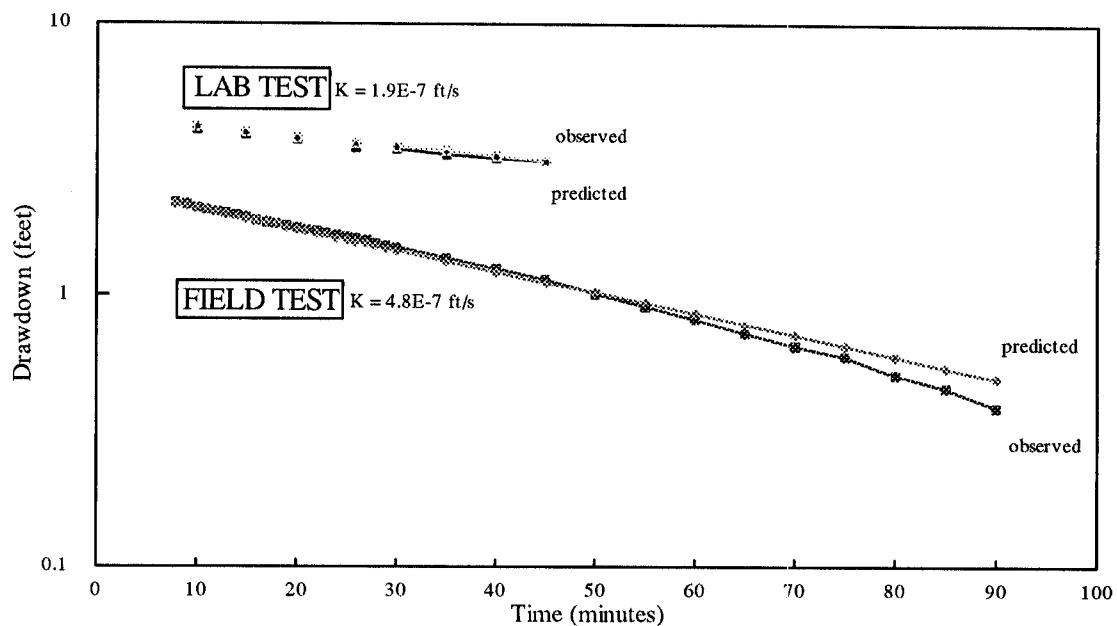


Figure 4.10 Results from the in-situ and lab slug tests.

**Table 4.4 Slug tests of station 1+80 3-foot piezometer**

Time	Field drawdown	Lab drawdown
10 minutes	0.40 feet	0.39 feet
15	0.57	0.56
20	0.73	0.72
26	0.90	0.93
30	1.01	1.03
35	1.13	1.16
40	1.26	1.27
45	1.37	1.35

of the piezometer. The visual nature of the material is the same for both piezometers, with the only difference the presence of iron oxide on the material from the 3-foot piezometer. The material could have been packed tighter in the 2-foot piezometer.

Extrapolating from the results exhibited, the presence of sediment in most of the piezometers in which slug tests were performed suggests that the results are indicative of the sediment and not the aquifer material. For this reason the results from the piezometer slug tests will not be used. It is important to note that the slug-test method is not in error here. Most of the slug tests were repeated on each piezometer, and analysis of the results indicates that the procedure produced very close results, generally within a factor of two. The high correlations obtained in the analyses indicate that the model used to interpret the data is valid. However, the large error variances obtained indicate that the results are very sensitive to errors in the data.

#### **4.7.2 Surface infiltration tests**

The results of the slug test analyses performed on the surface material at seven locations along the lower end of the stream are shown in Table 4.3. These results indicate that for the reach of stream analyzed the hydraulic conductivity of the streambed varies

between  $2.2 \times 10^{-6}$  and  $1.3 \times 10^{-4}$  ft/s. As with the piezometer slug tests the results are reproducible, the correlations are high, yet the error variances are also large. The two tests conducted at the 1+05 location were at two different locations while two tests were conducted at the same location at station 1+45. It appears that the hydraulic conductivities are clustered in two groups, one below and including the 0+85 test locations and the other including the two piezometer nests above it on which tests were conducted. Using a pooled t-test to determine whether the means of these two populations are equal shows that with a 5% level of significance they are statistically different. Because the material mapped downstream from station 1+05 is largely organic and upstream is fine-grained material, which has a lower hydraulic conductivity, this supports the occurrence of separate hydraulic conductivities.

#### 4.8 Grain Size Distribution

Results of the grain-size distribution analyses of surface sediments collected at the locations where the surface infiltration tests were conducted are presented graphically in Figure 4.11 and are tabulated in Appendix E. The samples collected are coarse-grained and moderately sorted as indicated by the range between  $D_{10}$  and  $D_{60}$  and the large coefficients of uniformity presented in Table 4.5. A large uniformity coefficient indicates that there is a wide range of grain sizes present and that the sample is poorly sorted (Fetter, 1988), while a high coefficient of gradation indicates that the distribution of materials is not even across all grain sizes. Thus, a material with a high uniformity coefficient and a low coefficient of gradation should have a lower hydraulic conductivity than a material with a low uniformity coefficient and a high coefficient of gradation. The Unified Soil Classification is also given for each sample. Most of the samples are poorly graded sands with some silt and well graded sands and gravels.

**Table 4.5 Grain size distribution of surface sediments**

	Station					1+05	1+05	1+15	1+45
	0+00	0+25	0+50	0+75	0+85	#1	#2		
D <sub>10</sub> (mm)	0.06	0.075	0.19	0.2	0.19	0.06	0.26	0.44	0.46
D <sub>30</sub> (mm)	0.16	0.26	0.48	0.45	0.48	0.2	0.5	3	1.9
D <sub>60</sub> (mm)	0.31	0.51	3.8	2.7	2.9	0.45	1.9	24	7.6
C <sub>u</sub>	5.2	6.8	20	13.5	15.3	7.5	7.3	54.5	16.5
C <sub>c</sub>	1.4	1.8	0.3	0.4	0.4	1.5	0.5	0.9	1
Unified Soil Classification	SM	SW-SM	SP	SP	SP	SW-SM	SP	GP	GW

G = Gravel, S = Sand, M = Silt, C = Clay

W = Well Graded, P = Poorly Graded.

#### 4.9 Air Permeameter

Hydraulic conductivity values calculated from the air permeameter measurements are presented in Table 4.6 and Figure 4.12. The shaded sections show the times required for the plunger to drop and the unshaded sections show the hydraulic conductivities calculated using the regression equation. The values presented in Table 4.6a and Figure 4.12a, obtained near stations 0+30 and 3+40, are the hydraulic conductivities at three-inch intervals across a traverse of the streambed at the indicated locations. The variation in hydraulic conductivity is small along both traverses perpendicular and parallel to the axis of the stream. Variation of hydraulic conductivity perpendicular to the streambed axis is small and the average hydraulic conductivity is equivalent for the four traverses. Using the pooled t-test with a 5% level of significance shows that the average hydraulic conductivities for the two sets of locations are not different. The stream environment of the two locations are very different, so it is interesting that the hydraulic conductivities are equivalent. The stream width and flow velocity of the downstream location are 33-39 inches and 1.5 feet per second, respectively, while at the upstream location 15-21 inches and 2.2 fps. This analysis shows that heterogeneities which may cause variation in

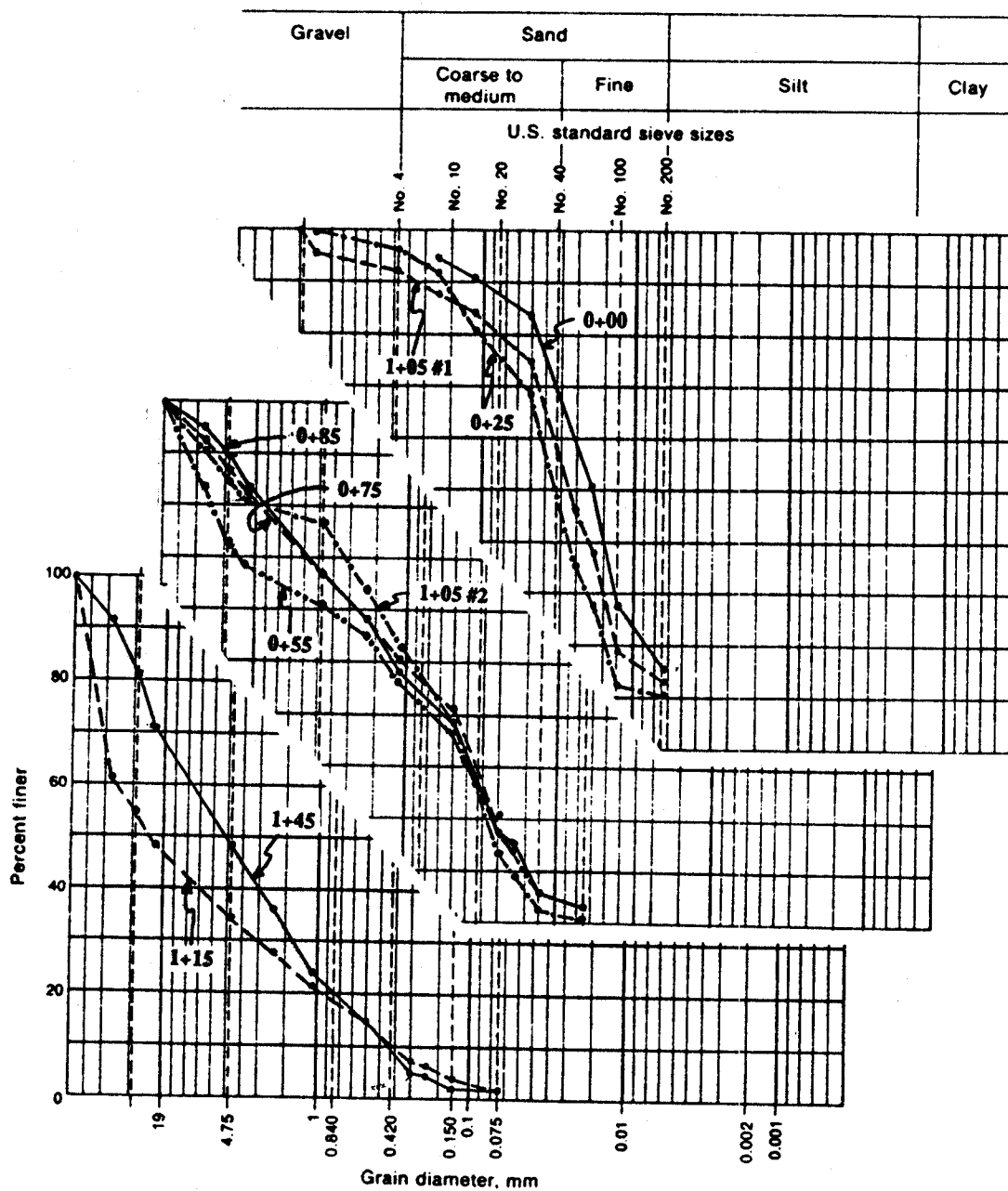


Figure 4.11 Results from grain size distribution analyses.



hydraulic conductivity of the streambed were not detected with the air permeameter. This data conflicts with the hydraulic conductivities measured using the surface infiltration test technique, and measurements at additional locations should be taken before a definitive statement is made.

The values presented in Table 4.6b and Figure 4.12b show the hydraulic conductivities measured using the air permeameter in a pit dug at station 1+80 where a piezometer nest was located. Slug tests were performed on the three piezometers at this location. Unfortunately the results do not compare well. The 1-foot piezometer, which contained no sediment, has a slug test hydraulic conductivity of  $2.3 \times 10^{-6}$  ft/s and an air permeameter hydraulic conductivity of  $6.3 \times 10^{-5}$  ft/s. The limitations and sensitivities of the two methods, as stated before, are probably responsible for this large discrepancy. The 3-foot piezometer slug test measured the hydraulic conductivity of the sediment in the piezometer, so it should not compare to the hydraulic conductivity determined with the air permeameter. Although the absolute value of hydraulic conductivity measured with the air permeameter may be incorrect, the distribution of relative values provide insight to the heterogeneity of the porous medium. The results from the air permeameter analysis show that there is some variation within the pit but it is within an order of magnitude. The average of all the readings is  $2.4 \times 10^{-4}$  ft/s with a standard deviation of  $1.2 \times 10^{-4}$  ft/s. Visual inspection of the pit did not reveal layering or other sorting of materials which would suggest a change in hydraulic conductivity. At this location the variation in hydraulic conductivity was not appreciable and no layering of the porous media was detected.

The values presented in Table 4.6c and Figure 4.12c shows the hydraulic conductivities measured at a pit located at station 3+80. The pit was located in an area where the stream gradient is shallow and so the streambed is wide with fine-grained material present. Streamflow velocity was not measured at this point so those data are not available. Layering was visually apparent at this location with approximately 12 inches of fine-grained sand and silt forming the streambed overlying the cobbly-sand alluvial aquifer material. Measurements were taken along two walls of the pit and the average hydraulic conductivities for each depth were calculated. From these data two populations are apparent with the boundary between 12 and 15 inches below the surface. The upper layer has an average hydraulic conductivity of  $1.7 \times 10^{-4}$  ft/s and the lower layer  $3.9 \times 10^{-4}$  ft/s.

Using a pooled t-test with a 5% level of significance supports the conclusion that the two mean hydraulic conductivities are statistically different.

The hydraulic conductivity obtained along four traverses across the stream using the air permeameter suggests that variability of the streambed hydraulic conductivity is small. This limited amount of data does not represent an unbiased sample of hydraulic conductivity of the streambed because the traverses were chosen so that the air permeameter would work at that location. More work should be done to establish the actual unbiased variability of streambed hydraulic conductivity before conclusions are drawn.

Table 4.6 Hydraulic conductivities from air permeameter.

Table 4.6a Streambed traverse at various locations

		0"	3"	6"	9"	12"	15"	18"	21"	24"	27"	30"	33"	36"	39"	Average	SDEV
Sta 0+29	Time(sec)		0.99	1.40	1.01	1.06	0.99	1.12	1.33	0.97	1.01	1.06	3.41				
	K(ft/s)		3.7E-04	2.5E-04	3.7E-04	3.5E-04	3.7E-04	3.3E-04	2.7E-04	3.8E-04	3.7E-04	3.5E-04	9.4E-05				3.2E-04
Sta 0+30	Time(sec)		2.10	1.06	1.18	1.17	1.22	1.02	1.00	0.97	1.08	2.00	0.97	1.64	1.53		
	K(ft/s)		1.6E-04	3.5E-04	3.1E-04	3.1E-04	3.0E-04	3.6E-04	3.7E-04	3.8E-04	3.4E-04	1.7E-04	3.8E-04	2.1E-04	2.3E-04		3.0E-04
Sat 3+40	Time(sec)		1.37	1.14	1.41	1.18	1.09	1.39	1.59	1.60							
	K(ft/s)		2.6E-04	3.2E-04	2.5E-04	3.1E-04	3.4E-04	2.6E-04	2.2E-04	2.2E-04							2.7E-04
Sta 3+41	Time(sec)		1.11	1.23	1.20	1.67	1.43										
	K(ft/s)		3.3E-04	2.9E-04	3.0E-04	2.1E-04	2.5E-04										2.8E-04

Table 4.6b Vertical section at station 1+80 piezometer set

Depth	Times (sec)						Hydraulic conductivity (ft/s)						Average	SDEV	
	1 Foot		2 Foot		3 Foot		1 Foot		2 Foot		3 Foot				
	U/S*	D/S	U/S	D/S	U/S	D/S	U/S	D/S	U/S	D/S	U/S	D/S			
3"			1.33	3.74		1.07					2.7E-04	8.5E-05	3.4E-04	2.3E-04	1.3E-04
6"					2.18	0.94					1.6E-04	4.0E-04		2.8E-04	1.7E-04
9"				1.05							3.5E-04			3.5E-04	
12"	4.86		1.07	1.06	1.49	0.95	6.3E-05		3.4E-04	3.5E-04	2.4E-04	3.9E-04		2.8E-04	1.3E-04
15"			2.66	1.13					1.2E-04	3.2E-04				2.2E-04	1.4E-04
18"			3.67	14.30					8.7E-05	1.9E-05				5.3E-05	4.8E-05
21"			12.13	1.77	3.34	1.85			2.3E-05	2.0E-04	9.7E-05	1.9E-04		1.3E-04	8.2E-05
24"			1.06	1.43	3.67	1.51			3.5E-04	2.5E-04	8.7E-05	2.3E-04		2.3E-04	1.1E-04
27"					1.11	1.25					3.3E-04	2.9E-04		3.1E-04	2.9E-05
30"					1.28	1.63					2.8E-04	2.1E-04		2.5E-04	4.8E-05
33"					0.95						3.9E-04			3.9E-04	
36"					1.07	1.25					3.4E-04	2.9E-04		3.2E-04	3.9E-05
Average	2.43		3.13	3.06	1.68	1.16	6.3E-05		2.0E-04	2.2E-04	2.4E-04	2.9E-04	All measurements:	2.4E-04	1.2E-04
SDEV			4.15	4.66	1.18	0.53			1.4E-04	1.3E-04	1.2E-04	7.9E-05		2.4E-04	1.2E-04

\* U/S = upstream side of piezometer tube; D/S = downstream side of piezometer tube.

Table 4.6c Vertical section at pit at station 3+80

Depth	Times (sec)		Calculated K (ft/s)		Average SDEV		
	NW Wall	SW Wall	NW Wall	SW Wall	Average	SDEV	
3"	0.98		3.8E-04		3.8E-04		
6"	1.71	10.27	2.0E-04	2.8E-05	1.2E-04	1.2E-04	Upper layer:
9"	1.22	3.12	3.0E-04	1.0E-04	2.0E-04	1.4E-04	Average SDEV
12"	1.18	3.25	3.1E-04	1.0E-04	2.0E-04	1.5E-04	1.7E-04 1.1E-04
15"	0.94	0.97	4.0E-04	3.8E-04	3.9E-04	9.6E-06	
18"		0.99		3.8E-04	3.8E-04		Lower layer:
21"	1.04	0.94	3.6E-04	4.0E-04	3.8E-04	3.1E-05	Average SDEV
24"		0.91		4.1E-04	4.1E-04		3.9E-04 2.0E-05
Average	1.18	2.92	3.2E-04	2.6E-04			
SDEV	0.28	3.41	7.0E-05	1.7E-04			

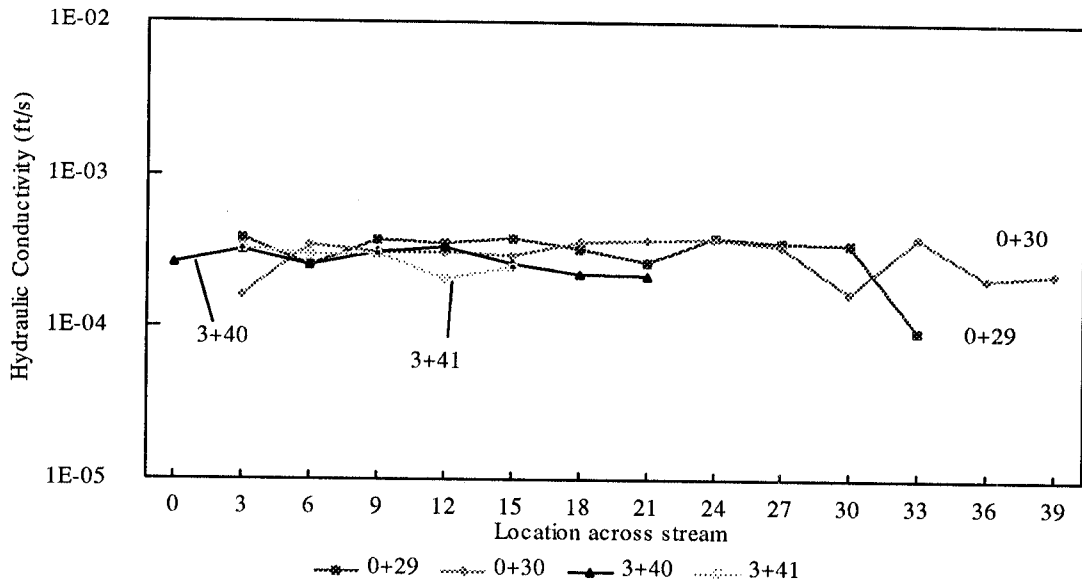


Figure 4.12a Hydraulic conductivity across streambed traverse.

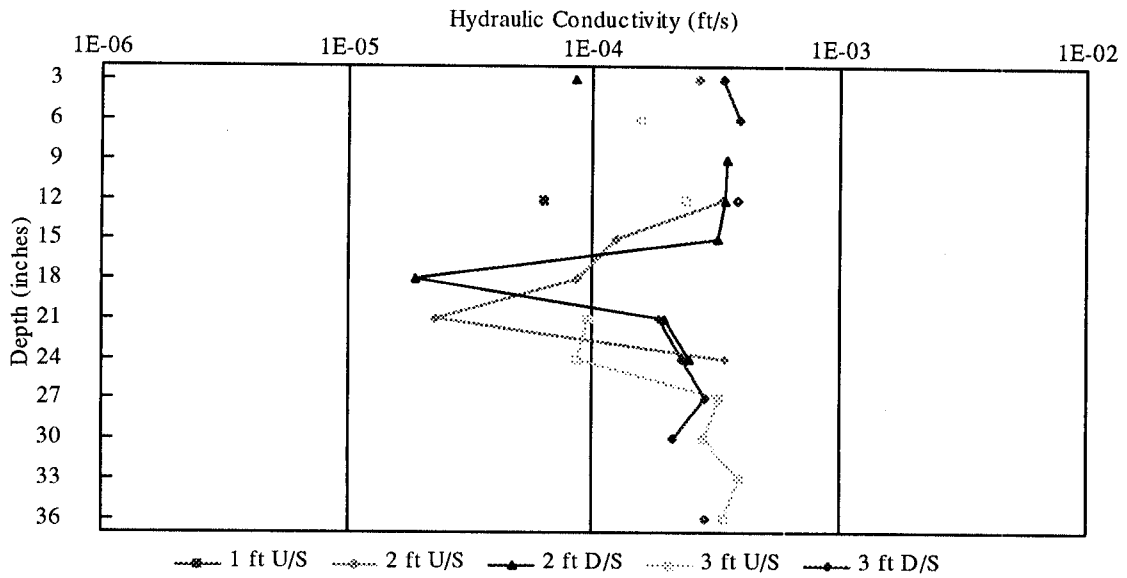


Figure 4.12b Vertical section at station 1+80 piezometer nest.

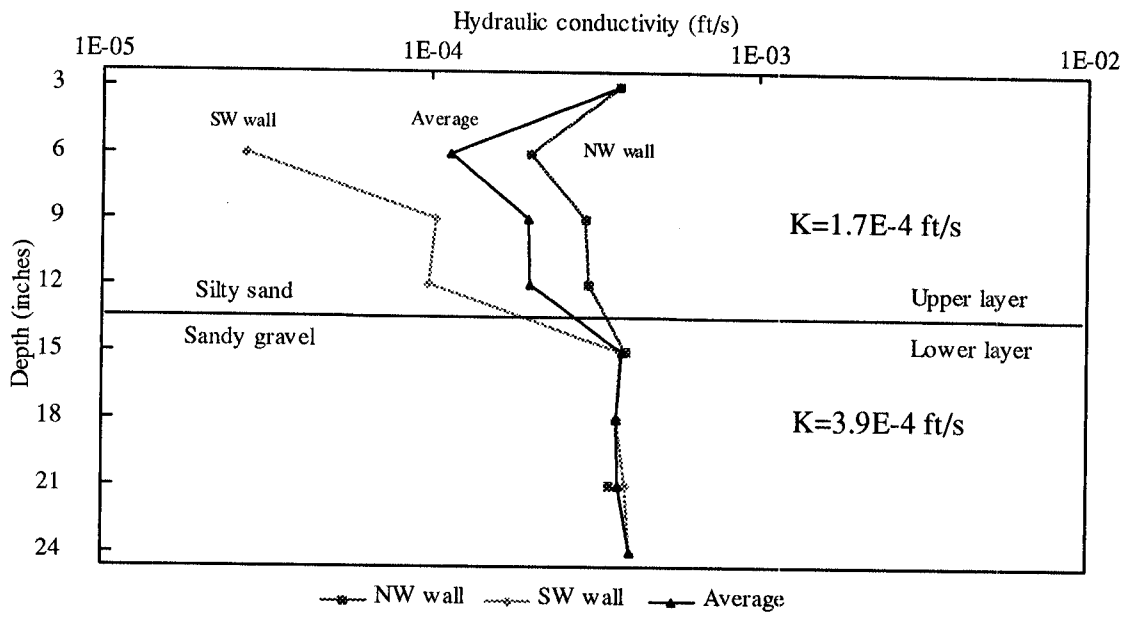


Figure 4.12c Vertical section at pit at station 3+80

## Section 5. STREAMFLOW PREDICTION

An objective of this study is to incorporate all the data gathered and predict the amount of streambed seepage given specific values of hydraulic parameters measured in the field, and compare this to the observed difference between discharge measured above and below a stream reach. The purpose of this part of the report is to state the model and assumptions upon which the calculation of the streamflow is based and then discuss the success of the predictions. As mentioned in Section 2 of this report, a number of different components contribute to streamflow within a channel. As stated in the conceptual approach section of this report, for a given reach of stream the flow measured at a downstream point can be calculated as (after Freeze, 1974):

$$Q_{out} = Q_{in} + Q_{precip} + Q_{over} + Q_{sub} \pm Q_{seep} - Q_{evap} \pm \Delta storage \quad (5.1)$$

where  $Q_{out}$  = streamflow measured at downstream point,

$Q_{in}$  = streamflow measured at upstream point,

$Q_{precip}$  = storm flow from precipitation falling directly on stream,

$Q_{over}$  = overland storm flow from excess precipitation ,

$Q_{sub}$  = storm flow derived from shallow subsurface,

$Q_{seep}$  = sustained baseflow derived from seepage through streambed,

$Q_{evap}$  = flow lost to evaporation from the free water surface, and

In order to accurately predict the flow at any given point either all these parameters must be measured or assumptions must be made to eliminate unknown terms. Since precipitation, overland flow, and subsurface flow terms are all storm event related, and the flow at the weirs was not measured during a storm, these terms can be neglected. The evaporation was not measured in this study, so this term will not be included in the seepage calculation. The prediction of streamflow will be made for the lowest 180 feet of stream in the study area. This reach was selected because there were days when there was no inflow and all the flow can be attributed to groundwater discharge. Based on these assumptions, the flow at the downstream point is:

$$Q_{out} = Q_{seep} \quad (5.2)$$

Darcy's law is used to calculate the seepage term as:

$$Q_{seep} = KiA \quad (5.3)$$

where  $K$  = vertical hydraulic conductivity of streambed,

$i$  = hydraulic head gradient between stream and groundwater system, and

$A$  = area of flow through streambed.

A two-layered system is used to calculate the hydraulic conductivity. This is based on the observations made at the two pits located at stations 0+25 and 3+40. Because a two-layered system was not observed at the third trench at station 1+80, the thickness of the upper layer is taken as minimal in some areas, letting the lower layer dominate. The geometry used in the calculations is presented in Figure 5.1. The effective hydraulic conductivity for flow perpendicular to layering is calculated as:

$$K_{eff} = \frac{\sum d_i}{\sum \frac{d_i}{K_i}} \quad (5.4)$$

where  $K_{eff}$  = effective hydraulic conductivity,

$d_i$  = thickness of layer  $i$ , and

$K_i$  = hydraulic conductivity of layer  $i$ .

The hydraulic conductivities measured in the trench at station 3+40 were used to calculate the effective hydraulic conductivity. The measurements were made with the air permeameter and since the regression equation and its associated uncertainty was used to calculate the hydraulic conductivity, it is possible to also calculate the 95% joint confidence interval using the Working-Hotelling approach (Table 5.1). Only the surface to 1-foot gradient was used to predict streamflow and so a total thickness of 1 foot was used for calculation of effective hydraulic conductivity. The thickness of each layer used to calculate the effective hydraulic conductivity varied with location (Figure 5.1). The ranges of hydraulic conductivity for each layer and effective hydraulic conductivity for each location are shown in Table 5.2.

The gradients for the days of interest were used in the calculations (Figure 5.2). The two most downstream piezometer nests consistently exhibited negative gradients while the upstream piezometer nests start positive and either become zero when the

Table 5.1 Hydraulic conductivities used in streamflow prediction.

Vertical section at pit at station 3+80

Depth	Times (sec)		Calculated K (ft/s)		Average SDEV		
	NW Wall	SW Wall	NW Wall	SW Wall			
3"	0.98		3.8E-04		3.8E-04		
6"	1.71	10.27	2.0E-04	2.8E-05	1.2E-04	1.2E-04	Upper layer:
9"	1.22	3.12	3.0E-04	1.0E-04	2.0E-04	1.4E-04	Average SDEV
12"	1.18	3.25	3.1E-04	1.0E-04	2.0E-04	1.5E-04	1.7E-04 1.1E-04
15"	0.94	0.97	4.0E-04	3.8E-04	3.9E-04	9.6E-06	
18"		0.99		3.8E-04	3.8E-04		Lower layer:
21"	1.04	0.94	3.6E-04	4.0E-04	3.8E-04	3.1E-05	Average SDEV
24"		0.91		4.1E-04	4.1E-04		3.9E-04 2.0E-05
Average	1.18	2.92	3.2E-04	2.6E-04			
SDEV	0.28	3.41	7.0E-05	1.7E-04			

Depth	NW Wall:				SW Wall:				Average:		
	tbar	Ws{Yh}	Lower K	Upper K	tbar	Ws{Yh}	Lower K	Upper K	Lower K	Upper K	
3"	0.98	0.494	1.2E-04	1.2E-03					1.2E-04	1.2E-03	
6"	1.71	0.436	7.5E-05	5.6E-04	10.27	0.285	1.4E-05	5.3E-05	4.4E-05	3.0E-04	Average of upper layer:
9"	1.22	0.472	1.0E-04	8.8E-04	3.12	0.377	4.4E-05	2.5E-04	7.2E-05	5.6E-04	Lower K Upper K
12"	1.18	0.475	1.0E-04	9.2E-04	3.25	0.374	4.2E-05	2.4E-04	7.3E-05	5.8E-04	7.8E-05 6.6E-04
15"	0.94	0.499	1.3E-04	1.3E-03	0.97	0.496	1.2E-04	1.2E-03	1.2E-04	1.2E-03	
18"					0.99	0.494	1.2E-04	1.2E-03	1.2E-04	1.2E-03	Average of lower layer:
21"	1.04	0.489	1.2E-04	1.1E-03	0.94	0.500	1.3E-04	1.3E-03	1.2E-04	1.2E-03	Lower K Upper K
24"					0.91	0.503	1.3E-04	1.3E-03	1.3E-04	1.3E-03	1.2E-04 1.2E-03

tbar = average of measured times  
 Ws{Yh} = Working-Hoteling coefficient  
 Lower and upper K = Confidence interval



Figure 5.1 Geometry used in streamflow prediction.

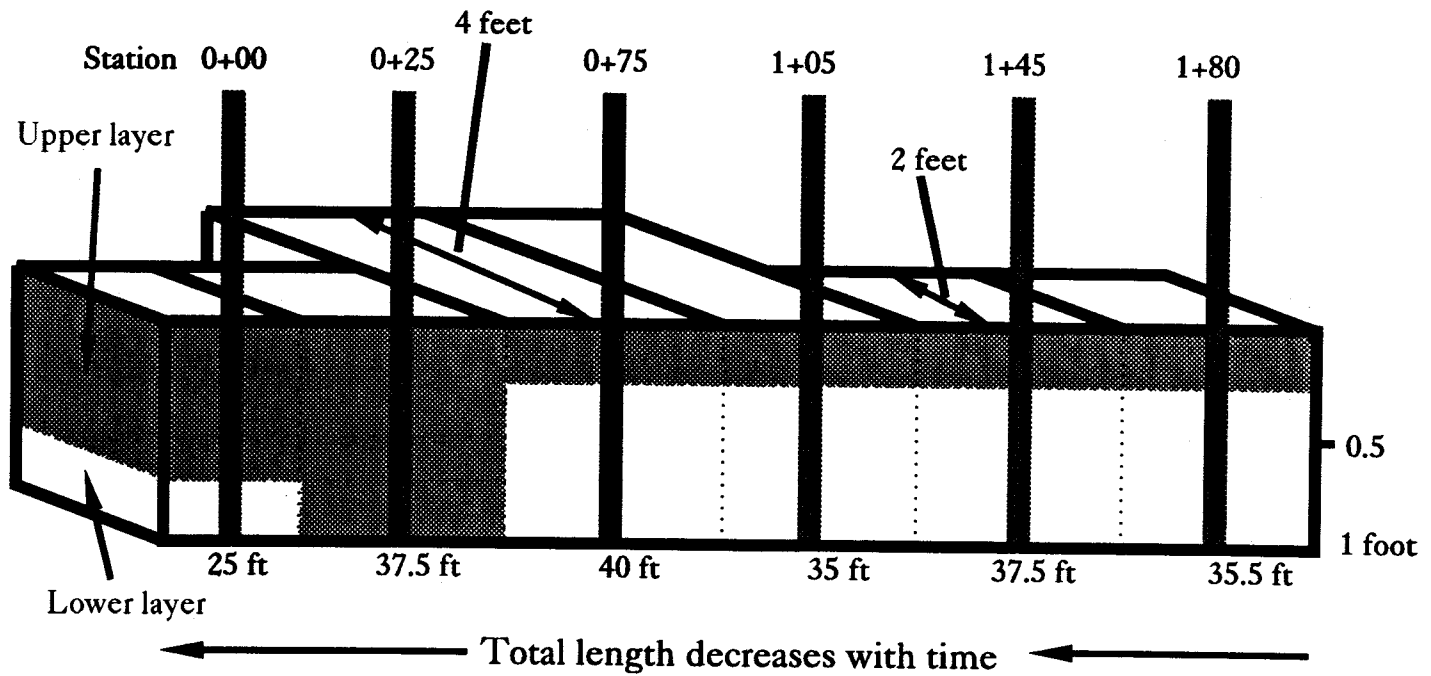


**Table 5.2 Effective hydraulic conductivities used in streamflow prediction**

	Lower Confidence Interval	Average	Upper Confidence Interval
Upper layer	$7.8 \times 10^{-5}$ ft/s	$1.7 \times 10^{-4}$ ft/s	$6.6 \times 10^{-4}$ ft/s
Lower layer	$1.2 \times 10^{-4}$	$3.9 \times 10^{-4}$	$1.2 \times 10^{-3}$
Effective Conductivity:			
0+00	$8.5 \times 10^{-5}$	$2.0 \times 10^{-4}$	$7.4 \times 10^{-3}$
0+25	$7.8 \times 10^{-5}$	$1.7 \times 10^{-4}$	$6.6 \times 10^{-3}$
0+75	$1.1 \times 10^{-4}$	$3.5 \times 10^{-4}$	$1.1 \times 10^{-3}$
1+05	$1.1 \times 10^{-4}$	$3.5 \times 10^{-4}$	$1.1 \times 10^{-3}$
1+45	$1.1 \times 10^{-4}$	$3.5 \times 10^{-4}$	$1.1 \times 10^{-3}$
1+80	$1.1 \times 10^{-4}$	$3.5 \times 10^{-4}$	$1.1 \times 10^{-3}$

piezometer becomes dry or become negative. The precipitation event at the end of May and beginning of June can be seen from the gradients in several of the piezometers increasing to reflect the influx of water into the system. A total of 0.27 inches of precipitation fell on the study area in late June and is reflected by the small increase in

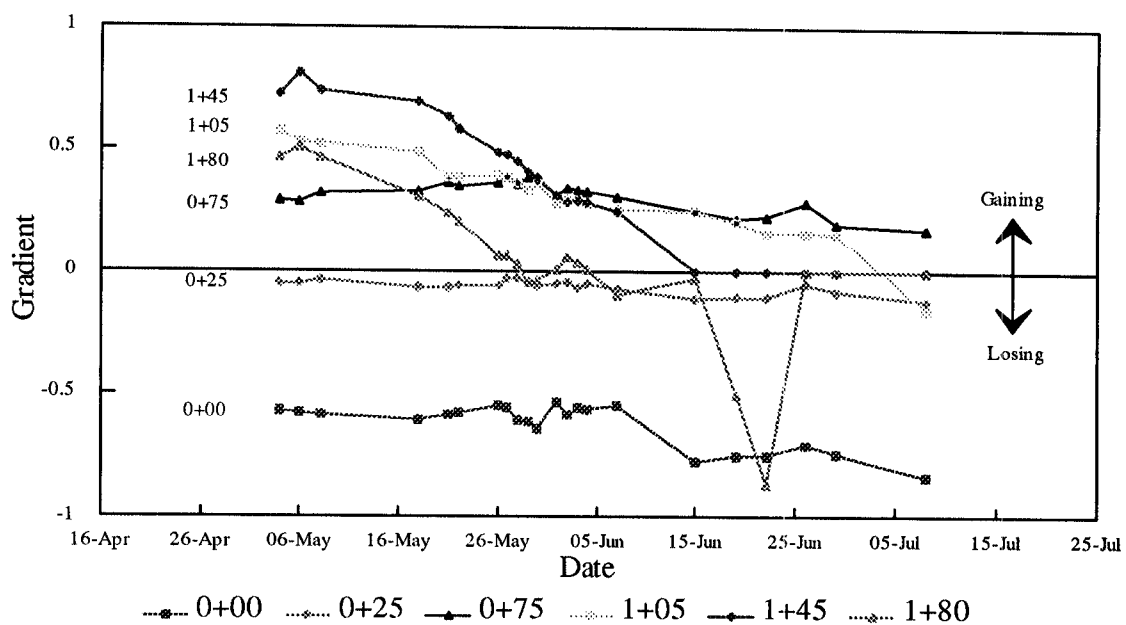


Figure 5.2 Gradients used in streamflow prediction.

gradients. These data suggest that the lag time in the piezometers is not a critical issue for the purposes of flow prediction. Response to these events is not seen in each piezometer, but the events are reflected in at least half of the piezometers. The limitations this lack of response will have on streamflow prediction are that peaks in flow will not be predicted as accurately. It is assumed that the gradient between the surface and 1-foot piezometer applies to the entire 1-foot thickness, varying linearly between piezometer locations.

The final parameter necessary to calculate Darcian flow is cross-sectional area. The width, and especially wetted perimeter, of the stream varied along the reach where flow was observed. Because of the upward gradients in the lower discharge zone, considerable seepage faces on the sides of the stream above the water surface were observed which contribute to area of flow. The width of flow was assumed to vary linearly between the piezometers locations, and the length of flow extended halfway between the locations. The width and length of flow for each location is shown on Figure 5.1. Because the stream progressively went dry, the length of flow for the uppermost active section was progressively decreased. Figure 5.3 shows the relative area assigned to

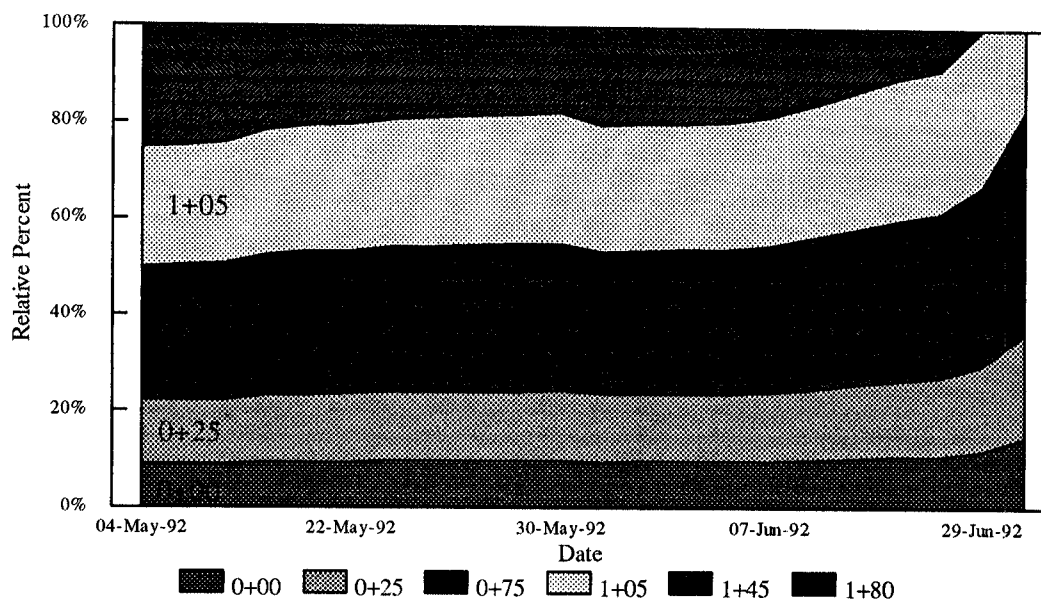


Figure 5.3 Relative areas assigned to each piezometer as a function of date.

each piezometer as a function of time. This clearly shows that the area assigned to the piezometers decreases to zero as the stream goes dry, and the relative areas assigned to the other piezometers increase.

Given this mathematical model, streamflow was predicted for the 25 days when flow could be entirely attributed to groundwater discharge. Only the gradients and area of flow were varied with time in the calculations. The predicted flows were calculated for a range of hydraulic conductivities using the average and upper and lower confidence interval to reflect the uncertainty associated with the measurements of hydraulic conductivity. The values of hydraulic conductivity used are shown in Table 5.2. The predicted flows, both as a total flow and as a percent of observed flow, are shown in Table 5.3 and Figure 5.4.

The results of this analysis are promising, considering the problems with the piezometers and the number of assumptions necessary to formulate a mathematical model. Using the average hydraulic conductivity the predicted flows consistently estimate the observed flows within 15 percent for the month of May and within 30 percent for most of the month of June. As the upper and lower confidence intervals span an order of magnitude range around the average hydraulic conductivity, the predicted flow exhibits the same trend. The close match between observed and predicted flows using the average hydraulic conductivity suggest the constraints on hydraulic conductivity are tighter than reflected in the measurement uncertainty. Flow rates in early May are consistently overestimated, with a few exceptions, while later flows are consistently underestimated. The possible mechanisms responsible for this over and under-estimation will be discussed later. The mathematical model breaks down when predicting flows in the middle of June as piezometers go dry and gradient information is unavailable. This problem proceeds from the top of the discharge area, where the gradients are generally positive, and progresses downstream. The effect on the predicted flow is that the strong negative gradients downstream predominate, and flow is significantly under predicted. Again, the response time of the water levels could be responsible for this effect. This can work both ways: a slow response time may imply that gradients should decrease faster and so flow rate is actually overestimated compared to observed flows.

Table 5.3 Observed and predicted streamflows

Date	Observed Flow (cfs)	Lower Confidence Interval		Average		Upper Confidence Interval	
04-May-92	0.071	0.022	31%	0.069	97%	0.216	304%
06-May-92	0.070	0.022	31%	0.069	99%	0.217	311%
08-May-92	0.063	0.021	34%	0.067	107%	0.210	335%
18-May-92	0.052	0.018	35%	0.059	112%	0.183	350%
21-May-92	0.055	0.016	30%	0.052	95%	0.163	298%
22-May-92	0.055	0.015	28%	0.050	90%	0.155	279%
26-May-92	0.044	0.015	34%	0.047	108%	0.146	335%
27-May-92	0.044	0.015	34%	0.048	110%	0.149	342%
28-May-92	0.044	0.014	31%	0.044	100%	0.136	311%
29-May-92	0.041	0.013	31%	0.042	100%	0.129	311%
30-May-92	0.040	0.013	32%	0.042	103%	0.129	318%
01-Jun-92	0.047	0.010	22%	0.034	71%	0.104	221%
02-Jun-92	0.047	0.011	23%	0.036	76%	0.110	235%
03-Jun-92	0.047	0.011	23%	0.035	74%	0.107	227%
04-Jun-92	0.045	0.010	23%	0.033	75%	0.103	230%
07-Jun-92	0.040	0.009	22%	0.029	72%	0.089	220%
15-Jun-92	0.038	0.004	12%	0.017	44%	0.048	126%
19-Jun-92	0.033	0.003	10%	0.013	41%	0.037	115%
22-Jun-92	0.026	0.003	11%	0.012	45%	0.032	123%
26-Jun-92	0.018	0.004	25%	0.016	91%	0.047	265%
29-Jun-92	0.011	0.002	21%	0.010	90%	0.027	244%
08-Jul-92	0.001	-0.002	-167%	-0.003	-259%	-0.017	-1266%

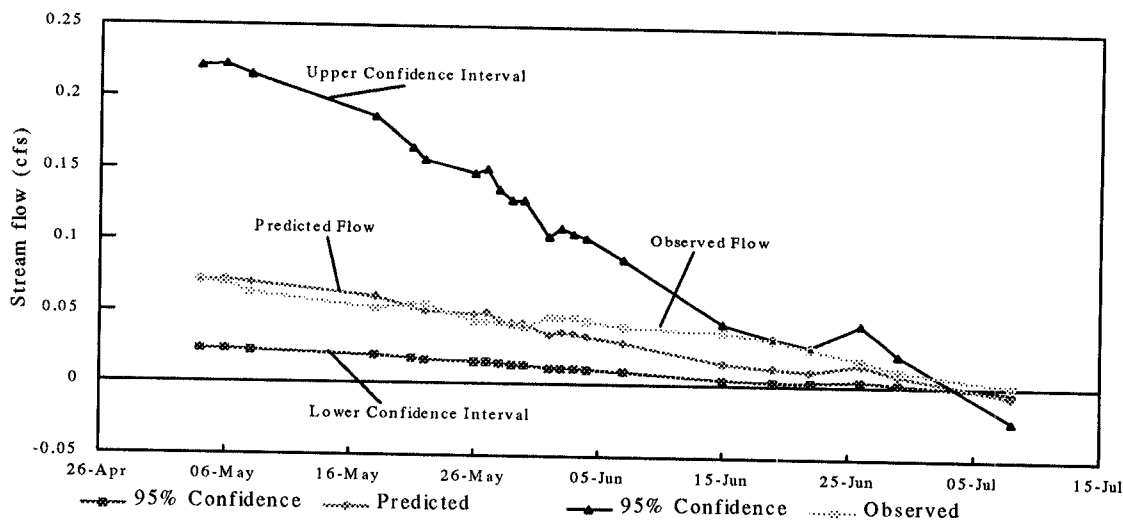


Figure 5.4 Streamflow predictions.

The observed streamflows which are compared to the predicted flows also have measurement uncertainty associated with them. Because the flow is calculated from the flow depth using a power law equation, a small error in the measured flow depth results in a large error in calculated streamflow. For example, flow depths of 0.23 and 0.24 feet give flow rates of 0.064 and 0.072 cfs, respectively, for a difference of approximately 10%. The discrepancies grow with decreasing flow depth. This suggests that the uncertainty in the observed flows could encompass the differences between the predicted and observed flows.

An alternative method to determine the effective hydraulic conductivity is to use the hydraulic conductivity obtained from the surface infiltration tests and to estimate the hydraulic conductivity using the grain size distribution analysis. The correlation between hydraulic conductivity and some measure of grain diameter was recognized early in this century by Hazen (1910). Refinement of this method through empirical studies led to the Hazen approximation:

$$K = Cd_{10}^2 \quad (5.5)$$

where  $K$  = hydraulic conductivity (cm/s),  
 $C$  = empirical material coefficient, and  
 $d_{10}$  = effective grain size (cm).

A range for the material coefficient is given for various unconsolidated material types. For the materials encountered in this study, Fetter (1988) recommends a range of 40-80 be used for very fine-grained, poorly sorted sand and a range of 80-120 for medium-grained, well sorted sand. More recent work by Uma et al. (1989) statistically correlating reliable pump testing hydraulic conductivity with grain size data from forty-seven wells in two groups of unconsolidated to moderately consolidated aquifers in southeastern Nigeria indicates that the Hazen method consistently overestimates the hydraulic conductivity. This study recommends a value of 6.0 be used for unconsolidated to poorly consolidated sands and sandstones. The hydraulic conductivity was estimated using the two methods outlined above for the samples on which grain size distribution analyses were performed, and then the effective hydraulic conductivity was calculated using equation 5.4. The hydraulic conductivities and the effective hydraulic conductivities from the surface infiltration tests, the Hazen method, and the Uma et al. are presented in Table 5.4 along with the effective grain sizes.

The streamflow was predicted using the hydraulic conductivities from the surface infiltration tests, the Hazen method, and the Uma et al. method and the results are presented in Figure 5.5. The differences in hydraulic conductivity are exhibited as different predicted flows. The Uma et al. method predicts the highest amount of streamflow because the hydraulic conductivities in the gaining reach of the stream are higher than the other methods and in the losing reach are lower. Even though the Hazen method estimates the highest hydraulic conductivity, the predicted streamflows are in the middle because the strong losing gradients predominate. The same is true for the streamflow predicted using the surface infiltration test hydraulic conductivities, however the predicted streamflows at locations where the gradients indicate a gaining stream are low because they have low hydraulic conductivities.

All of the methods used to estimate the hydraulic conductivity of the streambed overpredict the streamflow for the early period and underpredict the streamflow for the later period. This suggests that the values of one or more of the parameters used to predict the streamflows have a time dependence which has not been incorporated into this analysis. Possible explanations for this time dependence are that measured gradients are not reflective of the actual field conditions, the areas of flow are different than

**Table 5.4 Predicted hydraulic conductivity using surface infiltration and grain size distribution analysis**

	Station 0+00	0+25	0+75	1+05	1+45	1+80
Surface infiltration hydraulic conductivity (ft/s)	$2.2 \times 10^{-6}$	$7.9 \times 10^{-6}$	$1.1 \times 10^{-5}$	$8.2 \times 10^{-5}$	$1.3 \times 10^{-4}$	$1.3 \times 10^{-4}$
<b>Effective hydraulic conductivity (ft/s)</b>	$5.9 \times 10^{-6}$	$1.0 \times 10^{-5}$	$1.6 \times 10^{-4}$	$3.4 \times 10^{-4}$	$3.6 \times 10^{-4}$	$3.6 \times 10^{-4}$
d10 (mm)	0.06	0.075	0.20	0.16	0.46	0.46
Hazen hydraulic conductivity	$4.6 \times 10^{-5}$	$2.7 \times 10^{-4}$	$4.9 \times 10^{-4}$	$4.6 \times 10^{-5}$	$5.6 \times 10^{-5}$	$5.6 \times 10^{-5}$
<b>Effective hydraulic conductivity</b>	$1.0 \times 10^{-4}$	$2.9 \times 10^{-4}$	$4.0 \times 10^{-4}$	$3.0 \times 10^{-4}$	$4.1 \times 10^{-4}$	$4.1 \times 10^{-4}$
Uma hydraulic conductivity	$7.2 \times 10^{-6}$	$4.3 \times 10^{-5}$	$7.9 \times 10^{-5}$	$7.2 \times 10^{-5}$	$4.3 \times 10^{-4}$	$4.3 \times 10^{-4}$
<b>Effective hydraulic conductivity</b>	$1.9 \times 10^{-5}$	$5.5 \times 10^{-5}$	$3.4 \times 10^{-4}$	$3.3 \times 10^{-4}$	$3.9 \times 10^{-4}$	$3.9 \times 10^{-4}$

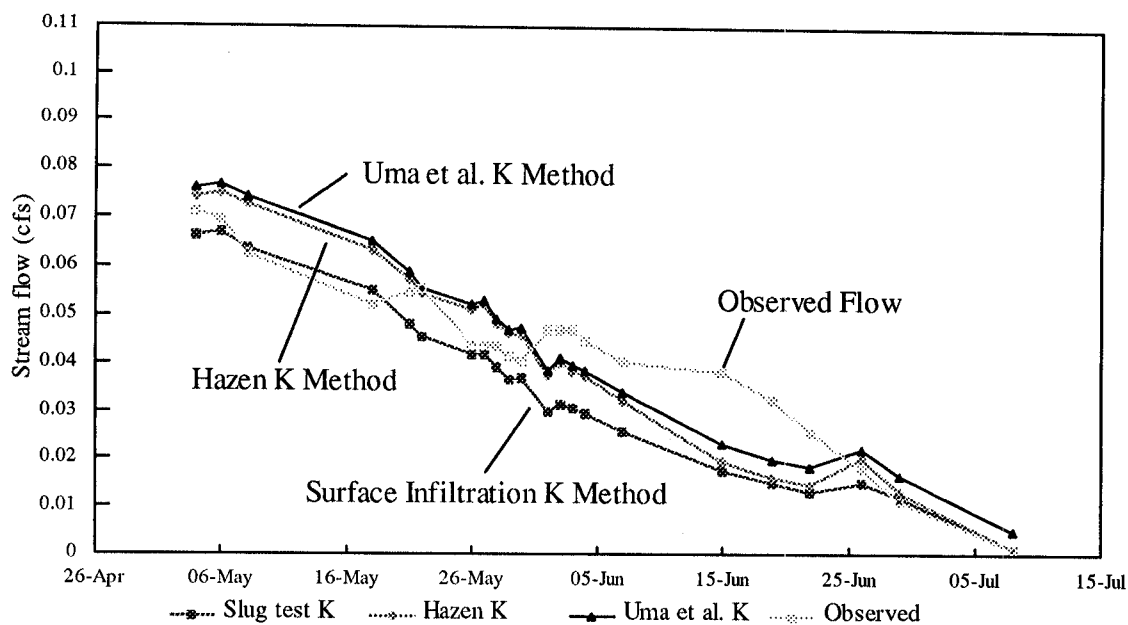


**Figure 5.5 Streamflow predictions using hydraulic conductivity from surface infiltration tests and grain size distribution analysis.**



represented, or hydraulic conductivity increases with time. The gradients are somewhat uncertain because the piezometers were plugged. Changes in evapotranspiration rate may have impacted accuracy of measurement of gradient. Plant life became prevalent during late spring and summer of the study period. The effect which evapotranspiration of the plants will have on measurement of the shallow groundwater system depends on the relative location of the head measurement and the plant root intake and on the direction of flow between the stream and aquifer. Plant roots withdrawing water near the piezometer will lower the head measured in the piezometer but may not lower heads near the streambed. If the gradient is upward, this will cause the calculated gradient to be lower than the actual conditions and the calculated seepage will underpredict the observed gain in streamflow. If the gradient is downward, the calculated gradient will be greater than the actual condition and the calculated flow will overpredict the observed loss in flow. In either case, evapotranspiration would lead to the under prediction of stream seepage.

There are several hypotheses for the time dependence of hydraulic conductivity. Fine material deposited on the streambed in the early spring could be eroded away during the late spring, increasing the hydraulic conductivity of the streambed. Similarly, increasing plant life in the summer could be responsible for the increase in hydraulic conductivity, by roots opening new pathways for seepage. Assuming that the hydraulic conductivity is homogeneous over each stream reach where flows were calculated, the observed streamflows, gradients, and seepage areas can be used to predict the time dependence of hydraulic conductivity. The results from these calculations are presented in Figure 5.6, showing that the possible increase in hydraulic conductivity with time is approximately half an order of magnitude. Additional field work is necessary to identify the process responsible for this under- and over-prediction of stream flow.

As the method used here to predict streamflow is the same one that most numerical models use, namely Darcy's Law, the success of streamflow prediction gives validity to the models. Given the data obtained in this study, it can be concluded that variations in the shallow hydraulic head gradient outweigh variations in hydraulic conductivity when predicting streamflow. This conclusion is based on the fact that observed streamflows were adequately predicted incorporating little variation in hydraulic conductivity and more variation in head gradient. The order of magnitude range in the uncertainty of hydraulic conductivity as directly measured in the field is reflected in the

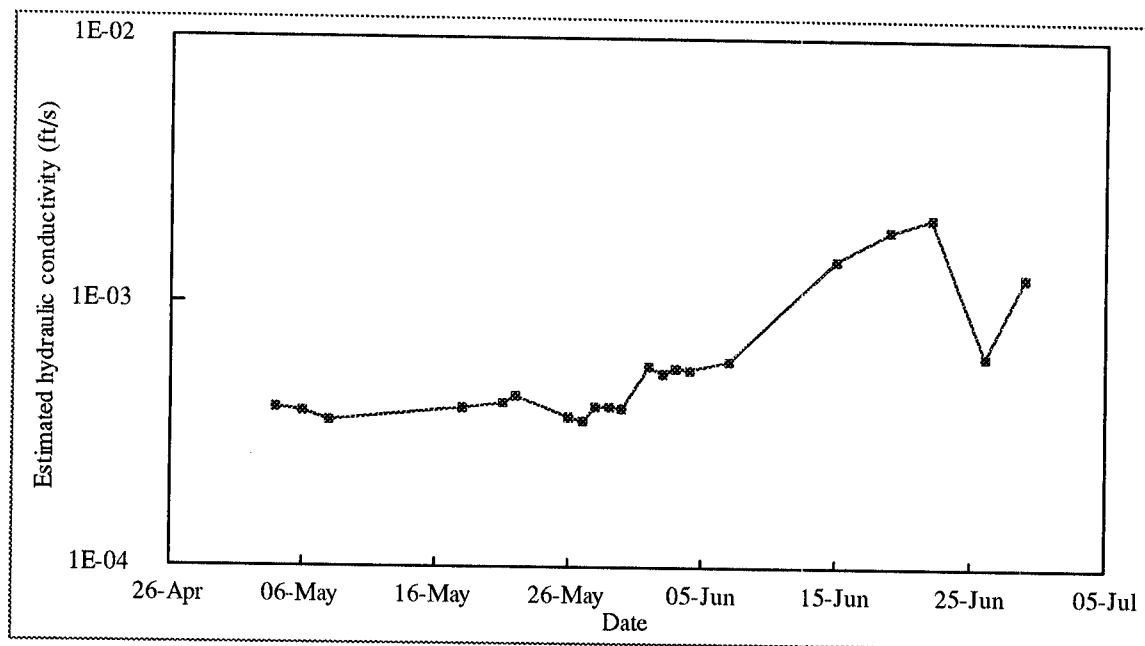


Figure 5.6 Estimated time dependence of hydraulic conductivity.

order of magnitude range in predicted flows. The close match of seepage and streamflows using the mean hydraulic conductivities indicates the other field data impose tighter constraints on the hydraulic conductivity. While there is an infinite number of combinations of hydraulic conductivity, head gradient, and cross-sectional area of flow which will result in the same calculated flows, the governing equation is linear. Consequently if the hydraulic conductivity of the aquifer material varies with time or location from those values used, then the values of the other parameters must vary as well to compensate and obtain the same seepage. Observations made in the field can constrain some of the input parameters. First, the area is well constrained by observations made in the field of the width and wetted perimeter of the stream. Second, it has been assumed that the gradients apply over the one foot section below the streambed being modeled. If, on the other hand, most of the head drop actually occurs over a shorter distance (i.e. across a very low hydraulic conductivity "skin" on the stream bottom), the calculated gradients would be larger. Finally, some other process, such as evapotranspiration, could cause an inaccurate measurement of the shallow head gradient and thus inaccurate prediction of stream seepage.

## Section 6 CONCLUSIONS

A number of conclusions can be drawn from this study, both with regard to the stream/aquifer system in the study area as well as the techniques applied during the study. As one of the implicit purposes of this study was to develop techniques to gather site specific data regarding stream/aquifer interactions, it is enlightening to evaluate the success of those techniques. The conclusions drawn here will be discussed in two parts: the system behavior and the techniques.

### 6.1 Stream/aquifer system

- The duration of groundwater discharge in summer months is dependent on the amount of precipitation the area has received. Since 1992 was relatively drier than 1991, groundwater did not discharge as long in 1992 as in 1991. Given that the alluvial valley is basically a large reservoir, if all other parameters are constant, more recharge will result in a longer discharge period. Given enough years of data, the storage volume of the alluvial aquifer could be inferred.
- The response of the groundwater system to precipitation is on the order of days rather than hours. That is, infiltration takes a number of days to be detected at the piezometers. Fluctuation of the piezometer water levels in response to water level changes in the stream could be greater than the response to precipitation and so the response is not seen.
- The response of the groundwater system to changes in stream stage is almost immediate for most of the piezometers.
- The shallow groundwater gradients calculated from the water level data indicate the presence of two groundwater discharge zones. These zones are in the vicinity of and can be partially attributed to sharp breaks in stream slope. Variation in

subsurface topographic features may be responsible for the longevity of the lower discharge zone but this could not be verified.

- For the period when streamflow data are available, the total reach of stream is generally gaining water from the groundwater system. The spring runoff event ended in mid-April after which only unconnected segments of stream were flowing. Flow stopped in the middle of July. From the beginning of June through mid-July there was only flow from the lower discharge zone, resulting in 5.7 acre-feet of discharge from groundwater.
- Stream flow velocity is fairly uniform along the stream reach with peaks corresponding to breaks in stream slope. The range of velocities observed is sufficient to transport unconsolidated sediments up to 2 mm in diameter, typical of sand. Mapping of the streambed surface material type shows that it is highly variable along the stream reach, with larger grain sizes predominating. Finer material is present filling the space between the large cobbles.
- Hydraulic conductivity of the streambed surface materials ranges from  $2.2 \times 10^{-6}$  to  $3.2 \times 10^{-4}$  ft/s, depending on the type of testing procedure used. Variation in air permeameter hydraulic conductivity was much less than surface infiltration hydraulic conductivity. While there is some variability in hydraulic conductivity, results from four locations where traverses were performed using the air permeameter suggest that the range of hydraulic conductivity of the stream bed is within an order of magnitude and the average hydraulic conductivities are statistically similar. The heterogeneous nature of the alluvial material suggests that variation in hydraulic conductivity should be greater than those observed and additional work should be done to verify the unbiased nature of the sampling.
- Hydraulic conductivity of the shallow aquifer material measured using the air permeameter is generally higher exhibits a wider range than the surface stream bed materials. The range observed is from  $9.5 \times 10^{-6}$  to  $4.3 \times 10^{-4}$  ft/s. At two locations a two-layer system was observed with a fine grain silty-sand surface layer overlying a material with grain size ranging from silt to cobbles. No layering was apparent at a third location where coarser aquifer material predominated.
- Grain size analysis of streambed surface materials indicates the predominance of poorly sorted sand and gravels.

- Given the measured hydraulic conductivities, shallow head gradients, and stream geometry the stream seepage was adequately predicted using Darcy's Law and a two-layer aquifer system. Hydraulic conductivities were also estimated from grain size distribution data, predicting similar streamflows. All methods consistently overestimated flow in the early period and underestimated flow in the later period, suggesting a time-dependence of one or more of the parameters used to predict flow.

## 6.2 Observation Techniques

- The low cost and somewhat easy installation of the piezometers make them attractive for general use. However, some sort of fine screening material attached inside the electrical conduit is necessary to prevent the introduction of fine-grained material into the piezometer.
- V-notched weirs are an adequate means of gathering streamflow data but have a number of drawbacks. The requirement of a large pool of backwater introduces the complication of leakage underneath the weir as well as perhaps unduly influencing the groundwater system. Additionally, weirs are difficult to install if the stream is flowing. A Parshall flume of adequate size would overcome these drawbacks.
- The mini air permeameter holds great promise as a technique for the rapid and non-destructive determination of hydraulic conductivity. The main drawback associated with the air permeameter is the need for a dry, open face of fine grained (sand and smaller) aquifer material. In some types of unconsolidated material this is a nontrivial task; on outcrops it could be invaluable. Further work is necessary to validate the calibration obtained in this study.

## REFERENCES CITED

- Bachu, S., and Cuthiell, D., 1990, Effects of Core-Scale Heterogeneity on Steady State and Transient Fluid Flow in Porous Media: Numerical Analysis, *Water Resour. Res.*, 26(5), 863-874.
- Bachu, S., Cuthiell, D., Kramers, J. and Yuan, L.P., 1990, Reservoir Characterization Case Study: Bimodally Heterogeneous Facies, In: S. Bachu (ed) *Proceedings Fifth Canadian/American Conference on Hydrology, Parameter Identification and Estimation for Aquifer and Reservoir Characterization*, National Water Well Assoc., Dublin, Ohio, 87-100.
- Bouwer, H. and Jackson, R.D., 1974, Determining Soil Properties, in *Drainage for Agriculture, ASA Monogr. 17*, chapter 23, sect. 10, edited by J. van Schilgaarde, pp. 611-672, American Society of Agronomy, Madison, Wis.
- Bouwer, H., and Rice, R.C., 1976, A Slug Test for Determining Hydraulic Conductivity of Unconfined Aquifers With Completely or Partially Penetrating Wells, *Water Resour. Res.*, 12, 3, 423-428.
- Bouwer, H., 1989, The Bouwer and Rice Slug Test - An Update, *Groundwater*, 27, 3, 304-309.
- Bowles, J.E., 1986, *Engineering Properties of Soils and Their Measurement*, McGraw-Hill Book Co., U.S.A.
- Buchanan, T.J., and Somers, W.P., 1969, Discharge Measurements at Gaging Stations, *Techniques of Water-Resources Investigations of the U.S.G.S.*, Chapter A8, Book 3, 57-58.
- Castro, N.M., and Hornberger, G.M., 1991, Surface-Subsurface Water Interactions in an Alluviated Mountain Stream Channel, *Water Resour. Res.*, 27, 7, 1613-1621.
- Coates, D.R., 1990, Geomorphic Controls of Groundwater Hydrology, in C.G. Higgins and D.R. Coates (ed) *G.S.A. Special Paper 252 Groundwater Geomorphology; The Role of Subsurface Water in Earth-Surface Processes and Landforms*, 341-356.
- Cooper, H.H., Jr., Bredehoeft, J.D. and Papadopoulos, I.S., 1967, Response of a Finite Diameter Well to an instantaneous Charge of Water, *Water Resour. Res.*, 3, 263-269.

- Davis, J.M., Phillips, F.M., and Wilson, J.L., unpublished, An Air-Permeameter for the Rapid and Non-Destructive Sampling of Moderately Consolidated Materials, New Mexico Institute of Mining & Technology, Socorro, New Mexico.
- Dillon, P.J., and Liggett, J.A., 1983, An Ephemeral Stream/aquifer Interaction Model, *Water Resour. Res.*, 19, 3, 621-626.
- Fetter, C.W., 1988, Applied Hydrogeology, Macmillan Publishing, Co., New York.
- Flug, M., Abi-Ghanem, G.V., and Duckstein, L., 1980, An Event-Based Model of Recharge From an Ephemeral Stream, *Water Resour. Res.*, 16, 4, 685-690.
- Freeze, R.A., 1969, The Mechanism of Natural Ground-water Recharge and Discharge 1. One-dimensional, Vertical, Unsteady, Unsaturated Flow above a Recharging or Discharging Ground-water Flow System, *Water Resour. Res.*, 5, 1, 153-171.
- Freeze, R.A., 1972a, Role of Subsurface Flow in Generating Surface Runoff 1. Base Flow Contribution to Channel Flow, *Water Resour. Res.*, 8, 3, 609-623.
- Freeze, R.A., 1972b, Role of Subsurface Flow in Generating Surface Runoff 2. Upstream Areas, *Water Resour. Res.*, 8(5), 1272-1283.
- Freeze, R.A., 1974, Streamflow Generation, *Review of Geophys. and Space Physics*, 12(4), 627-647.
- Goggin, D.J., Thrasher, R.L., and Lake, L.W., 1988, A Theoretical and Experimental Analysis of Minipermeameter Response Including Gas Slippage and High Velocity Flow Effects, *In Situ*, 12(1&2), 79-116.
- Harrison, S.S., and Clayton, L., 1970, Effects of Ground-water Seepage on Fluvial Processes, *G.S.A. Bulletin*, 81, 1217-1226.
- Hansen, W.R., Chronic, J., and Matelock, J., 1978, Climatology of the Front Range Urban Corridor and Vicinity, Colorado, U.S.G.S. Professional Paper 1019, U.S. Government Printing Office, Washington, D.C., 59 pp.
- Harza, L.F., 1935, Uplift and Seepage Under Dams, *Trans. Am. Soc. Civ. Eng.*, 100, 1352-1406.
- Hazen, 1910, in Koenig, A.C., Discussion of Dams on Sand Formation, *Trans. of The A.S.C.E.*, 73, 199-221.
- Hill, B.R., 1990, Groundwater Discharge to a Headwater Valley, Northwestern Nevada, U.S.A., *Journ. of Hydro.*, 113, 265-283.
- Hornberger, G.M., Ebert, J., and Remson, I., 1970, Numerical Solution of the Boussinesq Equation for Aquifer-Stream Interaction, *Water Resour. Res.*, 6, 2, 601-608.

- Hvorslev, M.J., 1951, Time Lag and Soil Permeability in Groundwater Observations, Corps of Engineers, U.S. Army, Vicksburg, MS Bull. No. 36 Waterways Experiment Station, 1-50.
- Keller, E.A., Kondolf, G.M., and Hagerty, D.J., 1990, Groundwater and Fluvial Processes; Selected Observations, in C.G. Higgins and D.R. Coates (ed) G.S.A. Special Paper 252 Groundwater Geomorphology; The Role of Subsurface Water in Earth-Surface Processes and Landforms, 319-340.
- Kemblowski, M.W., and Klein, C.L., 1988, An Automated Numerical Evaluation of Slug Test Data, *Groundwater*, Vol. 26, No. 4, 435-438.
- Kennedy, V.C., Kendall, C., Zellweger, G.W., Wyerman, T.A., and Avanzino, R.J., 1986, Determination of the Components of Stormflow Using Water Chemistry and Environmental Isotopes, Matole River Basin, California, *Journ. of Hydro.*, 84, 107-140.
- Larkin, R.G. and Sharp, J.M., 1992, On The Relationship Between River-basin Geomorphology, Aquifer Hydraulics, and Ground-water Flow Direction in Alluvial Aquifers, *Geol. Soc. of Amer. Bull.*, v. 104, p. 1608-1620.
- Leet, L.D., Judson, S. and Kauffman, M.E., 1982, *Physical Geology*, Prentice-Hall, Inc., Englewood Cliffs, NJ, p. 271.
- Lohman, S.W., 1972, Groundwater Hydraulics, *U.S. Geol. Surv. Prof. Pap. 708*, 70 pp.
- Masch, F.D., and Denny, K.J., 1966, Grain Size Distribution and Its Effect on the Permeability of Unconsolidated Sands, *Water Resour. Res.*, 2(4), 665-677.
- McDonald, M.G. and Harbaugh, A.W., 1988, A Modular Three-Dimensional Finite-Difference Ground-Water Flow Model, TWRI of the USGS, Book 6, Chapter A1.
- McKenna, S.A., 1990, Examination of Water Quality and Groundwater/Surface Water Interaction During Drought Periods, Truckee River, California/Nevada, Masters Thesis, University of Nevada, Reno.
- Morel-Seytoux, H.J., 1975, A Combined Model of Water Table and River Stage Evolution, *Water Resour. Res.*, 11, 6, 968- 972.
- Neter, J., Wasserman, W., and Kutner, M.H., 1990, *Applied Linear Statistical Models*, Irwin, Homewood, Illinois, pp. 163-4.
- Pinder, G.F., and Sauer, S.P., 1971, Numerical Simulation of Flood Wave Modification Due to Bank Storage Effects, *Water Resour. Res.*, 7(1), 63-70.
- Scott, G.R., 1972a, Geologic Map of the Morrison Quadrangle, Jefferson County, Colorado, U.S.G.S. I-790-G.



- Scott, G.R., 1972b, Map Showing Inferred Relative Permeability of Geologic Materials in the Morrison Quadrangle, Jefferson County, Colorado, U.S.G.S. I-790-A.
- Skibitzke, H.E., 1958, An Equation for Potential Distribution About a Well Being Bailed, open file report, U.S. Geol. Surv., Washington, D.C.
- Taylor, D.W., 1948, Fundamentals of Soil Mechanics, John Wiley & Sons, New York, 700 p.
- Uma, K.O., Egboka, B.C.E., and Onuoha, K.M., 1989, New Statistical Grain-Size Method for Evaluating Hydraulic Conductivity of Sandy Aquifers, *Journ. of Hydro.*, 108, 343-366.
- Watters, G.Z., and Rao, V.P., 1971, Hydrodynamic Effects of Seepage on Bed Particles, *Proc. of the A.S.C.E. Hyd. Div. Journ.*, HY3, 421-439.

## SELECTED BIBLIOGRAPHY

- Bachu, S., 1991, On The Effective Thermal and Hydraulic Conductivity of Binary Heterogeneous Sediments, *Tectonophysics*, 190, 299-314.
- Bjerg, P.L., Hinsby, K., Christensen, T.H., and Gravesen, P., 1992, Spatial Variability of Hydraulic Conductivity of an Unconfined Sandy Aquifer by a Mini Slug Test, *Journ. of Hydro.*, 136, 107-122.
- Freeze, R.A. and Cherry, J.A., 1979, *Groundwater*, Prentice-Hall, Inc., Englewood Cliffs, N.J., 604 pp.
- Hinsby, K., Bjerg, P.L., Andersen, L.J., Skov, B., and Clausen, B.S., 1992, A Mini Slug Test Method for Determination of a Local Hydraulic Conductivity of an Unconfined Sandy Aquifer, *Journ. of Hydro.*, 136, 87-106.
- Karasaki, K., Long, J.C.S., and Witherspoon, P.A., 1988, Analytical Models of Slug Tests, *Water Resour. Res.*, 24(1), 115-126.
- Keller, E.A., 1972, Development of Alluvial Stream Channels: A Five Stage Model, *G.S.A. Bulletin*, 83, 1531-1536.
- Kruseman, G.P. and de Ridder, N.A., 1991, Analysis and Evolution of Pumping Test Data, International Institute for Land Reclamation and Improvement, The Netherlands, pp. 237-247.
- McKee, C.R., Permeability Theory, unpublished.
- Pandit, N.S., and Miner, R.F., 1986, Interpretation of Slug Test Data, *Groundwater*, 24, 6, 743-749.
- Shepherd, R.G., 1989, Correlations of Permeability and Grain Size, *Groundwater*, 27(5), 633-638.

**APPENDIX A**

**FORTRAN Code for Automated Numerical Analysis of Slug Test Data**

```

PROGRAM SLUG.FOR
REAL RW,RC,LW,LE,H,A,B,KINIT,YINIT,Y(100),T(100),YT(2,100)
REAL D(2),DELTAK,KSTAR,E,R,SIGMA,LNRRW,SUM,SUMSQ,YBAR,RSQD
INTEGER I,J,L
CHARACTER*80 TITLE
C-----
C      Program SLUG.FOR to calculate the hydraulic conductivity
C      of subsurface materials from a slug test using Horvslev
C      and Bouwer and Rice analysis methods.
C-----
C      Written by Evan R. Anderman for ER-4313   March 1993
C      Department of Geological Engineering
C      Colorado School of Mines
C      Golden, Colorado   80401
C-----
C      The slug test procedure is outlined in Bouwer & Rice (1976)
C      in WRR 12(3) pp. 423-428.
C      The basis for the automated numerical analysis is outlined
C      by Kemblowski & Klein (1988) in Groundwater 26(4) pp. 435-438.
C-----
C READ IN THE VARIABLES:
C      N=NUMBER OF OBSERVATIONS
C      RW=EFFECTIVE WELL RADIUS
C      RC=CASING RADIUS
C      LW=DISTANCE FROM INITIAL WATER TABLE TO BOTTOM OF WELL
C      LE=SCREEN LENGTH
C      H=DISTANCE FROM INITIAL WATER TABLE TO BASE OF AQUIFER
C      YINIT=
C      KINIT=
C      READ (10,5) TITLE
5      FORMAT(A80)
C      WRITE (11,5) TITLE
C      READ (10,10) N,RW,RC,LW,LE,H,YINIT,KINIT
10     FORMAT(I5,6F8.4,E8.2)
C      WRITE(11,15) N,RW,RC,LW,LE,H,YINIT,KINIT
15     FORMAT(' N = ',I5,/,
1      'RW = ',F8.4,/,
2      'RC = ',F8.4,/,
3      'LW = ',F8.4,/,
4      'LE = ',F8.4,/,
5      ' H = ',F8.4,/,
6      'YINIT = ',F8.3,/,
7      'KINIT = ',E8.2)
C      READ(10,20) A,B
20     FORMAT(16F5.2)
C      WRITE(11,25) A,B
25     FORMAT('A = ',F8.2,5X,'B = ',F8.2)
C      READ(10,20) (T(I),I=1,N)

```

```

      READ(10,20) (Y(I), I=1,N)
C
C COMPUTE FACTORS NEEDED IN PARAMETER ESTIMATION
C
      LNRRW=1.0/((1.1/LOG(LW/RW))+((A+B*LOG((H-LW)/RW))/(LE/RW)))
      D(1)=(LNRRW*RC*RC)/(2.0*LE)
      D(2)=((RC*RC)*LOG(LE/RC))/(2.*LE)
C
C PERFORM PARAMETER ESTIMATION FOR TWO METHODS
C
      DO 900 K=1,2
      KSTAR=KINIT
      DO 100 J=1,50
      SUM=0.0
      SUMSQ=0.0
      DO 200 I=1,N
      YT(K,I)=YINIT*EXP(-KSTAR*T(I)/D(K))
      SUM=SUM+(Y(I)-YT(K,I))*YT(K,I)*T(I)
      SUMSQ=SUMSQ+YT(K,I)*YT(K,I)*T(I)*T(I)
200    CONTINUE
      DELTAK=-D(K)*SUM/SUMSQ
      KSTAR=KSTAR+DELTAK
      WRITE(11,*) KSTAR
      L=J
      IF((DELTAK/KSTAR).LT.0.000001) GOTO 110
100    CONTINUE
      WRITE(6,*) 'TOO MANY ITERATIONS'
      GOTO 1000
110    CONTINUE
C
C COMPUTE STATISTICS OF PARAMETER ESTIMATION
C
      YBAR=0.0
      DO 250 I=1,N
      YBAR=YBAR+Y(I)
250    CONTINUE
      YBAR=YBAR/N
      E=0.0
      R=0.0
      DO 300 I=1,N
      E=E+(Y(I)-YT(K,I)+(YT(K,I)*T(I)*DELTAK/D(K)))**2
      R=R+(YT(K,I)-(YT(K,I)*T(I)*DELTAK/D(K))-YBAR)**2
300    CONTINUE
      SIGMA=(E/(N-1))**0.5
      RSQD=R/(R+E)
C
C PRINT OUT RESULTS
C

```

```
IF(K.LT.2) WRITE(11,*) 'BOUWER AND RICE METHOD'  
IF(K.EQ.2) WRITE(11,*) 'HORSLEV METHOD'  
WRITE(11,30) L,KSTAR,SIGMA,RSQD  
30  FORMAT('CONVERGED IN',I3,' ITERATIONS',/,/  
1  'KSTAR =',1X,E8.3,/,/  
1  'SIGMA =',1X,E8.3,/,/  
2  'R SQUARED =',1X,E15.4)  
900  CONTINUE  
WRITE(11,*) ' TIME      OBSERVED  BOUWER  HORSLEV'  
WRITE(11,*) '-----'  
DO 400 I=1,N  
    WRITE(11,40) T(I),Y(I),YT(1,I),YT(2,I)  
400  CONTINUE  
40   FORMAT(F8.1,F9.3,F9.3,F9.3)  
1000 CONTINUE  
STOP  
END
```

**APPENDIX B**

Daily Precipitation

Month	1	2	3	4	5	6	7	8	9	10	11	12	13	14	15	16	17	18	19	20	21	22	23	24	25	26	27	28	29	30	31	Total	
January																																0.00	
February																																	0.00
March				0.30	2.50							0.50	0.30	0.30	0.55													0.40			0.27	4.32	
April			0.30	1.00	0.50															0.17	0.03	0.39					0.04	0.10	0.19		3.52		
May	0.38	0.04	0.11																2.58	0.05	0.05	0.02	0.03					0.28	0.55	0.03	4.12		
June	0.03	0.11		0.02	0.36	0.02	0.04		0.01	0.02		1.06	1.03												1.45	0.13	0.02				4.30		
July										0.19							0.05	0.03		0.35	0.12	1.35	0.10								2.19		
August												0.03		1.00						0.30	0.15	0.28						0.06	0.03		1.85		
September			0.19					0.05		0.05		0.06		0.10					0.11												0.45		
October														0.02				0.75					0.70	0.04		1.30	1.30		0.20		5.07		
November					0.10		0.70																									0.15	
December				0.05										0.10		0.20							0.10	0.30			0.10	0.60			1.45		
1984																																27.42	
January											0.10		0.15				0.05															0.30	
February														0.30			0.50										1.30					2.10	
March			0.10	0.30					0.15							0.05	0.20								0.50		0.10					2.70	
April		0.50	0.05				0.30		0.26		0.20							0.05	1.80	0.80						0.05	0.20	0.45			4.66		
May					0.13	0.02																										0.66	
June	0.03		0.28		0.03			0.15					1.75			0.05	0.14							0.03						0.12	0.66		
July																																2.69	
August	0.50		0.06													0.20	0.18		1.10	0.18					0.30	0.48		0.26	0.03	0.26	0.10	0.67	
September	0.11																			0.15				0.13						0.10	3.23		
October		0.03	0.68	3.00	0.15			0.10				0.70	2.20							0.15							1.20				1.59		
November																																7.01	
December	0.05	0.05										0.10	0.40											0.10	0.08						0.18		
1985																																1.10	
January							0.16			0.08								0.40								0.05				0.20		0.89	
February									0.30				0.20													0.50						1.70	
March			0.30																									0.03		0.80	0.30	0.02	1.65
April				0.05																0.07					0.26	0.60	0.26		0.84	0.24		2.32	
May					0.15											0.14	0.22		0.30							0.06						1.66	
June		0.04	0.48	0.01	0.05					0.10																	0.25	0.90				1.83	
July							0.29					0.14	0.01							0.45	0.56	0.10		0.02	0.10	0.06				0.10	0.35	2.28	
August			0.10									0.15																				0.77	
September	0.80	0.01	0.94									0.30																	0.46			0.06	3.55
October			0.08				0.05	0.11				0.08	0.28						0.06	0.12		0.36		0.16			0.80				1.16		
November								0.40	0.10	0.10		0.07	0.20							0.50			0.01							0.05	1.75		
December																																0.60	
1986																																	20.16
January					0.45																											0.47	
February					0.30	0.15					0.10																					1.00	
March		0.02										0.30		0.08		0.15	0.22	0.05		0.40							0.05				1.13		
April		0.07	2.40								0.06									0.24										0.07	3.28		
May						0.42	0.15		0.08	0.18										0.30						0.15					3.47		
June						0.09	0.14	1.25	0.40											0.04								0.50	0.22		0.13	2.45	
July		0.12		0.26	0.05		0.06	0.31												0.07	0.07										0.93		
August												0.10	0.05		0.11					0.12	0.24	0.20									1.66		
September		0.09				0.26	0.09	0.15	0.01																0.05	0.05	0.03	1.05				0.60	
October			0.54						0.30	0.30	0.50																					2.69	
November	0.70						0.45			0.03		0.13							0.32		0.06		0.07							0.60	2.26		
December	0.20						0.10	0.50																	0.03	0.02			0.90			0.80	



Month	1	2	3	4	5	6	7	8	9	10	11	12	13	14	15	16	17	18	19	20	21	22	23	24	25	26	27	28	29	30	31	Total			
<b>1987</b>																																			
January						0.10	0.20								0.70				0.80															20.74	
February				0.10										0.25	0.20	0.20	0.50	0.45	0.15						0.40	0.03								1.80	
March							0.80							0.20	0.05				0.01		0.36	0.08	0.01				1.10	0.25					2.08		
April	0.50											0.74	0.10						0.65															2.86	
May	0.21	0.36	0.75	0.05	0.45					0.02	0.04	0.43		0.61		0.02	0.54	0.06	0.62	0.60			0.42	0.02	0.01	0.25				0.01	0.11		2.11		
June									1.10	0.08								0.70		0.07				0.30				0.10	2.90	0.13			5.55		
July																																	0.13	0.43	
August				0.02			0.15																		0.30	0.62	0.86	0.15	0.15	0.30				2.55	
September				0.26			0.05								0.05	0.05	0.26	0.09																0.76	
October													0.76		0.26																0.02	0.50		1.54	
November	0.04					0.09	0.18								0.70	1.00																		2.41	
December													0.35	0.10										0.40		0.40							2.65		
<b>1988</b>																																			
January					0.04														0.30	0.10													30.12		
February					0.02						0.35						0.42	0.08	0.11					0.10										0.44	
March	0.15	0.30							0.11	0.13						0.30														0.22	0.05	0.65		1.08	
April																	0.55	0.07																1.89	
May		0.60									0.20							0.13	2.25	0.63				0.30	0.06				0.05				1.22		
June						0.21													0.09								0.26	0.04		0.35				3.86	
July				0.49			0.19	0.10		0.01	0.20		0.05	0.34	0.06				0.09											0.06	0.12		1.43		
August		1.60				0.20						0.06	1.15	0.12	0.24	0.04			0.26	0.08													1.99		
September																				0.49	0.19		0.03										2.26		
October					0.10															0.02	0.10											0.10		1.61	
November			0.25					0.10			0.05				0.35																			0.20	
December							0.55							0.75										0.02			0.15							0.77	
<b>1989</b>																																			
January												0.32														0.03							1.45		
February	0.03			0.58	0.10							0.14	0.10							0.03								1.10					1.09		
March			0.46																	0.23														0.95	
April	0.05	0.02							0.68	0.06	0.05																	0.06	0.23	0.07	0.63			1.85	
May		0.01					0.28	0.24		0.03	0.30			0.74	0.79	0.03	0.01												0.06	0.23	0.07	0.63		3.91	
June	0.02	0.18	0.21		0.33	0.07		0.01	0.06	0.04	0.11	0.17	0.04									0.44	0.06	0.05	0.01		0.44			0.05	0.14	0.90	3.91		
July																											0.01			0.11	0.60	0.29		1.86	
August		0.06				0.01	0.49									0.91	0.21	0.02		0.50													1.50		
September				0.05			0.03	0.91	0.03	0.44	0.64	0.46				0.91	0.21	0.02		0.02	0.01					0.10							1.81		
October																																		2.73	
November	0.53															0.45	0.25	0.14																0.84	
December						0.20			0.52	0.18					0.04					0.23								0.04						0.57	
<b>1990</b>																																			
January																																		1.37	
February		0.29																	0.02	0.54														1.93	
March					0.72	2.15							0.72						0.10							0.10								0.56	
April			0.02		0.43			0.03	0.12	0.01						0.16		0.03	0.12		0.02			0.08	0.03		0.34	0.18	0.46	0.03			0.76		
May				0.19				0.07			0.23					0.25													0.07	0.23					4.81
June																																0.45		2.15	
July																			0.28								0.04		0.15	0.50				1.88	
August			0.05			0.18	0.05	1.61	0.03	0.11	0.07					0.02				0.80	0.34													0.28	
September	0.49	0.13				0.10				0.07	0.30	0.17		0.07	0.15			0.12		0.10												0.19	1.69		
October				0.27	0.03													0.05	0.69				0.29											2.09	
November		0.09					0.37													0.20						0.17		0.11	0.06	0.02				0.98	
December		0.23	0.39		0.07	0.48																						0.23						1.40	
						0.05														0.15											0.08			0.28	

Month	1	2	3	4	5	6	7	8	9	10	11	12	13	14	15	16	17	18	19	20	21	22	23	24	25	26	27	28	29	30	31	Total		
1991																																		
January																0.28				0.37			0.09		0.14									20.14
February																								0.17										1.06
March		0.02			0.18																													0.17
April							0.22																											0.37
May				0.64							0.56	0.70								0.02			0.15	0.02										2.87
June	0.77	0.17	0.03		0.07	0.17		0.14	0.14			0.02			0.55	1.93					0.07		0.15	0.17	0.10	0.03	0.03				0.15		4.06	
July		0.03	0.05						0.31							1.43																		2.40
August		0.15	2.52			0.63			0.11							0.38				0.33	0.42		0.29	0.32	0.21	0.15	0.06					0.16	0.23	4.31
September							0.04			0.07	0.06	0.07	0.14				0.12	0.03		0.07	0.33	0.42		0.29	0.32	0.21	0.15	0.06				0.03		3.60
October				0.16																				0.13										4.31
November	0.33					0.04	0.06				0.12						0.41	0.09	0.37	0.70	0.35	0.32									0.26		0.94	
December													0.05										0.08	0.03		0.13	0.05			0.43	0.30		1.07	
1992																																		3.55
January							0.26					0.45		0.16																				0.10
February																																		24.50
March				1.37				1.23	1.56														0.05		0.02									0.87
April										0.10				0.16	0.12	0.07																		0.07
May									0.13														0.13											5.76
June	0.30				0.14		0.10	0.05													0.18	0.39	0.18		0.06	0.58	0.15	0.18	0.08		0.02	0.36		0.58
July	0.06	0.23				0.04	0.02			0.04	0.07	0.19		0.02	0.01					0.05	0.06	0.02			0.10	0.10		0.03					2.31	
August	0.02		0.10																															1.01
September																																		1.30
October																							0.28	0.13	2.85	0.05								3.74
November																																		0.00
December																																		0.00

**APPENDIX C**

**Water Level Observations**





2 foot piezometer water levels

DOWNSTREAM															UPSTREAM				
Piezometer Date	Stream Flow	Farthest d/s		Original					Packed		Stream Flow	Stream				Stream Flow			
		0+00	0+25	0+25	0+75	1+05	1+45	1+80	1+80	3+30		4+80	6+30	7+30	9+30		10+80	Stream Flow	
25-Feb-92	n/a	5887.55	5888.83	5889.19				5894.11	5895.13	n/a									
05-Mar-92	n/a	5887.54	5888.85	5889.20				5894.28	5895.49	n/a									
09-Mar-92	n/a	5887.57	5888.88	5889.21				5894.49	5896.40	n/a									
10-Mar-92	n/a	5887.57	5888.89	5889.25				5894.62	5896.57	n/a									
12-Mar-92	n/a	5887.61	5888.94	5889.25	5891.28			5894.71	5896.83	n/a									
27-Mar-92	n/a	5887.75	5889.04	5889.42	5891.39			5894.92	5896.97	n/a									
30-Mar-92	n/a	5887.76	5889.07	5889.47	5891.46			5894.93	5896.98	n/a									
31-Mar-92	n/a	5887.76	5889.08	5889.47	5891.48			5894.94	5896.97	n/a									
01-Apr-92	n/a	5887.76	5889.05	5889.46	5891.45			5894.92	5896.94	n/a									
02-Apr-92	n/a	5887.74	5889.03	5889.45	5891.44			5894.90	5896.94	n/a									
03-Apr-92	n/a	5887.75	5889.04	5889.47	5891.46			5894.90	5896.95	n/a									
04-Apr-92	n/a	5887.74	5889.03	5889.45	5891.48			5894.89	5896.95	n/a									
05-Apr-92	n/a	5887.73	5889.03	5889.47	5891.45			5894.89	5896.95	n/a									
06-Apr-92	n/a	5887.72	5889.02	5889.45	5891.40			5894.88	5896.95	n/a									
07-Apr-92	n/a	5887.70	5889.01	5889.44	5891.38			5894.88	5896.95	n/a									
09-Apr-92	n/a	5887.68	5888.99	5889.43	5891.38			5894.85	5896.96	n/a									
13-Apr-92	n/a	5887.66	5888.99	5889.40	5891.35			5894.84	5896.97	n/a									
16-Apr-92	n/a	5887.67	5888.98	5889.40	5891.35			5894.86	5896.97	n/a									
20-Apr-92	n/a	5887.59	5888.94	5889.43	5891.37			5894.80	5896.97	n/a									
22-Apr-92	0.149	5887.57	5888.93	5889.40	5891.32			5894.83	5896.97	n/a									
24-Apr-92	0.127	5887.52	5888.93	5889.31	5891.30			5894.79	5896.93	n/a									
29-Apr-92	0.072	5887.48	5888.87	5889.30	5891.29			5894.79	5896.95	n/a									
04-May-92	0.071	5887.47	5888.90	5889.29	5891.33			5894.79	5896.95	0.000									
06-May-92	0.070	5887.45	5888.84	5889.27	5891.34			5894.79	5896.94	0.000									
08-May-92	0.063	5887.44	5888.87	5889.28	5891.29			5894.76	5896.93	0.000									
18-May-92	0.052	5887.44	5888.85	5889.27	5891.31			5894.63	5896.90	0.000									
21-May-92	0.055	5887.44	5888.90	5889.28	5891.36			5894.58	5896.88	0.000									
22-May-92	0.055	5887.46	5888.91	5889.30	5891.39			5894.53	5896.85	0.000									
26-May-92	0.044	5887.45	5888.88	5889.30	5891.38			5894.32	5896.82	0.000									
27-May-92	0.044	5887.51	5888.93	5889.35	5891.34			5894.35	5896.86	0.000									
27-May-92	0.044	5887.51	5888.93	5889.35	5891.34			5894.35	5896.86	0.000									
28-May-92	0.044	5887.49	5888.91	5889.35	5891.33			5894.29	5896.83	0.000									
28-May-92	0.044	5887.49	5888.91	5889.33	5891.30			5894.30	5896.83	0.000									
29-May-92	0.041	5887.49	5888.92	5889.34	5891.28			5894.27	5896.81	0.000									
30-May-92	0.040	5887.49	5888.88	5889.34	5891.30			5894.22	5896.83	0.000									
01-Jun-92	0.047	5887.49	5888.94	5889.35	5891.31			5894.28	5896.81	0.000									
01-Jun-92	0.053	5887.52	5888.92	5889.36	5891.30			5894.26	5896.81	0.000									
02-Jun-92	0.047	5887.50	5888.94	5889.36	5891.26			5894.25	5896.81	0.000									
02-Jun-92	0.046		5888.93	5889.35	5891.28			5894.24	5896.81	0.000									
03-Jun-92	0.047		5888.91	5889.36	5891.25			5894.23	5896.79	0.000									
04-Jun-92	0.045		5888.93	5889.35	5891.24			5894.22		0.000									
04-Jun-92	0.040		5888.91	5889.33	5891.25			5894.23		0.000									
07-Jun-92	0.040		5888.93	5889.35	5891.23			5894.23		0.000									
15-Jun-92	0.038		5889.23	5889.37	5891.25			5894.27		0.000									
19-Jun-92	0.033		5889.04	5889.39	5891.14					0.000									
22-Jun-92	0.026		5889.01	5889.39	5891.12					0.000									
26-Jun-92	0.018		5889.71	5889.39	5891.09					0.000									
29-Jun-92	0.013		5889.25	5889.35	5891.03					0.000									
08-Jul-92	0.003		5888.91	5889.27	5890.96					0.000									
13-Jul-92	0.000		5888.85	5889.22	5890.90					0.000									
24-Jul-92	0.000		5888.59	5888.78	5890.93					0.000									
27-Jul-92	0.000		5888.38	5888.50	5890.17					0.000									
31-Jul-92	0.000		5888.12	5888.28	5889.91					0.000									
03-Aug-92	0.000		5887.93	5888.12	5889.76					0.000									
07-Aug-92	0.000		5887.62	5887.97						0.000									
13-Aug-92	0.000									0.000									
20-Aug-92	0.000									0.000									
25-Aug-92	0.000		5887.53							0.000									
26-Aug-92	0.000									0.000									
03-Sep-92										0.000									



**APPENDIX D**

**Calculated Shallow Groundwater Gradients**



	25-Feb-92	05-Mar-92	09-Mar-92	10-Mar-92	12-Mar-92	27-Mar-92	30-Mar-92	31-Mar-92	01-Apr-92	02-Apr-92	03-Apr-92
<b>Surf-1 foot</b>											
0+00	-0.5	-0.6	-0.5	-0.5	-0.5	-0.5	-0.6	-0.5	-0.4	-0.5	-0.5
0+25	-0.2	-0.1	-0.1	-0.1	-0.1	-0.1	-0.1	-0.1	-0.1	-0.1	-0.1
0+25	-0.1	-0.1	-0.1	-0.1	-0.1	-0.1	-0.1	-0.1	-0.1	-0.1	-0.1
0+75	0.2	0.2	0.2	0.2	0.2	0.2	0.2	0.2	0.1	0.1	0.2
1+05	0.3	0.4	0.4	0.4	0.5	0.4	0.4	0.4	0.4	0.4	0.4
1+45	0.1	0.2	0.4	0.5	0.5	0.7	0.6	0.6	0.6	0.6	0.6
1+80	-0.7	-0.3	0.1	0.2	0.2	0.5	0.4	0.3	0.3	0.3	0.3
3+30			-0.7	-0.6	-0.5	-0.2	-0.9	-1.0	-1.1	-1.1	-1.1
4+80			-0.5	-0.4	-0.3	-0.4	-0.5	-0.5	-0.6	-0.6	-0.6
6+30		-0.3	-0.3	-0.2	-0.1	-0.3	-0.5	-0.5	-0.6	-0.6	-0.6
7+80		-0.2	-0.4	-0.5	-0.7						
9+30	-0.4	0.1	0.1	0.1	0.1	0.0	0.1	0.1	0.1	0.1	0.1
10+80	-0.5	0.1	0.3	0.3	0.3	0.5	0.6	0.5	0.5	0.5	0.5
<b>1-2 foot</b>											
0+00	-0.5	-0.5	-0.5	-0.5	-0.5	-0.5	-0.5	-0.5	-0.6	-0.5	-0.5
0+25	-0.2	-0.2	-0.2	-0.2	-0.2	-0.2	-0.2	-0.2	-0.2	-0.2	-0.2
0+25	0.1	0.1	0.1	0.1	0.1	0.2	0.2	0.2	0.2	0.2	0.2
0+75					-0.0	-0.0	0.0	0.0	0.0	0.1	0.1
1+05											
1+45	-0.1	-0.1	-0.2	-0.1	-0.1	-0.1	-0.1	-0.1	-0.1	-0.1	-0.1
1+80	-0.0	-0.0	0.3	0.5	0.7	0.4	0.4	0.5	0.5	0.5	0.5
3+30			-0.2	-0.1	-0.1	-0.5	0.0	0.0	0.0	0.1	0.0
4+80			0.0	0.0	0.1	-0.0	0.0	-0.2	0.0	0.0	-0.0
6+30		-0.4	-0.1	-0.1	-0.1	-0.1	-0.1	-0.0	-0.1	-0.0	0.1
7+80		-1.7	-1.3	-1.1	-1.0						
9+30	-0.0	-0.0	0.0	0.0	0.0	0.1	0.1	0.0	0.1	0.1	0.1
10+80	-0.0	0.0	0.1	0.1	0.1	0.1	0.1	0.1	0.1	0.1	0.1
<b>2-3 foot</b>											
0+00	-1.3	-1.2	-1.3	-1.2	-1.3	-1.3	-1.3	-1.3	-1.3	-1.2	-1.3
0+25	0.4	0.4	0.4	0.4	0.4	0.5	0.4	0.4	0.5	0.5	0.4
0+25											
0+75					3.2	4.3	3.2	2.9	3.2	2.9	2.4
1+05											
1+45	-0.0	-0.0	0.1	0.1	0.1	0.2	0.1	0.1	0.1	0.1	0.1
1+80	0.6	-0.1	-0.1	-0.1	-0.1	0.2	0.1	0.1	0.2	0.1	0.1
3+30			0.3	0.2	0.1	-0.2	-0.1	-0.1	-0.1	-0.3	-0.1
4+80			-0.1	-0.1	0.0	0.0	-0.0	0.0	-0.0	-0.0	-0.0
6+30		-0.4	-0.2	-0.2	-0.1	-0.2	-0.2	-0.2	-0.2	-0.2	-0.7
7+80		6.6	-19.8	-19.8	-17.5						
9+30	0.1	0.2	0.2	0.2	0.2	0.2	0.3	0.3	0.2	0.2	0.2
10+80	0.1	-0.1	-0.0	-0.1	-0.1	-0.2	0.0	-0.0	0.1	0.0	0.0

	04-Apr-92	05-Apr-92	06-Apr-92	07-Apr-92	09-Apr-92	13-Apr-92	16-Apr-92	20-Apr-92	22-Apr-92	24-Apr-92	29-Apr-92
<b>Surf-1 foot</b>											
0+00	-0.5	-0.5	-0.5	-0.6	-0.6	-0.5	-0.5	-0.5	-0.5	-0.5	-0.6
0+25	-0.1	-0.0	-0.1	-0.1	-0.1	-0.0	-0.0	-0.0	-0.0	-0.0	-0.0
0+25	-0.0	-0.0	-0.0	-0.1	-0.0	-0.0	-0.0	-0.0	-0.0	0.0	-0.0
0+75	0.2	0.2	0.2	0.2	0.2	0.2	0.2	0.2	0.2	0.3	0.3
1+05	0.5	0.5	0.5	0.5	0.5	0.5	0.5	0.5	0.6	0.5	0.5
1+45	0.6	0.8	0.7	0.7	0.7	0.7	0.7	0.7	0.7	0.7	0.7
1+80	0.4	0.5	0.4	0.4	0.4	0.5	0.5	0.4	0.5	0.5	0.5
3+30	-1.2	-1.2	-1.2	-1.2	-1.1	-1.0	-1.1	-1.0	-1.0	-1.0	
4+80	-0.7	-0.4	-0.7	-0.7	-0.7	-0.8	-0.9				
6+30	-0.8	-0.8	-0.8	-0.9	-1.0	-1.1	-1.2				
7+80											
9+30	0.1	0.1	0.1	0.1	0.1	0.2	0.2	0.2	0.2	0.2	0.2
10+80	0.4	0.6	0.5	0.5	0.5	0.5	0.5	0.5	0.4	0.4	0.4
<b>1-2 foot</b>											
0+00	-0.5	-0.5	-0.5	-0.5	-0.5	-0.4	-0.5	-0.5	-0.5	-0.5	-0.5
0+25	-0.2	-0.2	-0.2	-0.2	-0.2	-0.2	-0.2	-0.2	-0.2	-0.1	-0.2
0+25	0.2	0.2	0.2	0.2	0.2	0.2	0.2	0.3	0.2	0.2	0.2
0+75	0.1	0.1	0.1	0.0	0.1	0.1	0.1	0.2	0.1	0.1	0.1
1+05											
1+45	-0.1	-0.2	-0.1	-0.1	-0.1	-0.1	-0.1	-0.1	-0.0	-0.0	-0.0
1+80	0.5	0.3	0.4	0.5	0.5	0.5	0.5	0.6	0.6	0.6	0.7
3+30	0.0	0.0	0.0	0.0	0.0	0.0	0.0				
4+80	0.0	-0.3	0.0	0.0	-0.1	0.0	0.1	0.0	0.0	0.0	
6+30	-0.0	-0.0	-0.1	-0.0	-0.0	-0.0	-0.1				
7+80											
9+30	0.0	0.2	0.1	0.1	0.1	0.1	0.1	0.0	0.0	0.0	-0.1
10+80	0.2	0.0	0.0	0.0	0.0	0.0	-0.0	0.2	0.0	0.0	0.1
<b>2-3 foot</b>											
0+00	-1.2	-1.2	-1.2	-1.2	-1.1	-1.1	-1.1	-1.0	-1.0	-0.9	-0.9
0+25	0.5	0.4	0.4	0.4	0.5	0.4	0.4	0.4	0.4	0.4	0.4
0+25											
0+75	1.6	2.4	3.5	4.0	3.5	3.7	4.3	4.3	3.7	3.2	3.5
1+05											
1+45	0.2	0.3	0.1	0.1	0.1	0.1	0.1	0.3	0.3	0.1	0.1
1+80	0.3	0.1	0.1	0.3	0.1	0.2	0.1	0.0	0.0	0.0	-0.0
3+30	0.7	0.7	-0.1	-0.1	-0.1	-0.1	-0.1	-0.1	-0.1	1.3	0.0
4+80	0.0	0.1	-0.0	0.0	0.0	0.0	0.0	0.0	0.0	0.0	0.0
6+30	-0.2	-0.1	-0.2	-0.2	-0.2	-0.2	-0.1	-0.1	-1.4	-0.2	-0.2
7+80											
9+30	0.2	0.0	0.2	0.2	0.2	0.2	0.2	0.2	0.1	0.1	0.2
10+80	0.0	0.1	0.0	0.0	0.1	0.0	0.0	-0.3	0.1	0.0	0.0

	04-May-92	06-May-92	08-May-92	18-May-92	21-May-92	22-May-92	26-May-92	27-May-92	27-May-92	28-May-92	28-May-92
<b>Surf-1 foot</b>											
0+00	-0.6	-0.6	-0.6	-0.6	-0.6	-0.6	-0.6	-0.6	-0.6	-0.6	-0.6
0+25	-0.1	-0.1	-0.0	-0.1	-0.1	-0.1	-0.1	-0.0	-0.0	-0.0	-0.0
0+25	0.0	-0.0	0.0	-0.0	-0.0	-0.1	-0.0	-0.0	-0.0	-0.0	-0.0
0+75	0.3	0.3	0.3	0.3	0.4	0.3	0.4	0.4	0.4	0.4	0.4
1+05	0.6	0.5	0.5	0.5	0.4	0.4	0.4	0.4	0.4	0.4	0.4
1+45	0.7	0.8	0.7	0.7	-0.2	0.6	0.5	0.5	0.5	0.5	0.4
1+80	0.5	0.5	0.5	0.3	0.2	0.2	0.1	0.1	0.1	0.0	0.0
3+30											
4+80											
6+30											
7+80											
9+30	0.2	0.1	0.1	-0.8				-0.6	-0.6	-0.4	-0.3
10+80	0.3	0.3	0.2	-0.6			-0.1	-0.0	0.0	0.1	0.1
<b>1-2 foot</b>											
0+00	-0.5	-0.5	-0.5	-0.5	-0.6	-0.5	-0.5	-0.5	-0.5	-0.5	-0.5
0+25	-0.1	-0.2	-0.2	-0.2	-0.2	-0.1	-0.1	-0.2	-0.2	-0.2	-0.2
0+25	0.2	0.2	0.2	0.2	0.2	0.3	0.2	0.2	0.2	0.2	0.2
0+75	0.2	0.2	0.1	0.1	0.2	0.2	0.2	0.0	0.0	0.1	-0.0
1+05											
1+45	-0.0	-0.1	-0.1	-0.1	-0.1	-0.1	-0.2	-0.2	-0.2	-0.2	-0.2
1+80	0.7	0.7	0.7	0.9	0.9	0.9	1.0	1.1	1.1	1.1	1.1
3+30											
4+80											
6+30											
7+80											
9+30	0.1	-0.1	-0.0	-0.3				-0.3	-0.3	-0.2	-0.2
10+80	0.0	0.1	0.1	0.2			-0.1	-0.0	-0.0	-0.0	-0.0
<b>2-3 foot</b>											
0+00	-0.8	-0.8	-0.8	-0.7	-0.7	-0.7	-0.7	-0.7	-0.7	-0.7	-0.7
0+25	0.4	0.4	0.4	0.4	0.5	0.4	0.4	0.4	0.4	0.4	0.4
0+25											
0+75	2.2	1.9	2.9	2.7	1.9	0.8	-0.5	1.9	1.9	1.1	2.4
1+05											
1+45	0.0	0.0	0.1	0.0		0.0	0.2	0.0	-0.0	0.0	-0.0
1+80	-0.1	-0.2	-0.1	-0.6	-0.7	-0.8	-1.1	-1.1	-1.1	-1.2	-1.2
3+30	0.1										
4+80	0.0										
6+30											
7+80											
9+30	-0.1	0.1	0.0	0.7				-0.0	-0.0	-0.0	-0.0
10+80	0.0	-0.1	-0.1	-0.4		-0.4	0.1	0.1	0.1	0.1	0.1

	29-May-92	30-May-92	01-Jun-92	01-Jun-92	02-Jun-92	02-Jun-92	03-Jun-92	04-Jun-92	04-Jun-92	07-Jun-92	15-Jun-92
<b>Surf-1 foot</b>											
0+00	-0.6	-0.6	-0.5	-0.6	-0.6	-0.5	-0.6	-0.6	-0.6	-0.5	-0.8
0+25	-0.0	-0.1	-0.1	-0.0	-0.0	-0.1	-0.1	-0.1	-0.1	-0.1	-0.1
0+25	-0.0	-0.0	-0.0	-0.0	-0.0	-0.0	-0.0	-0.0	-0.0	-0.1	-0.1
0+75	0.4	0.4	0.3	0.3	0.3	0.3	0.3	0.3	0.3	0.3	0.2
1+05	0.3	0.4	0.3	0.3	0.3	0.3	0.3	0.3	0.3	0.3	0.2
1+45	0.4	0.4	0.3	0.3	0.3	0.3	0.3	0.3	0.3	0.3	0.2
1+80	-0.0	-0.0	0.0	0.1	0.1	0.1	0.0	0.0	0.3	0.2	0.0
3+30									-0.0	-0.1	-0.0
4+80											
6+30											
7+80											
9+30	-0.3	-0.4	-0.2	-0.1	-0.1	-0.0	-0.0	-0.0	-0.0	-0.1	
10+80	0.2	0.1	0.1	0.2	0.3	0.3	0.2	0.2	0.2	0.1	
<b>1-2 foot</b>											
0+00	-0.5	-0.4	-0.6	-0.5	-0.5						
0+25	-0.2	-0.2	-0.2	-0.2	-0.2	-0.2	-0.2	-0.2	-0.2	-0.2	0.1
0+25	0.2	0.2	0.2	0.2	0.2	0.2	0.2	0.2	0.2	0.2	0.2
0+75	-0.0	0.0	0.1	0.0	-0.0	-0.0	-0.0	-0.0	-0.0	-0.0	0.1
1+05											
1+45	-0.2	-0.2	-0.1	-0.1	-0.1	-0.1	-0.1	-0.1	-0.1	-0.0	
1+80	1.1	1.1	1.1	1.0	1.0	1.0	1.0				
3+30											
4+80											
6+30											
7+80											
9+30	-0.2	-0.1	-0.2	-0.2	-0.1	-0.1	-0.1	-0.1	-0.1	-0.1	
10+80	-0.0	0.0	0.0	-0.0	-0.0	-0.0	-0.0	-0.1	-0.0	-0.1	
<b>2-3 foot</b>											
0+00	-0.7	-0.7	-0.7	-0.7	-0.7						
0+25	0.4	0.5	0.4	0.4	0.4	0.4	0.4	0.4	0.4	0.2	0.1
0+25											
0+75	2.7	1.4	1.6	1.9	1.9	1.6	2.4	2.4	2.4	2.4	0.3
1+05											
1+45	0.0	0.0	-0.0	0.0	0.0	0.0	0.0	0.0	0.0	0.0	
1+80	-1.2	-1.2	-1.2	-1.0	-1.1	-1.1	-1.1	0.0	-0.0	-0.1	
3+30											
4+80											
6+30											
7+80											
9+30	0.1	0.2	-0.0	0.0	0.0	0.1	0.1	0.1	0.1	0.2	
10+80	0.0	-0.1	0.0	0.0	0.1	0.0	0.0	0.0	0.1	-0.2	-0.2

**Surf-1 foot**

	19-Jun-92	22-Jun-92	26-Jun-92	29-Jun-92	08-Jul-92	13-Jul-92	24-Jul-92	27-Jul-92	31-Jul-92	03-Aug-92	07-Aug-92
0+00	-0.8	-0.8	-0.7	-0.7	-0.8	-0.9	N/A				
0+25	-0.1	-0.1	-0.1	-0.1	-0.1	-0.1	-0.3	-0.6			
0+25	-0.1	-0.1	-0.1	-0.1	0.0	-0.1	-0.5	-0.8	-1.0	-1.0	
0+75	0.2	0.2	0.3	0.2	0.2	0.1	-0.3	-0.6	-0.7		
1+05	0.2	0.2	0.2	0.1	-0.2	-0.5					
1+45											
1+80	-0.5	-0.9									
3+30											
4+80											
6+30											
7+80											
9+30											
10+80											

**1-2 foot**

0+00											
0+25	-0.1	-0.1	0.6	0.2	-0.1	-0.2	0.0	0.0			
0+25	0.2	0.2	0.2	0.2	0.1	0.1	0.2	0.2	0.2	0.1	
0+75	-0.1	-0.1	-0.2	-0.2	-0.2	-0.2	0.6	-0.2	-0.4		
1+05											
1+45											
1+80											
3+30											
4+80											
6+30											
7+80											
9+30											
10+80											

**2-3 foot**

0+00											
0+25	0.3	0.4	-0.3	0.1	0.3	0.4	0.2	0.2	0.1	0.1	0.1
0+25											
0+75	2.9	2.9	3.2	3.5	2.9	3.2	-12.3	1.6	1.9	0.1	
1+05											
1+45											
1+80											
3+30											
4+80											
6+30											
7+80											
9+30											
10+80											

	13-Aug-92	20-Aug-92	25-Aug-92	26-Aug-92	03-Sep-92
<b>Surf-1 foot</b>					
0+00					
0+25					
0+25					
0+75					
1+05					
1+45					
1+80					
3+30					
4+80					
6+30					
7+80					
9+30					
10+80					
<b>1-2 foot</b>					
0+00					
0+25					
0+25					
0+75					
1+05					
1+45					
1+80					
3+30					
4+80					
6+30					
7+80					
9+30					
10+80					
<b>2-3 foot</b>					
0+00			0.1		
0+25					
0+25					
0+75					
1+05					
1+45					
1+80					
3+30					
4+80					
6+30					
7+80					
9+30					
10+80					

**APPENDIX E**

**Grain Size Analysis of Surface Sediments**

	Percent Finer	Diameter (mm)	Station		0+55	0+75	0+85	1+05	1+05	1+15	1+45
			0+00	0+25				#1	#2		
	2"	50.8			100%	100%	100%		100%	100%	100%
	1"	26.67			84%	91%	97%		92%	61%	92%
	3/4"	18.85			73%	88%	90%		87%	55%	84%
Gravel	1/2"	13.33		100%	69%	84%	85%	100%	97%	85%	48%
	#4	4.75	100%	97%	63%	68%	68%	94%	78%	35%	48%
	#8	2.362	95%	92%	57%	60%	58%	89%	65%	28%	35%
	#16	1.19	91%	81%	47%	51%	49%	94%	54%	22%	25%
Sand	#30	0.6	84%	69%	38%	41%	39%	75%	39%	16%	16%
	#50	0.3		35%	24%	19%	20%	47%	14%	7%	7%
	#60	0.246	50%	28%	17%	15%	15%	39%	10%	5%	5%
	#100	0.147	28%	12%	8%	6%	7%	20%	3%	2%	2%
	#200	0.074	14%	11%	4%	3%	3%	12%	2%	1%	1%
Silt & Clay	0.032		9.2%	3.6%				5.4%			
	0.023		7.7%	2.9%				4.7%			
	0.017		6.8%	2.6%				4.2%			
	0.012		5.8%	2.3%				3.6%			
	0.009		5.0%	2.0%				3.2%			
	0.006		4.2%	1.8%				2.8%			
	0.004		3.6%	1.6%				2.5%			
	0.003		3.0%	1.4%				2.1%			
	0.0013		1.9%	1.2%				1.7%			
	0.0009		1.9%	1.0%				1.5%			
	0.0005		1.6%	1.0%				1.4%			